


5-2017

The Role of the DIRAS Family Members in Regulating Ras Function, Cancer Growth and Autophagy

Margie Nicole Sutton

Follow this and additional works at: https://digitalcommons.library.tmc.edu/utgsbs_dissertations

 Part of the [Biology Commons](#), [Cancer Biology Commons](#), [Cell Biology Commons](#), [Laboratory and Basic Science Research Commons](#), and the [Medicine and Health Sciences Commons](#)

Recommended Citation

Sutton, Margie Nicole, "The Role of the DIRAS Family Members in Regulating Ras Function, Cancer Growth and Autophagy" (2017). *The University of Texas MD Anderson Cancer Center UTHealth Graduate School of Biomedical Sciences Dissertations and Theses (Open Access)*. 741.
https://digitalcommons.library.tmc.edu/utgsbs_dissertations/741


This Dissertation (PhD) is brought to you for free and open access by the The University of Texas MD Anderson Cancer Center UTHealth Graduate School of Biomedical Sciences at DigitalCommons@TMC. It has been accepted for inclusion in The University of Texas MD Anderson Cancer Center UTHealth Graduate School of Biomedical Sciences Dissertations and Theses (Open Access) by an authorized administrator of DigitalCommons@TMC. For more information, please contact digitalcommons@library.tmc.edu.

THE ROLE OF THE *DIRAS* FAMILY MEMBERS IN REGULATING RAS FUNCTION,
CANCER GROWTH AND AUTOPHAGY

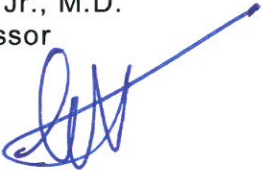
by

Margie Nicole Sutton, B.S.

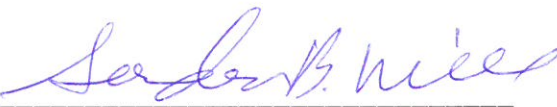
APPROVED:




Robert C. Bast Jr., M.D.
Advisory Professor



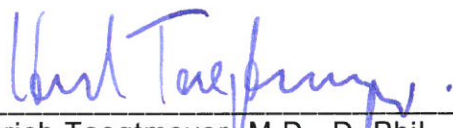
George Calin, M.D, Ph.D.



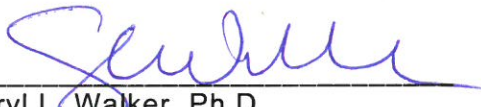
Gordon Mills, M.D., Ph.D.



Samuel Mok, Ph.D.



Heinrich Taegtmeyer, M.D., D. Phil.



Cheryl L. Walker, Ph.D.

APPROVED:

Dean, The University of Texas
MD Anderson Cancer Center UTHealth Graduate School of Biomedical Sciences

THE ROLE OF THE *DIRAS* FAMILY MEMBERS IN REGULATING RAS FUNCTION,
CANCER GROWTH AND AUTOPHAGY

by

Margie Nicole Sutton, B.S.

APPROVED:

Robert C. Bast Jr., M.D.
Advisory Professor

George Calin, M.D, Ph.D.

Gordon Mills, M.D., Ph.D.

Samuel Mok, Ph.D.

Heinrich Taegtmeyer, M.D., D. Phil.

Cheryl L. Walker, Ph.D.

APPROVED:

Dean, The University of Texas
MD Anderson Cancer Center UTHealth Graduate School of Biomedical Sciences

THE ROLE OF THE *DIRAS* FAMILY MEMBERS IN REGULATING RAS FUNCTION,
CANCER GROWTH AND AUTOPHAGY

A

DISSERTATION

Presented to the Faculty of

The University of Texas

MD Anderson Cancer Center UTHealth

Graduate School of Biomedical Sciences

in Partial Fulfillment

of the Requirements

for the Degree of

DOCTOR OF PHILOSOPHY

by

Margie Nicole Sutton, B.S.
Houston, Texas

May, 2017

Copyright © 2017 Margie N. Sutton
All Rights Reserved

DEDICATION

To

Those patients, family, and friends which have been affected by cancer.

ACKNOWLEDGEMENTS

My academic career would not be where it is today without the help and guidance of many. Without the example set forth by you, Dr. Robert C. Bast Jr., I would not truly understand the selflessness and dedication necessary to translate the important findings at the bench top to the clinic. Thank you Dr. Bast for standing by my side when the weight of my projects seemed unbearable, and as soon as I started to feel the weight lift, you were there to pile on a few more experiments pushing me to expect more from myself than I thought possible. Your commitment to the clinical needs of your patients is a driving force in the level of research conducted under your guidance, and I am fortunate to have your mentorship. I have learned what it means to be a collaborator, advisor, student and patient advocate, but most importantly a respected scientist from your exemplification. While graduate school is often one of the most challenging adventures in one's career path, it can also be one of the most rewarding and I am thankful that you were there to see me through. I would like to extend my sincere gratitude, and hope that I too will one day be able to provide the mentorship you gave me to students of my own.

I would be remiss if I did not also extend my appreciation to the members of my thesis committee who have spent countless hours with me discussing my progress and lending advice and guidance. Thank you Dr. George Calin for providing daily encouragement when I needed the extra push to keep going. Dr. Gordon Mills, I appreciate how you challenged me at every committee meeting to take my hypothesis to the next level and for reminding me that in science there is not a right or wrong outcome, but that only a well-designed experiment can test one's hypothesis. Thank you Dr. Samuel Mok for consistently offering disease site specific advice and direction during the preparation of my manuscripts. Your attention to detail continues to amaze me. Dr. Henrich Taegetmeyer, thank you for always conveying your support for me as

a scientist and leader helping me gain the confidence needed to succeed beyond my graduate school career. Dr. Cheryl Walker you have served as an inspiration and role model. I am thankful to have had such an extraordinary committee made up of brilliant and supportive scientists. Dr. Steven Millward I've enjoyed collaborating with you and your group over the past couple of years. Thank you for being someone I can count on and a great role model.

Over the past six years, the members of the Bast laboratory have had a daily impact on my mold as a scientist and young investigator. Thank you Dr. Zhen Lu for playing an instrumental role in my development and serving as a teacher, counselor, and friend throughout this journey. Your guidance and daily discussions of the literature, experimental design and protocol development are greatly appreciated. I would also like to extend my sincere gratitude to both past and present members of the Bast laboratory. I would like to thank Dr. Robert Langley for careful reading of my dissertation and manuscripts.

To our collaborators, Dr. Geoff Wahl, Dr. Yao-Cheng Li, Dr. Yong Zhou, Dr. John Hancock, Dr. Jinsong Liu, Dr. Xiaolin Nan, Dr. Tao Huang, Dr. Craig Logsdon, Dr. Timothy Palzkill, Dr. Albert Reger, Dr. Amy Hurwitz, Dr. Joe Gray, Dr. Jan Parker-Thornburg, Dr. Steven Millward, Dr. Daniel Carson, Dr. Micaela Morgado your support has been instrumental not only in helping to decipher the role of the DIRAS family members, but developing my role as a scientist. Collaboration is essential to propel discoveries forward and your example of how to do that successfully will always remain a valued part of my training.

As an undergraduate student, Dr. Doug Frantz gave me the opportunity to experience firsthand what a life dedicated to research would look like. His guidance and support drove me to choose biomedical research as my career path, and I could

not be more grateful to have had him as my first academic advisor. Dr. Frantz, your passion for organic chemistry ignited my desire to pursue a Ph.D. and for that I am forever indebted. To my colleges at The University of Texas at San Antonio, Dr. Hector Aguilar, Dr. David Babinski, Dr. Ian Crouch, and Robynne Neff your support during my time at UTSA and throughout graduate school has been heartening.

Graduate school would not be what it is without those who walk alongside you in the trenches. Thank you for supporting me from our interview weekend and beyond, Angie Torres-Adorno, Lisa Mustachio, Paloma Monroig, Emily Steinmetz, Alex Marshall, Ramon Flores, Sunil Acharya, Dennis Ruder, Smruthi Vijayaraghavan, Archana Sidalaghatta Nagaraja, Aarthi Goverdhan, Kimberly Vincent, Keri Callegari, Shelley Herbrich and my UTHHealth StudentIncercouncil colleagues, Alix Baycroft, Margaret Wang.

Houston would not feel like home without the love and support of my dearest friends who have been by my side throughout my thesis work. Thank you for providing a listening ear and sharing in the excitement of my discoveries. Julia, Kristy, Kelly, Kori, Chelsea, Courtney, Catherine, Christina, Sarah (you should move to Houston!) and the boys, you all mean the world to me and your support has been essential in my success. Without your unwavering friendship and encouragement this step in my career would not only be more stressful, but a lot less fun.

It is often said that as we age, our mold is ever changing and influenced by those around us. From an early age my family and friends have shaped not only who I have become as a scientist, but most importantly who I have become as an individual. There are never enough “thank you’s” or “I love you’s” to make up for the role models they have been. Dad, your influence led me to the crossroads of science and medicine and without your support my inquisitive mind may not have been pushed to its fullest

potential. Mom, your compassion and love is nothing short of everlasting and without you I would not be the person I am today; I am a direct reflection of everything that makes you so special and I hope you know how much I cherish that (even the excessive emotions). Amanda, I don't think you realize how influential it is to have you as my little sister and for that I will always be grateful. Bob and Sandy, thank you for always believing in me and raising the wonderful man that is my husband, we both benefit greatly from your continued love and support. To my extended family and cherished friends, I couldn't have asked for a better cheer squad; thank you so much!

To my dearest husband, words cannot describe how thankful I am for your support, not only in this journey, but in life. You truly are one of a kind and without you I would not be where I am today. You push me to be the best version of myself and without you my dreams would not become my reality. I am lucky to know your love and I cherish what we have deeply. I love you always.

THE ROLE OF THE *DIRAS* FAMILY MEMBERS IN REGULATING RAS FUNCTION, CANCER GROWTH AND AUTOPHAGY

Margie Nicole Sutton, B.S.

Advisory Professor: Robert C. Bast Jr, M.D.

DIRAS3 is a maternally imprinted tumor suppressor gene that is downregulated by multiple mechanisms across several tumor types. When re-expressed, *DIRAS3* decreases proliferation, inhibits motility, and induces autophagy and tumor dormancy. *DIRAS3* encodes a 26 kDa small GTPase with 60% homology to Ras and Rap, differing from oncogenic Ras family members by a 34-amino acid N-terminal extension that is required for its tumor suppressive function in ovarian cancer. By assessing the structure-function relationship, I found that *DIRAS3* inhibits Ras-induced transformation and is a natural antagonist of Ras/MAPK signaling. *DIRAS3* binds directly to Ras and disrupts cluster formation inhibiting the activation of Raf kinase, which is dependent upon membrane localization and the N-terminal extension. This observation provides a novel approach to target oncogenic Ras and assesses the functional significance of Ras clustering/multimerization.

The N-terminus of *DIRAS3* also plays an important role in the mechanism(s) by which *DIRAS3* induces autophagy. Expression of *DIRAS3* is required for the induction of autophagy in human cells. While *DIRAS3* is found in the genome of humans, pigs and cows, it maps to an apparent evolutionary breakpoint in the rodent lineage where chromosomes have been rearranged relative to the human genome since the two species shared a common ancestor. Mice and humans do express two homologous

Ras-related GTPases, *DIRAS1* and *DIRAS2*. These 22-kDa GTPases have 30-40% homology with H-Ras and 50-60% homology with *DIRAS3* where the major difference is the truncation of the N-terminal extension. *DIRAS1* and *DIRAS2* have not previously been studied extensively. I compared the roles of the *DIRAS* family in malignant transformation, proliferation, survival, motility and autophagy. My observations document the role of *DIRAS1* and *DIRAS2* as ovarian cancer tumor suppressors and demonstrate their role in autophagy and autophagic cell death. Similar to *DIRAS3*, *DIRAS1* and *DIRAS2* induce autophagy at several different levels, including transcription-dependent mechanisms. *DIRAS1* and *DIRAS2* likely serve as surrogates for *DIRAS3* in the murine genome, playing an essential role in murine autophagy. These studies are fundamentally important as they explore the functional significance of their N-terminal extensions, helping to explain how members of an oncogenic superfamily acquire tumor suppressor function.

TABLE OF CONTENTS

APPROVAL SIGNATURES.....	i
TITLE PAGE.....	ii
DEDICATION.....	iv
ACKNOWLEDGEMENTS.....	v
ABSTRACT.....	ix
TABLE OF CONTENTS.....	xi
LIST OF ILLUSTRATIONS.....	xiv
LIST OF TABLES.....	xvii
ABBREVIATIONS.....	xviii
Chapter 1: Introduction.....	1
1.1 Tumor Suppressor Genes	
1.2 Oncogenes	
1.3 <i>Ras</i> Oncogenes	
1.4 <i>DIRAS</i> Tumor Suppressor Genes	
1.5 Autophagy	
1.6 Role of Autophagy in Normal Tissues and in Cancer	
1.7 Ovarian Cancer	
1.8 Autophagy in Human Ovarian Cancer	
1.9 Autophagy in Murine Cells	
1.10 Aims and Hypotheses of the Study	
Chapter 2: Materials and Methods.....	17
2.1 List of reagents	
2.2 List of antibodies	
2.3 Experimental Methods	

Chapter 3: DIRAS family members inhibit Ras driven transformation and interact directly with Ras.....39

- 3.1 DIRAS family members inhibit transformation and anchorage independent growth.
- 3.2 The N-terminus of DIRAS family members are important for tumor suppressive function.
- 3.3 DIRAS family members interact with Ras at the A5 helical domain.

Chapter 4: DIRAS3 inhibits Ras driven cancers and downstream ERK signaling by disrupting Ras multimerization/clustering.....49

- 4.1 Ovarian, pancreatic and lung cancer cell lines depend on K-Ras for survival.
- 4.2 Re-expression of DIRAS3 inhibits Ras driven cancer viability.
- 4.3 DIRAS3 inhibits p-ERK downstream Ras/MAPK signaling.
- 4.4 DIRAS3 but not the N-terminal deleted construct, inhibits Ras multimerization/clustering.
- 4.5 Ras multimerization depends on GTP activation by Sos-1.

Chapter 5: DIRAS family members are conserved small GTPases with differential expression across multiple organs.....63

- 5.1 DIRAS family members are small GTPases with homology to Ras and Rap.
- 5.2 DIRAS family expression in normal tissues.
- 5.3 DIRAS family expression is downregulated in ovarian cancer.

Chapter 6: DIRAS1 and DIRAS2 inhibit ovarian cancer cell growth by inducing autophagic cell death.....71

- 6.1 Re-expression of DIRAS family members inhibits long-term and short-term viability.
- 6.2 Re-expression inhibits ovarian cancer xenograft growth in vivo.

- 6.3 Growth inhibition is not due to increased apoptosis, cell cycle arrest or cellular senescence.
- 6.4 DIRAS1 and DIRAS2 induce autophagy and autophagic cell death.
- 6.5 DIRAS family members inhibit ovarian cancer cell migration.

Chapter 7: DIRAS1 and DIRAS2 induce autophagy by regulating nuclear localization of autophagy-related transcription factors.....83

- 7.1 DIRAS1 and DIRAS2 inhibit the PI3K and Ras/MAPK signaling cascades which are necessary for the induction of autophagy.
- 7.2 DIRAS1 and DIRAS2 induce nuclear localization of FOXO3a and TFEB.
- 7.3 Nuclear localization of FOXO3a and TFEB induces transcription of several key autophagy-related genes.

Chapter 8: DIRAS1 and DIRAS2 serve as surrogates for DIRAS3 in the murine genome.....90

- 8.1 DIRAS3 is lost in the murine genome; DIRAS1 and DIRAS2 are conserved paralogues.
- 8.2 Overexpression of DIRAS1 and DIRAS2 induces autophagy in murine ovarian cancer cell lines.
- 8.3 Knockdown of DIRAS1 and DIRAS2 in murine cells inhibits autophagy induced by serum starvation or rapamycin.
- 8.4 Homozygous knockout of DIRAS1 or DIRAS2 results in early embryonic lethality.

Chapter 9: Discussion and future directions.....98

Bibliography.....106

Vita.....134

LIST OF ILLUSTRATIONS

Figure 1. Ras GTPases are molecular switches that activate cellular signaling cascades based on their nucleotide binding.....	5
Figure 2. DIRAS family GTPases differ primarily in the length of their N-terminal extension.....	7
Figure 3. The imprinted tumor suppressor gene DIRAS3 is downregulated by several mechanisms.....	8
Figure 4. Autophagy is a multistep process which includes several key regulators such as Beclin1, DIRAS3, LC3 and ATGs.....	10
Figure 5. Autophagy provides metabolites for many cellular functions.....	12
Figure 6. DIRAS3 inhibits Ras-induced malignant transformation of murine fibroblasts and Ras-induced anchorage independent growth of breast epithelial cells.....	41
Figure 7. DIRAS family members inhibit Ras-induced transformation of NIH3T3 murine fibroblasts.....	42
Figure 8. DIRAS family N-termini inhibit Ras-induced transformation of NIH3T3 mouse fibroblasts.....	43
Figure 9. DIRAS3 interacts with K-Ras.....	44
Figure 10. DIRAS3 interacts with K-Ras at the plasma membrane.....	46
Figure 11. DIRAS3 binds to Ras at the A5-helical domain.....	47
Figure 12. DIRAS family members share similar binding domains on Ras.....	48
Figure 13. Some ovarian, pancreatic and lung cancer cell lines with activating Ras mutations are dependent upon Ras for survival.....	50
Figure 14. Re-expression of DIRAS3 inhibits Ras driven cancer viability.....	51
Figure 15. DIRAS3, but not Δ NT DIRAS3, inhibits long term clonogenic growth.....	52
Figure 16. DIRAS3 inhibits downstream Ras/MAPK signaling.....	53

Figure 17. Relative mRNA expression of DIRAS3 across a panel of pancreatic cancer cell lines and normal pancreas.....	54
Figure 18. Transient knockdown of DIRAS3 increases cell viability and p-ERK signaling of SU86.86 pancreatic cancer cells.....	55
Figure 19. DIRAS3, but not Δ NT DIRAS3, disrupts K-Ras clustering and downstream signaling.....	56
Figure 20. DIRAS1 and DIRAS2 reduce Ras multimerization.....	57
Figure 21. DIRAS3 inhibits GTP-bound Ras and subsequent Ras:Raf interaction.....	58
Figure 22. DIRAS3 N-terminus inhibits GTP-bound Ras and downstream signaling.....	59
Figure 23. Ras multimerization and signaling depend on GTP-bound Ras.....	60
Figure 24. DIRAS3 inhibits Sos-1 protein expression	61
Figure 25. Model of DIRAS3 inhibition of Ras clustering.....	62
Figure 26. DIRAS family members are conserved small GTPases with homology to Ras and Rap.....	65
Figure 27. DIRAS family members are differentially expressed across tissues.....	66
Figure 28. DIRAS family proteins are differentially expressed across multiple organs.....	67
Figure 29. DIRAS1 and DIRAS2 immunohistochemical staining of ovarian cancer tissue microarrays.....	68
Figure 30. DIRAS family expression is a predictor of survival for ovarian cancer patients.....	69
Figure 31. DIRAS family expression is downregulated in ovarian cancers and cancer cell lines.....	70

Figure 32. Re-expression of DIRAS1 or DIRAS2 inhibit long term ovarian cancer clonogenic growth.....	72
Figure 33. Re-expression of DIRAS1 or DIRAS2 inhibits short term cell viability.....	73
Figure 34. Re-expression of DIRAS1 and DIRAS2 inhibit growth of orthotopic ovarian cancer xenografts <i>in vivo</i>	74
Figure 35. Growth inhibition of ovarian cancer cells following re-expression of DIRAS family members is not due to apoptosis.....	75
Figure 36. Growth inhibition of ovarian cancer cells following re-expression of DIRAS family members is not due to cell cycle arrest.....	76
Figure 37. Growth inhibition of ovarian cancer cells following re-expression of DIRAS family members is not due to senescence.....	77
Figure 38. Re-expression of DIRAS family members induce autophagy.....	78
Figure 39. Re-expression of DIRAS family members induces autophagy in SKOv3 and HeyA8 ovarian cancer cells.....	79
Figure 40. DIRAS1 and DIRAS2 induced growth inhibition is dependent upon functional autophagy.....	81
Figure 41. DIRAS family members inhibit ovarian cancer cell migration.....	82
Figure 42. Cartoon documenting the nuclear localization and transcriptional activation of autophagy-related genes by FOXO3a and TFEB.....	84
Figure 43. Re-expression of DIRAS1 and DIRAS2 inhibit the PI3K and Ras/MAPK signaling pathways.....	85
Figure 44. Autophagy induction by DIRAS1 and DIRAS2 is dependent upon inhibition of AKT.....	86
Figure 45. Re-expression of DIRAS1 and DIRAS2 results in nuclear localization of FOXO3a and TFEB.....	87

Figure 46. Re-expression of DIRAS1 and DIRAS2 increases transcription of autophagy- related genes.....	88
Figure 47. Knockdown of FOXO3a and TFEB inhibits autophagy induced by re-expression of DIRAS1 and DIRAS2.....	89
Figure 48. DIRAS3 was lost in the murine genome following chromosomal rearrangement, but DIRAS1 and DIRAS2 are conserved across species.....	91
Figure 49. Transient expression of murine DIRAS1 or DIRAS2 inhibit murine ovarian cancer cell clonogenic growth.....	92
Figure 50. Transient expression of murine DIRAS1 or DIRAS2 induce autophagy in murine ovarian cancer cells.....	93
Figure 51. Transient expression of murine DIRAS1 or DIRAS2 show classical double membrane autophagosomes by electron microscopy.....	94
Figure 52. Murine DIRAS1 and DIRAS2 are required for starvation-induced autophagy.....	95
Figure 53. Homozygous deletion of DIRAS1 or DIRAS2 resulted in early embryonic lethality.....	97

LIST OF TABLES

Table 1.	Functions of DIRAS3 compared to Δ NT DIRAS3.....	7
Table 2.1	List of Reagents.....	19
Table 2.2	List of Antibodies.....	22

ABBREVIATIONS

12-mer	12-amino acid peptide
15-mer	15-amino acid peptide
$\Delta\Delta CT$	delta delta threshold cycle
ΔNT	N-terminal deletion
μg	micrograms
μL	microliter
μM	micromolar
AIC	Autophagosome initiation complex
AKT	protein kinase b
Annexin V	Annexin A5
ATG(s)	autophagy-related gene(s)
ATP	adenosine triphosphate
BECN1	beclin1
BCA	bicinchoninic acid
Bcl2	B cell lymphoma 2 protein
BF	bright field
BSA	bovine serum albumin
Caspase	cysteine aspartate-specific protease
Cisplatin	cis-diaminedichloroplatinum (II)
CLEAR	CLEAR-box sequence (5'-GTCACGTGAC-3')
CO ₂	carbon dioxide
CQ	chloroquine
CRISPR-Cas9	Clustered Regularly Interspaced Short Palindromic Repeats-Cas9

Ctrl	control
DAB	3,3'-Diaminobenzidine
DAPI	4',6-diamidino-2-phenylindole
DMEM	Dulbecco's modified eagle's medium
DNA	deoxyribonucleic acid
Dox	doxycycline
ECL	enhanced chemiluminescence
EDTA	ethylenediaminetetraacetic acid
EGF	epidermal growth factor
EM	electron microscopy
ER	endoplasmic reticulum
ERK	extracellular signal-regulated kinase
ERO	Experimental Radiation Oncology
FBS	fetal bovine serum
FITC	fluorescence isotiocyanate
G418	geneticin selective antibiotic
GAP	GTPase activating protein
GAPDH	human glyceraldehyde-3-phosphate dehydrogenase
GDI	guanosine nucleotide dissociation inhibitors
GDP	guanine diphosphate
GEF	guanine nucleotide exchange factor
GTP	guanine triphosphate
HCQ	hydroxychloroquine
H&E	hematoxylin and eosin

HEPES	4-(2-hydroxyethyl)-1-piperazineethanesulfonic acid
hr	hour
HRP	horseradish peroxidase
IACUC	Institutional Animal Care and Use Committee
IF	immunofluorescence
IGF	insulin-like growth factor
IgG	immunoglobulin G
IHC	immunohistochemistry
i.p.	intraperitoneal
IRB	Institutional Review Board
LAMP	lysosome-associated membrane protein
LC3	microtubule-associated protein light chain
LC3-PE	LC3-phosphatidylethanolamine complex
MEK	MAP-kinase-extracellular signal-regulated kinase
mg	milligram
MgCl ₂	magnesium chloride
mL	milliliter
mm	millimeter
mTOR	mammalian target of rapamycin
NaCl	sodium chloride
Na ₃ VO ₄	sodium orthovanadate
NCI	National Cancer Institute
ng	nanogram
nm	nanometer

P62/SQSTM1	sequestome1
PBS	phosphate buffered saline
PBS-T	phosphate buffered saline-tween
PCR	polymerase chain reaction
PE	phosphatidyl-ethanolamine
PFA	paraformaldehyde
pH	logarithmic measure of hydrogen ion concentration
PI	propidium iodide
PI3K	phosphatidyl inositol 3 kinase
PLA	proximity ligation assay
PMSF	phenylmethylsulfonyl fluoride
PPI	protein-protein interactions
PVDF	polyvinylidene fluoride
ReBiLc	recombinase-enhanced bimolecular luciferase complementation
RNA	ribonucleic acid
RNase	ribonuclease
rpm	revolutions per minute
RPMI-1640	Roswell Park Memorial Institute media
rt	room temperature
rt-PCR	real time polymerase chain reaction
SA- β -Gal	senescence associated β -Galactosidase
s.d.	standard deviation
SDS-PAGE	sodium dodecyl sulfate polyacrylamide gel electrophoresis
s.e.	standard error

siRNA	small interfering ribonucleic acid
shRNA	short-hairpin ribonucleic acid
SRB	sulforhodamine B
TBS-T	Tris buffered saline-tween
TCA	Trichloroacetic acid
TCGA	The Cancer Genome Atlas
Tris	tris(hydroxymethyl)aminomethane (HOCH ₂) ₃ CNH ₂
TSC1/2	tuberous sclerosis 1/2 protein
ULK1/2	uno-51-like kinase1/2
UVRAG	UV-radiation-resistance-associated
WB	western blot
WT	wild-type

CHAPTER 1

Introduction

Cancer is a disease driven by genetic alterations that control how cells function with regard to cell proliferation, programmed cell death, motility and metastasis. Throughout decades of research, our understanding of this complex disease has provided insight into the fundamental mechanisms of tumor development, the multistep process of tumor pathogenesis and dissemination, and the contributions of the tumor microenvironment which collectively enable tumor growth. These genetic alterations include mutations, deletions, and gene amplifications, which can arise from a number of stimuli including carcinogen exposure and errors during cell replication. Often these genetic alterations target tumor suppressor genes and proto-oncogenes.

Tumor Suppressor Genes. Tumor suppressors are generally regarded as genes that limit cell proliferation, induce cell death, repair DNA damage or prevent invasion and metastasis. As a counter balance to growth promoting genes, they provide key checkpoints to ensure replication occurs when DNA damage has been repaired or to activate programmed cell death when necessary. While there are many mechanisms by which tumor suppressor genes and their encoded proteins work, the one thing they all have in common is the ability to reduce the likelihood of neoplastic transformation. The first tumor suppressor gene, *Rb1* was identified by Benedict, Cavanee, Sparkes and colleagues studying a rare childhood eye tumor, retinoblastoma. (Benedict, Murphree et al. 1983, Cavanee, Dryja et al. 1983, Sparkes, Murphree et al. 1983) The observation that retinoblastomas could arise in a statistically viable model where inactivation of both alleles of *RB1* was required for oncogenesis, explaining the involvement of both eyes with inherited familial disease, but only one eye in sporadic cases provided the first direct evidence of genetic loss of tumor suppressors. (Knudson 1971) This was later referred to as the two-hit hypothesis, in which Knudson and colleagues document that two inactivating “hits” must occur in a tumor suppressor gene for the cancer to arise, since often times a single functional tumor suppressor gene can be sufficient to protect from cancer development without additional insults to DNA. One particularly well studied tumor suppressor gene is *TP53*, the second ever discovered and also known as the “guardian of the genome.” (Baker, Fearon et al.

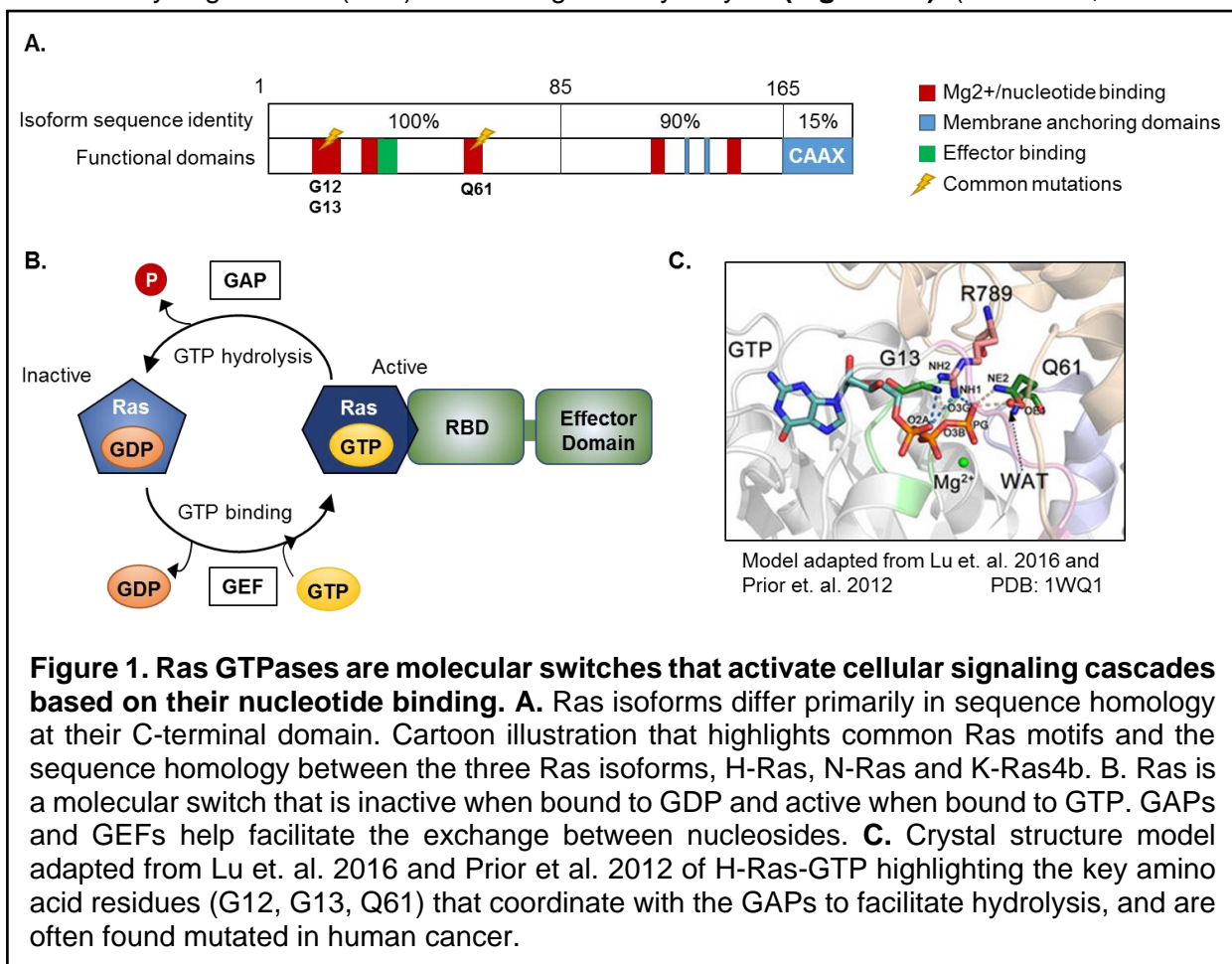
1989) P53 had a well-known role in cancer development for at least a decade before its true function was identified. It was documented that the p53 mutations which arose in transformed cells were identical to those seen in human cancer cases, suggesting that they were inactivating mutations likely working in a dominant-negative manner, and solidifying the role of p53 as a tumor suppressor. (Finlay, Hinds et al. 1989, Baker, Markowitz et al. 1990) Functionally, p53 uses several mechanisms to protect cells from uncontrolled proliferation, but best characterized is its role as a transcriptional activator. In a context dependent manner, p53 dictates whether a cell will undergo cycle arrest allowing for DNA repair, or trigger apoptotic cell death when stress signals and irreparable damage occur. (Kastan and Bartek 2004) Recent reports have also implicated a tumor suppressive role for p53 in response to oxidative stress, nutrient deprivation, hypoxia, and others by activating several intracellular pathways including senescence, autophagy, metabolism, and DNA repair. (Bieging and Attardi 2012) Whereas TP53 function is largely determined by intracellular sensors of stress and DNA damage from within the cell, RB halts cell proliferation from signals that are transduced from extracellular stimuli. (Hanahan and Weinberg 2011) Currently, there are four major mechanisms known by which tumor suppression occurs 1) cell cycle arrest and suppression of cell division, 2) induction of cell death cascades including apoptosis, 3) repairing DNA damage and 4) inhibiting metastasis. Despite the identification of more than 600 human tumor suppressor genes, thusfar none have been shown to bind directly to an oncogene and reverse its function.

Oncogenes. In addition to loss of tumor suppressor function, cancers may arise by activation of certain normal regulatory genes through one of the following 1) mutation, 2) overexpression of wild-type protein through gene amplification or 3) expression of a fusion protein produced by translocation to a gene under the influence of a strong promoter. Activated “oncogenes” drive persistent cell proliferation, enhance resistance to cell death, alter metabolism, and increase motility, invasion and metastasis. Evidence that viruses can cause cancer dates to the early 1900’s when Peyton Rous identified the first cell-free filtrate from a tumor homogenate that could

lead to new tumor development upon transplantation from one hen to another. (Rous 1910, Rous 1911) Discovery of the Rous sarcoma virus (RSV) opened the study of oncogenic retroviruses which were found to contain regulatory genes from mammalian cells. By the late 1970's, there was a growing consensus that cancer is a disease of genetically altered genes. Work by Weinberg, Cooper and colleagues demonstrated that chemically mutating the genome could result in transforming ability in the absence of any viral involvement, but the precise identity of the transforming gene remained elusive. (Shih, Shilo et al. 1979, Cooper and Neiman 1980) In 1982, the concept of cellular oncogenes were confirmed by cloning *Ras* from a rat sarcoma where a normal cellular signaling protein was activated by mutation, laying the groundwork for much of our modern understanding of cancer and the genetic aberrations that drive oncogenesis. (Der, Krontiris et al. 1982, Goldfarb, Shimizu et al. 1982, Parada, Tabin et al. 1982, Pulciani, Santos et al. 1982, Reddy, Reynolds et al. 1982, Santos, Tronick et al. 1982, Shih and Weinberg 1982, Tabin, Bradley et al. 1982, Taparowsky, Suard et al. 1982)

Ras Oncogenes. *Ras* has become one of the most intensively studied oncogenes, not only because it regulates normal cell functions, but also for its role in malignant transformation and cancer progression. Mutant *Ras* is associated with approximately 30% of all human cancers, including 95% of pancreatic cancers, 60% of low grade epithelial ovarian cancers and 35% of lung cancers. (Singer, Oldt et al. 2003, Prior, Lewis et al. 2012) *Ras* belongs to a class of proteins that hydrolyze GTP to GDP designated GTPases, which now include more than 150 family members. (Wennerberg, Rossman et al. 2005) Three distinct *Ras* genes encode four ~21 kDa proteins including H-*Ras*, N-*Ras*, K-*Ras4a* and K-*Ras4b* (**Figure 1A**). The conformational changes which occur in *Ras* proteins upon binding GTP or GDP serve as a switch that regulates signaling from cell surface receptors through several different cytoplasmic signaling cascades that influence proliferation, apoptosis, motility and metabolism. Small GTPases like *Ras*, contain a highly conserved domain composed of a six-stranded β -sheet surrounded by five α -helices

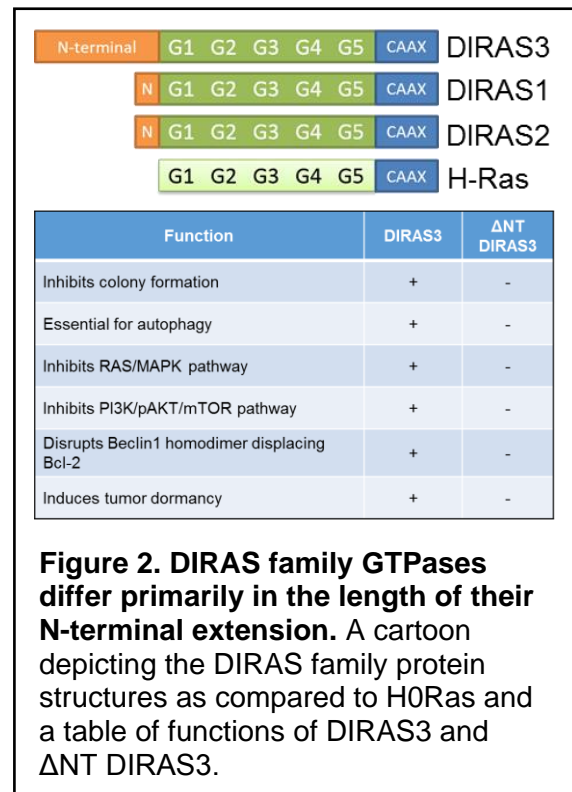
which contains the guanine nucleotide binding site. (Cherfils and Zeghouf 2013) This molecular switch depends not only on the intrinsic GTPase activity, but also on guanine nucleotide exchange factors (GEFs) that stimulate the exchange of GDP and GTP and GTPase-activating proteins (GAPs) that increase intrinsic GTP hydrolysis (**Figure 1B**). The GDP-bound form of Ras is often considered inactive, whereas the GTP-bound form of Ras undergoes a conformational change which facilitates binding of other downstream effector molecules leading to the activation of various signaling cascades. In the case of Ras, the four isoforms are not mutated with equal frequency, adding to the complexity of the isoform specific roles in oncogenesis. The somatic mutations that occur most frequently decrease GTPase activity, preserving GTP binding and locking the Ras protein into an 'on' state. Oncogenic substitutions at glycine 12 or 13 disrupt the van der Waals interaction between Ras and the associated GAP protein perturbs the orientation of the catalytic glutamine (Q61) attenuating GTP hydrolysis (**Figure 1C**). (Scheffzek, Ahmadian



et al. 1997, Prior, Lewis et al. 2012, Lu, Jang et al. 2016) Similarly, oncogenic point mutations of Q61 have been observed in human cancers, resulting in an uncoordinated water molecule which is critical to the nucleophilic attack of the γ -phosphate, once again decreasing GTPase activity and maintaining bound GTP. (Scheidig, Burmester et al. 1999, Buhrman, Holzapfel et al. 2010) GAP-catalyzed GTP hydrolysis of Ras is dependent upon the glutamine in this motif and while this is true of other small GTPases, it is not essential for all. These subtle changes in sequence homology and function allow for the separation of small GTPases into five major subgroups. Each subfamily has GEFs, GAPs, and for some guanosine nucleotide dissociation inhibitors (GDIs), which specifically associate with and modulate the major biological functions of each group resulting in sophisticated autoregulatory mechanisms which are still being elucidated. (Cherfils and Zeghouf 2013) Regulation of Ras by tumor suppressors has received much less attention. One goal of this dissertation is to elucidate the ability of the DIRAS family members to inhibit Ras-induced transformation of murine fibroblasts and human mammary epithelial cells as well as reveal how the interaction between DIRAS3 and Ras affects its binding to other well established proteins essential to the signaling cascade, such as Raf and Sos-1.

DIRAS Tumor Suppressor Genes. The Distinct subgroup of the Ras family (DIRAS) is a Ras-related group of three small GTPases including DIRAS1, DIRAS2 and DIRAS3. DIRAS family members have not been studied as extensively as the Ras proteins. In contrast to Ras, DIRAS3 has been functionally characterized as a tumor suppressor in ovarian cancer. DIRAS3 is a maternally imprinted gene that was found to be markedly downregulated in the majority of ovarian cancers when compared to normal ovarian epithelial cells. (Yu, Xu et al. 1999) Downregulation

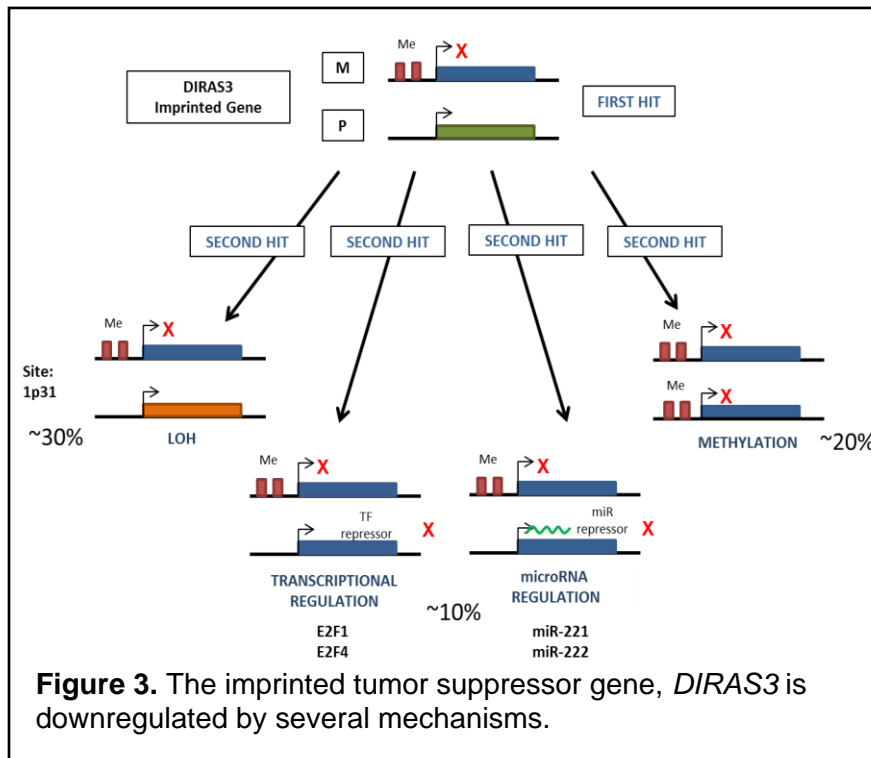
has been shown to be mediated by several different mechanisms described below. (Yu, Xu et al. 1999, Feng, Marquez et al. 2008) Sharing 50-60% homology to Ras and Rap, DIRAS3 is a ~26 kDa small GTPases which differs primarily in the addition of a 34-amino acid N-terminal extension, which is essential for most functions. (Luo, Fang et al. 2003) **(Figure 2)** Previous work from the Bast laboratory and others provided the molecular basis whereby DIRAS3 inhibits cell growth and motility, induces autophagy and establishes tumor dormancy. (Yu, Xu et al. 1999, Luo, Fang et al. 2003, Lu, Luo et al. 2008, Lu, Baquero et al. 2014, Lu, Yang et al. 2014) While many of the previously reported functions of DIRAS3 support its role in tumor suppression, classical experiments to



demonstrate this in knockout mouse models is not possible due to lack of *DIRAS3* in the murine genome. (Fitzgerald and Bateman 2004) Both mice and humans do, however, express *DIRAS1* and *DIRAS2*. DIRAS1 and DIRAS2 proteins share 30-40% overall amino acid homology with Ras and Rap and 50-60% homology with DIRAS3 where the only major difference is the truncation of the N-terminal extension from 34-amino acids to 4-amino acids. DIRAS1 and DIRAS2 are ~22 kDa proteins that have not been studied extensively. Only two reports have documented their impact on tumor progression. (Ellis, Vos et al. 2002, Zhu, Fu et al. 2013) Most recently, Bergom and colleagues described a tumor suppressive mechanism for DIRAS1, finding that its interaction with SmgGDS antagonizes the guanine nucleotide exchange factor and inhibits its binding to other small oncogenic GTPases. (Bergom, Hauser et al. 2016)

As an imprinted gene, DIRAS3 is expressed only from the paternal allele and expression is lost or silenced in ovarian cancer by several mechanisms including 1) loss of heterozygosity

(~60%), 2) transcriptional and miRNA regulation (~10%), or 3) hypermethylation of the paternal as well as the maternal allele (~30%). (Feng, Marquez et al. 2008) **(Figure 3)** In addition to



ovarian cancers, downregulation of *DIRAS3* has been demonstrated in carcinomas of the pancreas, lung, breast, thyroid, prostate and liver. (Weber, Aldred et al. 2005, Yu, Luo et al. 2006, Dalai, Missiaglia et al. 2007, Huang, Lin et al. 2009, Lin, Cui et al. 2011,

Wu, Liang et al. 2013) Previous work from the Bast laboratory and others, has demonstrated that re-expression of *DIRAS3* inhibits growth, slows motility and invasion, induces autophagy and establishes tumor dormancy.

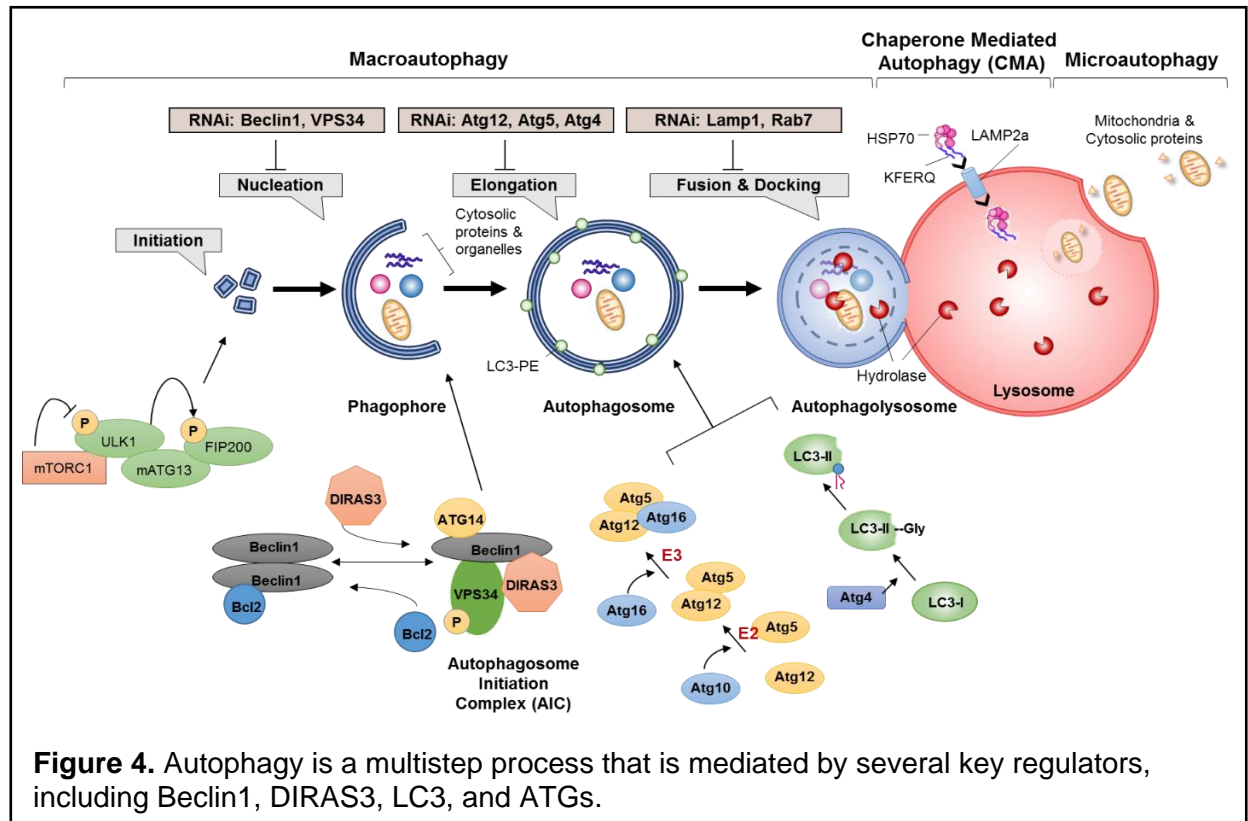
Much of this work has focused on the mechanisms by which *DIRAS3* plays an essential role in the induction of autophagy by 1) inhibiting the PI3K/AKT/mTOR signaling pathway, 2) participating in the autophagy initiation complex, 3) decorating autophagosomes, and 4) regulating the nuclear localization of FOXo3a, a master autophagy-related transcription factor. (Yu, Luo et al. 2006, Lu, Luo et al. 2008, Lu, Baquero et al. 2014, Lu, Yang et al. 2014) *DIRAS3*-induced autophagy can also sustain survival of dormant ovarian cancer xenografts, and disruption of autophagy with chloroquine, a functional inhibitor, significantly delayed outgrowth of tumors following downregulation of *DIRAS*. (Lu, Luo et al. 2008)

Autophagy. The process of autophagy, or cellular self-digestion, has been well characterized in both yeast and mammalian systems, documenting the dynamic process by which a cell can sequester and degrade cytosolic proteins and organelles, releasing amino acids and fatty acids to provide energy in nutrient poor conditions. (Cecconi and Levine 2008, Reggiori and Klionsky 2013) Unlike the ubiquitin-proteasome pathway, which targets individual short-lived proteins, autophagy functions as a bulk process capable of degrading the endoplasmic reticulum, mitochondria, peroxisomes, the nucleus and ribosomes. (Mizushima and Klionsky 2007, Stolz, Ernst et al. 2014) This tightly regulated catabolic process is more broadly classified into three types: macroautophagy, microautophagy and chaperone-mediated autophagy. In macroautophagy, cellular components are packaged in double-membrane vesicles that fuse with lysosomes, where acidification occurs and proteins and lipids are cleaved by hydrolases to release amino- and fatty acids. (Komatsu, Waguri et al. 2007) Microautophagy occurs when cytoplasmic content is directly engulfed by the lysosome following invagination of the lysosomal or endosomal membrane and then degraded by lysosomal proteases. (Li, Li et al. 2012) Chaperone-mediated autophagy (CMA) results in degradation of specific cargo that contains a pentapeptide motif 'KFERQ-like' which can be recognized by specific cytosolic chaperones and translocate the cargo directly to the lysosome via the lysosomal-associated membrane protein 2a (LAMP2A) without the formation of a membrane vesicle. (Cuervo and Wong 2014)

Macroautophagy, henceforth referred to as autophagy, is the best characterized of the three processes. A large body of work spanning several decades has provided detailed molecular mechanisms and insight into how this process occurs. The first of the autophagy-related genes (*ATG*) was discovered in yeast, and now some 30 autophagy-related proteins have been identified in yeast and in mammalian cells, of which about half are thought to be involved in the

highly conserved canonical autophagy shared by all organisms. (Lamb, Yoshimori et al. 2013)

Autophagy is characterized by six sequential steps; initiation, nucleation, elongation, maturation of the autophagosome, fusion and degradation. These steps begin with the sequestration of the cytoplasmic materials and end with lysosomal breakdown. (**Figure 4**)

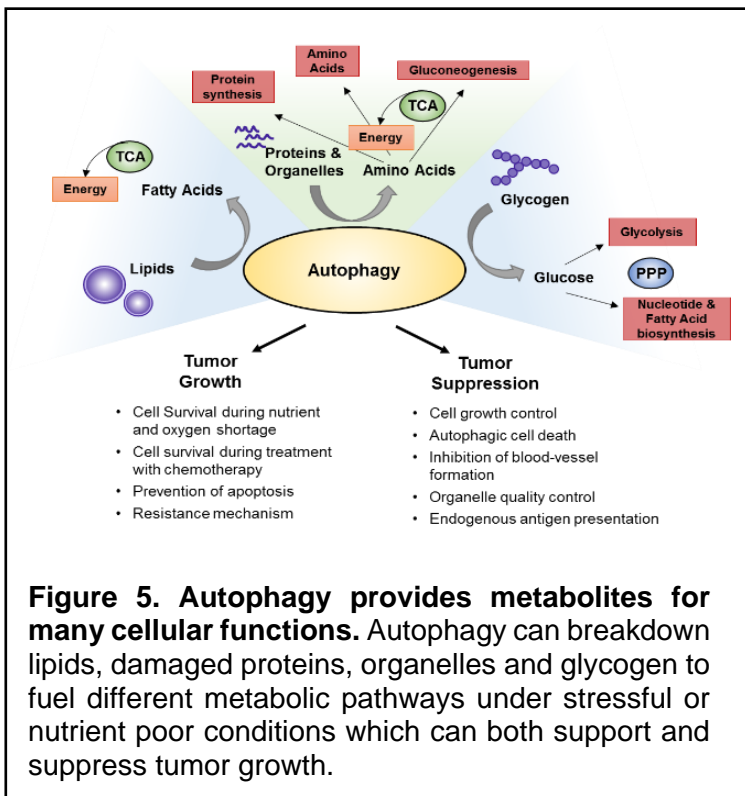


Biogenesis of autophagosomes is initiated by a phagophore assembly complex that contains ULK1/2, ATG13, FIP200 and ATG101 and is regulated by the UNC51-like kinase (ULK). Autophagy can be induced by several mechanisms, including downregulation of p-mTOR, which negatively regulates the ULK complex by interacting with and phosphorylating ULK1/2 and ATG13. (Vucicevic, Misirkic et al. 2011) Decreased p-mTOR levels result in dissociation of mTORC1 from the ULK complex resulting in partial dephosphorylation of p-ULK triggering localization of the phagophore and ULK1/2-mediated phosphorylation of ATG13, FIP200 and itself (ULK). (Glick, Barth et al. 2010) Further induction of autophagy requires the formation of an autophagosome initiation complex (AIC) which includes Beclin1 (BECN1), class III

phosphatidylinositol 3-kinase (PI3K), VPS34, p150, ATG14 and DIRAS3. (Hosokawa, Hara et al. 2009, Matsunaga, Saitoh et al. 2009, Lu, Baquero et al. 2014) In well fed cells, BECN1 dimers bind to Bcl-2 that prevents interaction with other components of the AIC. Following nutrient deprivation, DIRAS3 is upregulated and dissociates BECN1 dimers resulting in their dissociation from Bcl-2 (Lu, Baquero et al. 2014). Thus, permitting BECN1 monomer to bind with phosphatidylinositol 3-kinase catalytic subunit type 3 (PIK3C3) and VPS34. (Matsunaga, Saitoh et al. 2009) Subsequently, ATG14 associates with the AIC and directs it to a phagophore assembly site. (Itakura, Kishi et al. 2008, Sun, Fan et al. 2008, Matsunaga, Saitoh et al. 2009) Following nucleation, elongation of the autophagosomes occurs in a multistep ubiquitin-like conjugation process involving many of the ATGs and the LC3-PE complex. (Glick, Barth et al. 2010, Sridharan, Jain et al. 2011) The conversion of LC3 I to LC3 II is often used as a surrogate to document the elongation and formation of the autophagosome. (Klionsky, Abdelmohsen et al. 2016) Simultaneously, p62 binds and targets damaged proteins and organelles for degradation in the autophagolysosome and its decreased expression is associated with increased autophagic flux. (Klionsky, Abdelmohsen et al. 2016) DIRAS3 also decorates the autophagosomes and can be cross-linked to LC3-II. With its cargo engulfed, the autophagosome docks and fuses with the lysosome which was discovered in 1955 by de Duve and colleagues, forming the autophagolysosome, where degradation and recycling of amino and fatty acids provides energy in the form of ATP for nutrient-deprived cells.

Role of Autophagy in Normal Tissues and in Cancer. Some tissues like the heart, muscle, brain and liver are more dependent on autophagy to manage the buildup of damaged proteins and mitochondria. (Mizushima and Komatsu 2011) As a method to maintain cellular integrity, autophagy can mitigate ER stress and provide essential nutrients for yeast and mammals to survive starvation by recycling components into metabolic pathways. (Hoyer-Hansen and Jaattela 2007, Rabinowitz and White 2010) By breaking down lipids into fatty acids, autophagy provides catabolites for the TCA cycle resulting in ATP production. Likewise, the

breakdown of damaged proteins and organelles provides amino acids for protein synthesis and also fuels the TCA cycle, also resulting in ATP production. Autophagy can also generate glucose from glycogen resulting in nucleotide and fatty acid biosynthesis from the pentose phosphate pathway (PPP). (Kaur and Debnath 2015) **(Figure 5)** Autophagy deficiency is speculated to contribute to the pathogenicity of several diseases including neurodegenerative diseases, liver disease and aging. (Levine and Kroemer 2008) In cancer, the role of autophagy remains more ambiguous as some reports document a clear tumor suppressive phenotype during oncogenesis while others suggest the role of autophagy can promote oncogenesis by sustaining fully transformed nutrient-deprived cancer cells. (Cecconi and Levine 2008, White 2015) Likely, these phenotypes are dependent upon the context in which autophagy operates. Clinical trials have



been undertaken with hydroxychloroquine, a strongly basic lipophilic drug that penetrates autophagolysosomal membranes and decreases the acidification of their contents, preventing hydrolysis of proteins and lipids, functionally inhibiting autophagy. Promising studies which demonstrated antitumor activity and improved clinical outcomes have been ongoing for several disease sites

including melanoma, myeloma, colorectal cancer and renal cell carcinoma. (Mahalingam, Mita et al. 2014, Rangwala, Chang et al. 2014, Rangwala, Leone et al. 2014, Rosenfeld, Ye et al. 2014, Vogl, Stadtmayer et al. 2014, Patel, Hurez et al. 2016) In ovarian cancer, autophagy has been shown to play a critical role in the survival of dormant disease.

Ovarian Cancer. Clinically, epithelial ovarian cancers arise from flattened mesothelial cells that cover the surface of the ovary, from similar cells that line cysts immediately beneath the ovarian surface or from the cells that cover the fimbriae of the fallopian tube. (Crum, Drapkin et al. 2007) Like other solid tumors, ovarian cancers can metastasize through the blood or lymph, but most frequently metastasize across the abdominal cavity forming multiple tumor nodules on the parietal and visceral peritoneum.

Ovarian cancer is classified into two subgroups, type I and type II. Type I ovarian cancer refers to low grade cancers which typically grow slower and are diagnosed at an early stage (I-II). Low grade ovarian cancers are generally characterized by their stable genome, often being driven by activating mutations in Ras (60%) or PI3K signaling pathways and stimulation by insulin-like growth factor (IGF). Low grade cancers are also characteristically resistant to conventional chemotherapies. Type II ovarian cancers are high grade cancers which are more aggressive and often diagnosed in at late stage (III-IV). High grade serous ovarian cancer is the most common type of ovarian cancer and makes up the majority of Type II cancers, which are characterized by genomic instability, amplification of PIK3CA and AKT, and mutations in TP53 (>97%) and BRCA1/2 (15% germ line and 5% somatic). When high grade serous ovarian cancer is diagnosed early (where the disease is still confined to the ovary) more than 90% of patients can be cured with currently available therapy, including cytoreductive surgery and chemotherapy with a combination of carboplatin and paclitaxel. When the disease has disseminated, the long term survival drops drastically to ~30%. (Aletti, Dowdy et al. 2007, Espey, Wu et al. 2007, Ashworth, Balkwill et al. 2008) Treatment with six cycles of paclitaxel and carboplatin will produce a response in 70% of patients, but less than 30% will remain free from recurrence. While median survival now extends to 4-5 years with optimal and aggressive care, the fraction of women cured remains less than 30% and this has not changed over the last three decades. (Sutton 2014)

Autophagy in Human Ovarian Cancer. Previously, “second-look” operations were performed after primary surgery and chemotherapy to detect residual disease on the peritoneal cavity, but

due to lack of available treatment options for “positive second-looks” these operations have since been abandoned, but are now being reinstituted. These small deposits of disease were often found in small, poorly vascularized fibrotic nodules on the surface of the peritoneum, and analysis of these tumors revealed high expression of DIRAS3 and correlated with LC3 punctate and Beclin1 expression in >80% of cases, which are characteristic features of autophagic cells. (Lu, Baquero et al. 2014) In this setting, ovarian cancer cells are likely to be hypoxic and nutrient deprived where autophagy can have a positive impact to supply nutrients and maintain tumor dormancy. Efforts to modulate this balance are currently being explored in the Bast laboratory.

Autophagy in Murine Cells. In addition to the role in cancer, autophagy plays a critical role during embryogenesis and postnatal development, as determined by the developmental phenotypes resulting from genetically engineered mouse models with deficits in key autophagy related genes. (Cecconi and Levine 2008) Despite the absence of DIRAS3, which was lost during the evolution of mice, but retained in humans, pigs and cows, during a telomeric chromosomal re-arrangement that occurred ~60 million years ago, murine cells still have the ability to undergo autophagy. (Fitzgerald and Bateman 2004, An, Zhao et al. 2012, Shin, Lim et al. 2012, Kang, Louboutin et al. 2013) Both mice and humans express the two homologous DIRAS family members, DIRAS1 and DIRAS2. This dissertation addresses the role of DIRAS1 and DIRAS2 in regulating growth and survival of ovarian cancers, and more importantly, explores whether these GTPases serve as surrogates to DIRAS3 in the murine genome, playing an essential role in autophagy.

Aims and Hypotheses of the Study. The first goal of this study was to identify the structural features of DIRAS3 that are required to block mutant H-Ras- and K-Ras-driven malignant transformation of murine 3T3 cells and of partially transformed MCF10a breast epithelial cells. Experiments described in Chapter 3 demonstrate that DIRAS1, DIRAS2 and DIRAS3 inhibit H-Ras- and K-Ras-induced transformation in both cell types and DIRAS1, DIRAS2 and DIRAS3 are natural antagonists of Ras/MAPK signaling. These studies tested the hypothesis that

inhibition of malignant transformation is due to a direct interaction of DIRAS3 with Ras and that, in addition to binding, the N-terminus and CAAX-membrane anchoring domains of DIRAS3 are required. Chapter 4 explores the mechanism by which DIRAS3 inhibits growth of Ras-driven cancers and diminishes downstream ERK signaling. We tested the hypothesis that *DIRAS3 inhibits Ras activity by binding directly to Ras and disrupting Ras multimerization and clustering. DIRAS1 and DIRAS2 also inhibit Ras multimerization.* These observations provide the first example of direct interaction of a tumor suppressor with the oncogene that it suppresses and, moreover, identify the first endogenous protein to disrupt Ras clustering and activity. In addition to exploring the functional significance of DIRAS3 structure, this work holds translational promise. Peptides or small molecules that mimic *DIRAS3* activity could target the function of mutant Ras directly and specifically, filling a significant unmet clinical need to target mutant Ras in multiple types of cancer.

A second aim was to define the role of DIRAS1 and DIRAS2 in regulating proliferation, survival and migration of human ovarian cancer cells. In Chapter 5, expression of DIRAS1 and DIRAS2 was measured in multiple tissues and organs, and downregulation of DIRAS1 and DIRAS2 was documented for the first time. In chapter 6, we tested the hypothesis that *re-expression of DIRAS1 or DIRAS2 will inhibit proliferation and survival by inducing autophagic programmed cell death, but not by apoptosis, cell cycle arrest or senescence.* The ability of DIRAS1 and DIRAS2 to inhibit growth of ovarian cancer cell growth was documented in cell-based assays and in experimental xenograft models. We also determined that DIRAS1 and DIRAS2 inhibit cell motility. Collectively, these data build a case for the role of DIRAS1 and DIRAS2 as tumor suppressors.

A third goal was to determine the role of DIRAS1 and DIRAS2 in regulating autophagy in both human and murine cancer cells. In human cancer cells, re-expression of DIRAS3 induces autophagy and is required for the induction of autophagy. *DIRAS3* has been lost from the murine genome, but autophagy is still observed in mice. We tested the hypothesis that *DIRAS1 and*

DIRAS2 serve as surrogates for DIRAS3 and promote autophagy in mice. To examine the mechanism(s) by which DIRAS1 or DIRAS2 induce autophagy, we tested whether re-expression of DIRAS1 or DIRAS2 inhibit key signaling pathways resulting in transcriptional upregulation of autophagy-related genes. Re-expression of DIRAS1 or DIRAS2 decreased signaling through Ras/MAP and PI3K and increased nuclear localization of FOXo3a and TFEB as described in Chapter 7. In Chapter 8, murine DIRAS1 and DIRAS2 induced autophagy in murine ovarian cancer cells and knockdown of DIRAS1 and DIRAS2 blocked autophagy induced by amino acid starvation, supporting the possibility that DIRAS1 and DIRAS2 serve as surrogates for DIRAS3 in the murine genome. Homozygous knockout of DIRAS1 and DIRAS2 produced early embryonic lethality in mice, consistent with an important role for autophagy in normal embryonic development. In Chapter 9, these findings are discussed as are the future implications of this work.

CHAPTER 2

Materials and Methods

Cell Lines and Reagents. NIH3T3 Mouse fibroblast cells, AsPc-1, Capan-2, Panc-1, MiaPaca2, Su86.86 pancreatic cancer cells, H358 and H441 lung adenocarcinoma cells and SKOv3 ovarian cancer cells were obtained from the ATCC; MCF10a, OVCAR8 and Hey-A8 cells were provided by Dr. Gordon Mills, UT MD Anderson Cancer Center (Houston, TX); AsPc-1 cells were obtained from ATCC; TKOOV10, ID8, and IG10 cells were provided by Dr. Samuel Mok, UT MD Anderson Cancer Center; RCME-U2OS cell lines were generated and obtained from Dr. Geoffrey Wahl, The Salk Institute for Biological Studies (La Jolla, California); U2OS FK2 cells were obtained from Dr. Xiaolin Nan, Oregon Health and Science University (Portland, Oregon); TBR2 cells were obtained from Dr. Sandra Orsulic, Cedars-Sinai (Los Angeles, California) and all inducible sublines were generated in our laboratory.

NIH3T3 and **TBR2** cells were routinely grown in Dulbecco's modified minimal essential medium (Cellgrow, VA) supplemented with 2 mM L-glutamine, nonessential amino acids, 100 U of penicillin, 100 µg of streptomycin, 1% sodium pyruvate and 10% fetal bovine serum (FBS).

MCF10a cells were routinely grown in Dulbecco's modified minimal essential medium: nutrient mixture-F12 supplemented with 5% FBS, 20 ng/mL EGF (Peprotech), 0.5 mg/mL Hydrocortisone (Sigma H-0888), 100 ng/mL Cholera Toxin (Sigma C-8052), 10 µg/mL insulin (Sigma I-1882), and 100 U of penicillin, 100 µg of streptomycin.

AsPc-1, Panc-1, MiaPaca-2, H358, H441, TKOOV10, ID8, IG10, Hey-A8 and OVCAR8 cells were routinely grown in RPMI medium supplemented with 2 mM L-glutamine, nonessential amino acids, 100 U of penicillin, 100 µg of streptomycin and 10% FBS.

Capan2 and **SKOv3** cells were routinely grown in McCoy's 5A medium supplemented with 2 mM L-glutamine, nonessential amino acids, 100 U of penicillin, 100 µg of streptomycin and 10% FBS.

AsPc-1, Capan2, SKOv3, Hey-A8 and OVCAR8 inducible cell lines were maintained as previously specified using tetracycline free FBS (tet-FBS) and G418 to maintain clonal selections. DIRAS1, DIRAS2, or DIRAS3 expression was induced by adding 0.1 µg/mL doxycycline (Dox).

ReBiL-U2OS cell lines were routinely grown in Dulbecco's modified minimal essential medium: nutrient mixture-F12 supplemented with 10% tet- FBS, 400 µg/mL G418, 10 µg/mL ciprofloxacin, 5 ng/mL doxycycline, and 2-3 µg/mL blasticidin. Gene expression was induced by adding 0.01 µg/mL doxycycline (Dox).

U2OS FK2 cells were routinely grown in Dulbecco's modified minimal essential medium: nutrient mixture-F12 supplemented with 10% tet-FBS, 10 µg/mL ciprofloxacin. Gene expression was induced by adding 0.01 µg/mL doxycycline (Dox).

All cells were maintained at 37°C in a humidified atmosphere of 5% CO₂ and routinely checked for *Mycoplasma* contamination. Cell line fingerprinting was performed to confirm identity of each line.

OVCAR8-inducible Atg5^{-/-} cells and a corresponding double nickase control were generated by transfecting OVCAR8-DIRAS1 or OVCAR8-DIRAS2 ovarian cancer cells with Atg5 crispr plasmid or a control plasmid for 48 hours prior to sorting for GFP positive cells. A pooled population of sorted cells were expanded and then subjected to an enrichment sort to obtain the cells with the greatest GFP-signal.

Table 2.1 List of Reagents

Reagent Description	Company	Catalog	Lot Number
0.05% Trypsin-EDTA	Corning	25-052-CI	
0.25% Trypsin-EDTA	Corning	25-053-CI	
0.5 M EDTA	Gibco	15575-038	
1.0 M Tris HCl pH 7.0 (adjusted to 6.8)	TekNOVA	T1070	
1.5 M Tris HCl pH 8.8	TekNOVA	T1588	
10% SDS	Invitrogen	24730-020	
10X TAE Buffer	Ambion	AM 9869	
10X Tris Buffered Saline	RPI	T60075-4000.0	
10X Tris/Glycine Buffer	BioRad	161-0771	
10X Tris/Glycine/SDS Buffer	BioRad	161-0772	
20X TBS-Tween pH 7.4	USB	77500	

Reagent Description	Company	Catalog	Lot Number
2-mercaptoethanol	Sigma Aldrich	M6250-10ML	
30% Acrylamide	BioRad	161-0156	
4+ Biotinylated Goat anti-Mouse IgG	Biocare Medical	GM601H	111915
4+ Biotinylated Goat anti-Rabbit IgG	Biocare Medical	GR602H	71415
4+ Streptavidin HRP	Biocare Medical	HP604H	90315
488 Goat Anti-Mouse	Life Technologies	A11017	
488 Goat Anti-Rabbit	Life Technologies	A11008	
594 Goat Anti-Mouse	Life Technologies	A11020	
594 Goat Anti-Rabbit	Life Technologies	A11037	
5X siRNA Buffer	Thermo Scientific	B-002000-UB-1000	
Acetic Acid - Glacial	Fisher Scientific	BP 24015-212	
Agar	USB	1097 100GM	
All-In-One Mouse Tail Lysis	Allele Biotechnology	ABP-PP-MT01500	
Annexin V 488	Invitrogen	A 13201	
Annexin V-FITC Apoptosis Kit	Life Technologies	V13242	
Avidin	Biocare Medical	AB972H-A	62515
BCA Protein Assay	Thermo Scientific	23223, 23224	
Betazoid DAB Chromogen	Biocare Medical	BDB2004L	92016
Biotin	Biocare Medical	AB972H-B	20816
Bovine Serum Albumin	Sigma-Aldrich	A7906-500g	
Brilliant Blue	Sigma-Aldrich	B7920-50G	
BSA - Albumin Standard	Thermo Scientific	23209	
CAPS	Sigma-Aldrich	C2632-1KG	
Cat-Hematoxylin	Biocare Medical	CATHE-M	
Chamber slides - Regular 4 well/ 2 well	Labtek	154526/154461	
Chloroform	Mallinckrodt	4432	
Chloroquine	Sigma Aldrich	C6628-100.0	
Cholera Toxin (1mg/mL)	Sigma Aldrich	C-8052	
Ciprofloxacin	Chem-Impex	02884	
Coomassie (BioSafe)	BioRad	161-0786	
Dharmafect 1	Dharmacon	T-2001-03	
Dharmafect 4	Dharmacon	T-2004-03	
DMEM	Corning	15-17-CV	
DMEM/F12	Corning	10-090-CV	
Doxycycline (1mg/mL)	RPI	D43020-100.0	
D-Sucrose	Fisher Scientific	BP 220-10	
ECL Perkin Elmer	Perkin Elmer	NEL 104001	
EGF (100 µg/mL)	Peptotech	500-P45	
Ethanol 200 Proof	Decon Laboratory	2701	

Reagent Description	Company	Catalog	Lot Number
Fetal Bovine Serum	Sigma-Aldrich	F0926	15C487
G418	Thermo Scientific	11811031	6716010
Glycerol	Fisher Scientific	BP 229-1	
Hydrocortisone (1 mg/mL)	Sigma Aldrich	H-0888	
Insulin (10 mg/mL)	Sigma Aldrich	I1882	
iScript cDNA synthesis kit	BioRad	170-8897	
iTaq Universal SYBR Green PCR Mix	BioRad	172-5151	
LB Broth	Sigma-Aldrich	L-7275-500Tab	
L-Glutamine	Corning	25-005-CV	
McCoy's	Corning	10-050-CV	
Megatran 1.0	Origene	TT 200003	
Methanol	Fisher Scientific	BP 1105-4	
Mouse IgG	Santa Cruz	SC-2025	
Nuclear Fast Red	Sigma Aldrich	N3020-100 mL	
Nuclear/Cyto Extraction	Thermo Scientific	78835	
OPTIMEM	Gibco	31985-070	
Palbociclib PD: 0332991	Selleckchem	51116	07
PBS without Ca ²⁺ and Mg ²⁺	Corning	21-040-CV	
Penicillin/Streptomycin	Corning	30-002-CI	
PhosphoSTOP	Roche	04 906 837 001	
Protein A/G Magnetic Beads	Thermo Scientific	88803	
Puromycin (2.5 mg/mL)	Sigma Aldrich	P8833-1000	
QIA quick PCR Purification Kit	Qiagen	28106	
Rabbit IgG	Santa Cruz	SC-2027	
Ras Activation Assay	Cell Biolabs	STA-400-H/K/	
Restore Plus Stripping Buffer	Thermo Scientific	46430	
RPMI	Corning	15-040-CV	
SDS-PAGE Ladder "Page Ruler Plus"	Fisher Scientific	26619	
SDS-PAGE Ladder "Page Ruler"	Fisher Scientific	26616	
Senescence SA. β gal staining kit	Sigma-Aldrich	C50030-IKT	
Tag PCR Master Mix	Qiagen	201445	148027375
TEMED	BioRad	161-0801	
tet-FBS	Clontech	631106	A13020
Trichloroacetic Acid	RICCA	8693-16	
Trizol	Ambion	15596018	
Trypan Blue	Corning	25-900-CI	
Ultra-Pure Agarose	Invitrogen	15510-027	
Xylene	Fisher Scientific	X3P-1GAL	

Table 2.2 List of Antibodies

Antibody Description	Host	Company	Catalog	Dilution	Application
488 Goat Anti-Mouse	G	Life Technologies	A11017	1:250	IF
488 Goat Anti-Rabbit	G	Life Technologies		1:250	IF
594 Goat Anti-Mouse	G	Life Technologies	A11020	1:250	IF
594 Goat Anti-Rabbit	G	Life Technologies		1:250	IF
Actinin	R	CST	6487	1:5,000	WB
AKT	M	Santa Cruz	SC-514302	1:1000	WB
Anti-HA Tag	M	CST	2362	1:2000	WB, IP
Anti-HA Tag	M	Sigma	068K4806	1:3000	WB, IP
Atg 5	R	CST	26305	1:1000	WB
Atg 7	R	CST	85585	1:1000	WB
B-Actin	R	CST	4910L	1:10,000	WB
Beclin1	R	CST	3738S	1:1000	WB
Cleaved-Caspase3	R	Millipore	04-439	1:1000	WB
DIRAS1 #13A	M	Bast Laboratory	N/A	1:2000	WB, IF, IP
DIRAS1 #64	M	Bast Laboratory	N/A	1:3000 and 1:1000	WB, IHC, IF, IP
DIRAS2	M	Origene	TA 809398	1:15,000 and 1:10,000	WB, IHC, IF, IP
DIRAS3 15E11	M	Bast Laboratory	N/A	1:5000	WB
DIRAS3 1D8	M	Bast Laboratory	N/A	1:400 - 1:5000	WB, IHC, IF, IP
Flag M2	M	Sigma	F316S	1:3000	WB
FOX03a	R	CST	12829S	1:1000	WB, IF
Goat Anti-Mouse	G	Fisher Scientific	31439	1:10,000	WB
Goat Anti-Rabbit	G	Fisher Scientific	31463	1:10,000	WB
His-Tag	R	CST	2366	1:1000	WB
H-Ras	R	Cell Biolabs	240007	1:1000	WB
Kras	M	Sigma and Invitrogen	PAS-44339	1:1000	WB, IF
K-Ras Abcam	R	Abcam	172949	1:1000	WB, IF
LC3	R	CST	2775 S	1:1000	WB, IF
LC3 BXP	R	CST	3868S	1:700	IHC
mTOR	R	CST	2972	1:1000	WB

Antibody Description	Host	Company	Catalog	Dilution	Application
P62/WQSTM1	R	MBL	PM045	1:10,000	WB
Pan-Ras	M	Cell Biolabs	240002	1:1000	WB
PARP	M	Millipore	MAB3192	1:1,000	WB
Phospho-ERK	R	CST	43705	1:1000	WB
Phospho-mTOR	R	CST	2971	1:1000	WB
SOS-1 mAb	R	CST	12409S	1:1000	WB
TFEB	R	CST	4240S	1:500	WB, IF
α -Tubulin	R	CST	5335S	1:1,000	WB

Plasmids

pCMV-DIRAS3 Y2, pCMV- Δ NT DIRAS3, plasmids were constructed in our laboratory. pCMV-DIRAS1 and pCMV-DIRAS2 mouse and human plasmids were purchased from Origene. H-Ras plasmid was purchased from Clontech (631924) and site directed mutagenesis was used to create the H-Ras G12V plasmid in our laboratory. K-Ras, K-Ras G12V, NT-K-RasG12V, 4AA-K-RasG12V, 34-AAScramble-KRasG12V, and 4-AAScramble-K-RasG12V and the corresponding H-Ras constructs were custom synthesized by Blue Heron. DIRAS3 C226S and NT-H-RasG12V were constructed in our laboratory. Plasmids synthesized by Blue Heron were re-cloned into a pCMV promoter expression plasmid. Viral GFP-K-RasG12V was provided by Dr. John Hancock (McGovern Medical School UTHealth). ATG5^{-/-} CRISPR/Cas9 knockout plasmid was purchased from Santa Cruz Biotechnology sc-416847 and the control double nickase sc-437281. HA-tagged AKT-CA or AKT-DN plasmids (Myr-HA-AKT1-DD or Myr-HA-AKT1[AAA], respectively) were obtained from Dr. Gordon Mills (University of Texas MD Anderson Cancer Center).

Primers used for cloning include (5' \rightarrow 3'):

H-RasE153A	Forward	GTAGAAGGCATCCGCCACTCCCTGCCG
	Reverse	CGGCAGGGAGTGGCGGATGCCTTCTAC
H-RasY157A	Forward	CTCACGCACCAACGTGGCGAAGGCATCCTCCACT
	Reverse	AGTGGAGGATGCCTTCGCCACGTTGGTGCGTGAG

H-RasR161A	Forward	GTGCTGCCGGATCTCAGCCACCAACGTGTAGAAG
	Reverse	CTTCTACACGTTGGTGGCTGAGATCCGGCAGCAC

Purified Recombinant Protein

His-K-Ras (1-185) (ab96817), H-Ras (1-186) (ab93949), and H-RasG12V (2-186) (ab140571) were purchased from Abcam. Flag-K-Ras (1-188) and Flag-DIRAS2 (1-199) was purchased from Origene.

K-Ras (1-189), DIRAS3 (1-226) and DIRAS1 (1-189) were purified from BL21DE3 cells in our laboratory using a BioRad NGC Chromatography System.

Transformation Assay

Transformation of NIH3T3 cells was performed following standard protocols. (Clark, Cox et al. 1995) Low passage NIH3T3 cells were plated in 60 mm dishes at a density of $\sim 1.2 \times 10^6$ cells/plate. Transfection of single plasmids (20 μ g) or co-transfection of differing plasmids (10 μ g each) were completed 24 hours post seeding using MegaTran 1.0 (Origene) following manufacturers protocol. 24 hours post transfection, cells were trypsinized and plated onto 60 mm dishes at a ratio of 1:4 and kept in DMEM supplemented with dexamethasone (Sigma) or G418 to determine transfection efficiency for 14 days, with media changed every 3-4 days. Cells treated with DMEM supplemented with G418 media were stained by Coomassie blue and colonies were counted to ensure equal transfection efficiency. Those plates treated with DMEM supplemented with dexamethasone were examined microscopically for signs of contact-uninhibited growth and the appearance of morphologically transformed foci. Transformed foci were counted at 10x magnification as they appeared within two 10x10 mm areas per plate. The assay was performed three times with technical duplicates of each transfection group.

Anchorage Independent Growth

MCF10a cells were transfected with single or double DNA plasmids using MegaTran 1.0 according to the manufacturer's protocol. Twenty four hours following transfection, MCF10a cells were trypsinized and resuspended in RPMI containing 10% FBS and 0.35% noble agar, and plated on top of a layer of RPMI containing 10% FBS and 0.5% noble agar in a 35-mm dish. Media without epidermal growth factor (EGF) supplement was changed every 3 days and colonies were allowed to grow until they reached more than 50 cells/colony (~2-3 weeks). Colonies were visualized and quantified microscopically.

siRNA Transfection

Cells were transfected with control or DIRAS family siRNAs (single and pooled oligos) using the Transfection #1 or #4 reagent (Dharmacon Research, #T-2001-01, #T-2004-01). Briefly, a mixture of siRNA (100 nM final concentration) and transfection reagents were incubated for 20 minutes at room temperature. This mixture was then added to cells and allowed to incubate for 48-72 hours before cells were harvested for analysis.

Transient Transfection

Transient transfection was performed using MegaTran 1.0 (Origene, #TT200005) according to the manufacturer's protocol. For transfection of a 6-well plate, 3 μ g of DNA was combined with 9 μ L of transfection reagent in 250 μ L of OPTIMEM and allowed to incubate at room temperature for 10 minutes before being added to the cultured cells.

Cell Proliferation Assay

Cell proliferation was determined using clonogenic and sulforhodamine B (SRB) assays. Clonogenic assays were performed using inducible cell lines where 400-800 cells/well were cultured with or without Doxycycline for 72 hours, or following transient transfection and selection with G418. Cells were then allowed to grow in a clonogenic fashion for two weeks prior to staining and fixation with Coomassie blue. Clonogenic growth was quantified by manual analysis of

colonies containing at least 50 cells. SRB short-term viability assays were performed following siRNA knockdown or doxycycline induced expression. Cells were plated at specified cell densities and transfected with siRNA as described above, or treated with 0.1 µg/mL doxycycline. Seventy two hours following treatment cells were fixed with 30% TCA at 4°C for 1 hour, followed by washing. Cells were incubated with 0.4% SRB for 30 minutes at room temperature before being washed with 1% acetic acid. Tris base (pH=10.5) was used to solubilize the SRB dye prior to reading the plates with a microplate-reader (Tecan) at 510 nm.

Cell Migration Assay

SKOv3 and Hey-A8 ovarian cancer cells were seeded at 0.3×10^6 cells/well in a 6-well plates. Twenty-four hours later, cells were transfected with pLoc-DIRAS1, DIRAS2, or DIRAS3 DNA plasmids and an empty vector control. Twenty-four hours post transfection, cells were trypsinized and re-seeded at 1,000 cells/well into an Oris cell migration assay plate, which contained a mask as provided by the manufacturer to assess the basal migration towards the center of the well upon imaging. The cells were incubated for 24 hours to permit attachment to the outer annular region of the wells. The stopper, provided in the assay kit to create a circular area free from cellular attachment in the center of the well, was removed and the plates were assessed on an IN-Cell Analyzer HCA (GE Life Sciences). Re-assessment occurred every 4 hours for a period of 20 hours. Analysis was performed by quantifying the GFP-positive cells which had migrated to the center of the well at each time point. Experiments were performed in triplicate on three separate occasions.

Ras activity Raf-RBD Pull-down Assay

H-Ras and K-Ras specific activity assays were purchased from CellBioLabs (STA-400-K and STA-400-H) and performed following the manufacturer's protocol. NIH3T3 cells were plated in 100 mm dishes at ~80% confluence. Twenty-four hours post seeding, cells were

transfected with 10 µg of DNA using MegaTran 1.0 (Origene) following the manufacturer's protocol. 24 hours post transfection, cells were lysed as suggested following the CellBioLabs protocol and the assay was carried out according to the manufacturer's protocol.

Immunoprecipitation and Immunoblotting

Treated cells were incubated for 30 minutes on ice in lysis buffer (50 mM Hepes, pH 7.0, 150 mM NaCl, 1.5 mM MgCl₂, 1 mM EDTA, 10 mM NaF, 10 mM sodium pyrophosphate, 10% glycerol, 1% Triton X-100) plus protease and phosphatase inhibitors (1 mM PMSF, 10 µg/mL leupeptin, 10 µg/mL aprotinin and 1 mM Na₃VO₄) before being scraped and the lysate centrifuged at 17,000 x g for 20 minutes at 4°C. The protein concentration was assessed using a bicinchoninic acid (BCA) protein assay (ThermoScientific, Waltham, MA). Lysates (0.8-1.5 mg protein) were diluted with lysis buffer to a final volume of 1 mL. Immune complexes were incubated overnight with 2µg of the specified antibody or immunoglobulin control at 4°C with gentle agitation. Immune complexes were precipitated with protein A/G-magnetic beads for 1 hour, and washed three times with IP wash buffer for 5 minutes each wash followed by two washes in PBS for 5 minutes each wash. Immunoprecipitated proteins were separated by SDS-PAGE and transferred to PVDF membranes. Immunoblot analysis was performed with the indicated antibodies and visualized with an ECL enhanced chemiluminescence detection kit (GE Healthcare). Band intensity from western blots was quantified using the ImageJ program (Ferreira and Rasband, 2011).

Peptide Array Analysis

Peptide arrays were made using the MultiPep RS robot (Intavis, Bergisch Gladbach, Germany) according to the SPOT synthesis technique described by Frank *et al.* (Frank 2002). Arrays were developed by soaking membranes in 100% methanol for 10 minutes at room temperature followed by washing with PBS three times for 10 minutes each. Membranes were then blocked overnight at 4°C in 5% BSA/PBS. Recombinant proteins were added to the

membrane at a final concentration of 1 µg/mL in 1% BSA/PBS and shaken gently at room temperature for 2 hours. Membranes were washed three times for 10 minutes with 1% BSA/PBS prior to the addition of primary antibody diluted in wash buffer and incubation for 1 hour at room temperature. The membrane was washed 3x for 10 minutes and a diluted secondary antibody (1:10,000) was added for 45 minutes at room temperature, with gentle shaking. The membrane was washed 3x with wash buffer for 10 minutes, then followed with 3 washes with PBS-T for 10 minutes. Membranes were developed with HRP substrates and exposed to X-Ray film.

K-Ras4B Array (residues 1-189) 12-mer walk stepping by 3 amino acids.

H-Ras Array (residues 1-186) 12-mer walk stepping by 3 amino acids.

DIRAS3 Array (residues 1-229) 15-mer walk stepping by 3 amino acids.

ReBiL Analysis of Protein-Protein Interactions

Cells were seeded in 96-well or 384-well black wall, clear bottom plates and treated with doxycycline (1 µg/µL) to induce gene expression. 24-48 hours following gene expression the cells were washed briefly with 1X phosphate buffered saline (PBS) and luciferin was added. Plates were read for luciferase activity within 15 minutes using a Tecan plate reader. Each experiment was performed in triplicate on at least three separate occasions. Values for untreated cells were subtracted from the experimental values to reduce background.

DUOLINK in situ Assay

Duolink in situ PLA probes and Duolink in situ detection reagents were purchased from Sigma. K-Ras/DIRAS3 heterodimer formation was studied in Hey-A8-DIRAS3 ovarian cancer cells and AsPc-1-DIRAS3 pancreatic cancer cells. Procedures were performed following the manufacturer's instructions. Briefly, cells were seeded on chamber slides, fixed, blocked and incubated with primary antibodies and then with secondary antibodies conjugated with oligonucleotides (PLA probe MINUS and PLA probe PLUS). Finally, cells were incubated

sequentially with ligation solution and amplification solution followed by analysis with fluorescence microscopy.

Super-resolution fluorescence microscopy

The custom multispectral super-resolution microscope (MSSRM) for multicolor superresolution imaging was constructed as described elsewhere (Huang *et al.* submitted). Briefly, the MSSRM is housed on a Nikon Ti-U inverted microscope frame equipped with two lasers emitting at 405 and 638 nm, respectively, an oil immersion objective (60x, numerical aperture 1.49), and an EM-CCD (Andor iXon+). Signals from the sample was collected through the objective and split between a positional channel and a spectral channel to enable simultaneous imaging of multiple fluorophores without having to use emission filters. The MSSRM setup achieves ~10 nm spectral resolution and hence is able to distinguish single Alexa Fluor 647 and CF660C molecules reliably as previously demonstrated. MSSRM imaging of fluorescently stained cells was performed in PBS buffer supplemented with 1% beta-mercaptoethanol (β ME), 5 μ g/mL glucose oxidase (Sigma, G2133-50 kU), 0.4 μ g/mL catalase (Sigma, C100-50 MG), and 10% glucose (w/v, Fisher Chemicals D16-500). The EM-CCD was operated in the in frame transfer mode at 15 ms per frame with a gain setting of 300. Acquisition of raw images was performed using the open source micromanager software suite (<https://micromanager.org/>) (Edelstein, Amodaj *et al.* 2010). Image analyses for extracting single-molecule localization, spectra were all performed with custom MatLab (Mathworks, MA) scripts as described previously (Nickerson, Huang *et al.* 2014). Coordinates of single molecules were grouped based on their peak emission wavelength. Images in each channel were rendered separately and recombined in Fiji (<http://imagej.net/Fiji/>) (Schindelin, Arganda-Carreras *et al.* 2012) into a composite image.

EM Spatial Interaction and Cluster Analysis

Using methods previously reported by Hancock et. al. (Prior, Muncke et al. 2003, Prior, Parton et al. 2003, Plowman, Muncke et al. 2005) we assessed the co-localization of K-RasG12V and DIRAS3 on the plasma membrane of HeyA8 ovarian cancer cells. HeyA8-DIRAS3 inducible cells were seeded at 1.0×10^5 cells/well in a six well plate onto gold EM grids with pioloform and poly-L-lysine coating. Expression of DIRAS3 was achieved by adding doxycycline to the media for 24 hours. Lentiviral K-RasG12V was then used to infect both doxycycline negative and positive samples for 18 hours prior to harvesting the EM grids and adherent cells for analysis. Briefly, the basolateral membrane was exposed and fixed using 4% paraformaldehyde (PFA) and 0.1% glutaraldehyde (GA). For univariate experiments, 4.5-nm gold nanoparticles pre-coupled to GFP were used to immune-label GFP-Ras on the plasma membrane before embedding in uranyl acetate. Gold particle distribution was visualized by transmission electron microscopy (TEM) using JEOL JEM-1400 transmission EM. ImageJ was then used to assign x and y coordinates of gold particles in a $1\text{-}\mu\text{m}^2$ area on intact and featureless plasma membrane region. Ripley's *K*-Function was used to calculate the gold particle distribution and extent of nanoclustering. (Plowman, Muncke et al. 2005) Bi-variate analysis of co-localization was performed in a similar fashion where the basolateral membrane was exposed and fixed with 4% PFA and 0.1% GA before sequential labeling with 6-nm gold nanoparticles pre-coupled to GFP followed by 2-nm gold nanoparticles pre-coupled to DIRAS3 (antibody ID8). Membranes were embedded in uranyl acetate and then imaged. (Prior, Parton et al. 2003) At least 15 plasma membrane sheets were imaged, analyzed and pooled for each condition.

Measurement of mRNA expression

RNA from pooled ovarian scrapings and ovarian cancer cell lines was extracted using RNeasy kit (Qiagen, #217004). cDNA was synthesized from 1 μg of RNA using the Superscript II First Strand Synthesis Kit (Invitrogen, #11904-018). SYBR green based quantitative PCR was

used to measure RNA levels. Relative expression was calculated by the $2^{-\Delta\Delta CT}$ method using glyceraldehyde-3-phosphatase dehydrogenase (*GAPDH*) as the reference gene. The experiments were repeated at least three times, and samples were measured in triplicate.

Primers included (5' → 3'):

hDIRAS1	Forward 102	GTTCTTGCAGCTGGCAC
	Reverse 392	CTTGGAGATGGACAGGCG
hDIRAS2	Forward 48	CTCTGAGCGGAGTTGTGTTT
	Reverse 222	GATGTAGCTCTCCCGGAATG
hDIRAS3	Forward	GTACCTGCCGACCATTGAAAA
	Reverse	GGGTTTCCTTCTTGGTGAAGT
hSOS1 (Set 1)	Forward	GAGTGAATCTGCATGTCGGTT
	Reverse	CTCTCATGTTTGGCTCCTACAC
hSOS1 (Set 2)	Forward	ATGTATGTCGGCACTGGGTAG
	Reverse	GACCTGGTCCATTGTCTCTTG
mDIRAS1	Forward	TTGCTGGTCATGTGTAAGTCTG
	Reverse	AATTCTAAGTCACCCTCATCTGG
mDIRAS2	Forward	CGGCTGGATTTTGATTCTTGG
	Reverse	GATGGCTTAGAGAATGGTCGAG

OVCAR8-inducible cells were seeded in a 6-well plate at 1.5×10^5 cells/well, or following reverse transfection of siRNA at 1.0×10^5 cells/well. DIRAS1 or DIRAS2 expression was induced by adding DOX to the culture media for the indicated period of time. RNA was extracted with Trizol using the manufacturer's protocol, and cDNA was synthesized from 1 μ g of RNA using the Superscript II First Strand Synthesis Kit (Invitrogen, #11904-018). SYBR green based quantitative PCR was used to measure RNA levels. Relative expression was calculated by the $2^{-\Delta\Delta CT}$ method using glyceraldehyde-3-phosphatase dehydrogenase (*GAPDH*) as the reference

gene. The experiments were repeated at least three times, and samples were measured in duplicate on each occasion.

Primers included (5' → 3'):

ATG4	Forward	CAGACCCCGTTGGATACTG
	Reverse	TCTTCCTTTGTGTCCACCTC
ATG12	Forward	CTGCTGGCGACACCAAGAAA
	Reverse	CGTGTTGCTCTACTGCCC
ULK1	Forward	GGCAAGTTCGAGTTCTCCCG
	Reverse	CGACCTCCAAATCGTGCTTCT
LC3	Forward 356F	GAAGCAGCTTCCTGTTCTGG
	Reverse 588R	TCATCCCGAACGTCTCCTGG
Rab7	Forward F2	AGCTGACTTTCTGACCAAGG
	Reverse R2	TCGAGGTCAATCTTGTTT
Gabarap	Forward	AGAAGAGCATCCGTTGAGAA
	Reverse	CCAGGTCTCCTATCCGAGCTT
Beclin1	Forward	GAAGACAGAGCGATGGTAGTTC
	Reverse	CCTGGCGAGGAGTTTCAATAA
Bnip3	Forward	CAGGGCTCCTGGGTAGAACT
	Reverse	CTACTCCGTCCAGACTCATGC
Rab11a	Forward	GAAAGCAAGAGCACCATTGG
	Reverse	ATCTCTCAGTTCTTTCAGCC
LAMP1a	Forward 1280F	CAATTCCTACAAGTGCAACGC
	Reverse 1428R	GCATGCTGTTCTCGTCCA
GAPDH	Forward	ATGGAATCCATCACCATCTT
	Reverse	CGCCCCACTTGATTTTGG

qRT-PCR

Total RNA was extracted using Trizol reagent (Invitrogen) and 100 ng of RNA was reversely transcribed and SYBR green-based real-time PCR reactions were conducted in triplicate with a Real-Time PCR system (BioRad) using iTaq Universal SYBR Green 1-Step Kit (BioRad, Cat: 1725150). Human glyceraldehyde-3-phosphate dehydrogenase (GAPDH) served as an endogenous control and reference gene. Data were analyzed using the $2^{-\Delta\Delta CT}$ method.

Immunofluorescence Staining and Microscopy

Immunofluorescence staining was performed using two well chamber slides, fixed with 4% paraformaldehyde for 10 minutes prior to washing with PBS. Cells were permeabilized using 0.05% Triton X in PBS for 10 minutes at room temperature. Cells were washed 3x with PBS for 5 minutes each before being blocked with 0.5% BSA/PBS at room temperature for 1 hour. Primary antibodies were added at their specified dilution in 0.5% BSA/PBS and incubated overnight at 4°C. Cells were washed 3X with 0.5% BSA/PBS for 5 minutes each prior to the addition of secondary antibodies. Secondary antibodies were added at 1:250 dilution in 0.5% BSA/PBS and incubated at room temperature for 45 minutes. Cells were washed 3x with 0.5% BSA/PBS and DAPI staining at 1:10,000 dilution occurred at room temperature for 10 minutes. Slides were mounted, and imaged.

Immunofluorescence and bright field microscopy were performed on an Olympus lx71 microscope equipped with a DP72 camera (BF) and a XM10 camera (IF) (Olympus, Center Valley, PA). Confocal microscopy was performed on an Olympus FV1000 Laser Confocal Microscope.

Immunohistochemistry

Formalin-fixed, paraffin-embedded tissue microarrays were deparaffinized and rehydrated. Antigen retrieval was performed using a pressure cooker where the slides were

incubated in Tris-EDTA unmasking buffer for 10 minutes to retrieve latent epitopes, followed by sequential blocking steps with PeroxAbolish, avidin and biotin, and 5% BSA in PBS. The slides were incubated with a primary antibody or an isotype specific IgG control at the specified concentration listed above overnight at 4°C. The slides were washed and stained with a biotin-labeled 4plus anti-species specific secondary antibody for 30 minutes at room temperature followed by 4plus streptavidin horseradish peroxidase (HRP) for 10 minutes. The slides were developed using a DAB chromogen kit and then counterstain with hematoxylin. Staining reagents were purchased from Biocare Medical. For tumor tissue microarrays, the slides were read separately by two investigators. Cases in which <20% of the core contained tumor were excluded from the analysis.

Transmission Electron Microscopy

Cells were seeded in a 6-well plate and re-expression of DIRAS1, DIRAS2, and/or DIRAS3 was induced or transfected for a specified time period. After re-expression, samples were fixed with light Karnovsky's fixative solution containing 3% glutaraldehyde plus 2% paraformaldehyde in 0.1 M cacodylate buffer at pH 7.3 and stored at 4°C. After fixation, samples were submitted to the MD Anderson electron microscopy core facility for processing. Briefly, cells were washed in 0.1 M cacodylate buffer and treated with 0.1% Millipore-filtered buffered tannic acid, post fixed with 1% buffered osmium tetroxide for 30 minutes, and stained with 1% Millipore-filtered uranyl acetate. The samples were washed several time in water then dehydrated in increasing concentrations of ethanol, infiltrated, and embedded in LX-112 medium. The samples were polymerized in a 60°C oven for 2 days. Ultrathin sections were cut with a Leica Ultracut Microtome (Leica), stained with uranyl acetate and lead citrate in a Leica EM Stainer, and examined in a JEM 1010 transmission electron microscope (JEOL, USA, Inc.) at an accelerating voltage of 80 kV. Digital images were obtained using AMT Imaging System (Advanced Microscopy Techniques Corp).

AnnexinV and PI Staining for Apoptosis

Annexin V/PI staining was used to determine the percentage apoptotic cells following re-expression of DIRAS1 or DIRAS2 as indicated. Cells were washed with PBS and trypsinized before centrifugation at 1000 rpm for 5 minutes. Cells were re-suspended in binding buffer and incubated for 20 minutes with fluorescence isothiocyanate (FITC) conjugated annexin V and propidium iodide (PI). Cells were analyzed on Beckman Coulter Gallios™ flow cytometer. Experiments were conducted in triplicate and repeated at least three times.

Cell Cycle Analysis

The percentage of cells in different phases of the cell cycle was determined based on relative DNA content as determined by flow cytometry analysis. Inducible cells were treated with Doxycycline as indicated for the specific time to induce DIRAS1 or DIRAS2 expression. The cells were then detached by incubating with 0.05% trypsin-EDTA, washed with PBS and counted. Two million cells were fixed in 70% cold ethanol for 30 minutes. Cells were then pelleted by centrifugation at 1000 rpm for 5 minutes and washed in PBS two times. Cells were resuspended in PBS containing 1 µg/ml propidium iodide (PI) and RNaseA and incubated for 20 minutes at room temperature. Cells were analyzed on Beckman Coulter Gallios™ flow cytometer. Experiments were conducted in triplicate and repeated at least twice.

Senescence SA-βGal Staining

DIRAS1 and DIRAS2 inducible ovarian cancer cells were grown in 6-well plates at an initial density of 1.5×10^5 cells per well. After 72 hours incubation with DOX to induce DIRAS1 or DIRAS2 expression, cells were washed with PBS and fixed in 4% paraformaldehyde before staining with X-gal solution according to the manufacturer's instructions (Senescence Cell Histochemical Staining kit, Sigma-Aldrich #CS0030). After cells were incubated in the staining solution for 4-16 hours at 37°C, β-galactosidase positive cells with blue precipitate were counted

and analyzed using bright field microscopy. Treatment with 5 μ M Palbociclib (Selleckchem, #PD-0332991), a CDK4/6 inhibitor, was used as a positive control.

Ovarian Cancer Cell Lines and Tissue Samples

Twelve human ovarian cancer cell lines (CaOv3, DOV13, HEY, OC316, OVCA 420, OVCA 432, OVCA 433, OVCAR3, OVCAR5, OVCAR8, SKOv3ip, and HeyA8) and 5 pools of normal human ovarian surface epithelial scrapings were grown at 37°C in an atmosphere of 5% CO₂ and 95% air using the recommended cell culture medium for each cell line. Five pools of normal ovarian surface epithelium scrapings were obtained from the Division of Gynecologic Oncology at New York University using IRB approved protocols. All cancer and normal uterine specimens were snap frozen in liquid nitrogen and stored at -80°C. Normal ovarian epithelial scrapings were stored at -20°C in RNeasy® (Ambion, Foster City, CA). Protein and RNA extraction was performed as described elsewhere.

Autophagy modulation

Cells were treated as described and chloroquine (5 μ M) was added to inhibit lysosomal degradation for 18-24 hours prior to lysing the cells. To induce autophagy cells were rinsed briefly with PBS and the media was replaced with serum free media for 4-16 hours.

Tissue Microarrays

Ovarian cancer tissue microarrays (TMAs) were prepared by the Pathology Core Facility that supports the M.D. Anderson SPORE in Ovarian Cancer. The microarrays contained 148 distinct ovarian cancer specimens of which 122 were epithelial ovarian cancers where immunohistochemical staining could be interpreted. Protocols and informed consents to acquire and develop these arrays were approved by the respective Institutional Review Boards (IRB).

Mouse Xenografts and Measurement of Tumor Size

Five million DIRAS1-, DIRAS2-inducible cells and the parental SKOV3-IP and OVCAR8 cell lines were injected intraperitoneally into six-week old female athymic nu/nu mice were purchased from Taconic Biosciences. Each group contained 8-10 mice. 2 mg/mL DOX in 5% sucrose or sucrose alone water starting the day of injection, and supplemented every two days throughout the duration of the study. The tumor mass (g) was determined 4-6 weeks post injection after euthanizing mice with CO₂ and excising and pooling each intraperitoneal tumor nodule. All procedures were carried out according to an animal protocol approved by the IACUC of The University of Texas MD Anderson Cancer Center.

Generation of Knockout Mouse Models

Validated sgRNA constructs were purchased from SageLabs, and prepared at a desired concentration of 2.5 ng/μL and Cas9 at 5 ng/μL to a total volume of 600 μL. Pro-nuclear injection of C57Bl6 embryos was performed by the MD Anderson Genetically Engineered Mouse facility. Backcrosses were performed two times and germline transmission was confirmed by genotyping. Genotyping was performed by dissolving a 1-2 mm tail sample in All^{ele}-in-one tail direct lysis buffer (Allele Biotechnology, ABP-PP-MT01500) at 55°C overnight or until the tail was fully digested. Polymerase chain reaction (PCR) was performed on an optimized amount of direct lysis DNA (approximately 1:50 dilution) using Taq PCR Mastermix (Qiagen, #201443) and the following primers (5' → 3'):

DIRAS1 KO	Forward	TGCCAGAACAGAGCAATGAC
	Reverse	TCATCTTCGCTGAGGTTTCC
DIRAS2 KO	Forward	TACATCCCGACTGTGGAAGA
	Reverse	GGTTGAGGAGTTCCTGAAAGAG

PCR conditions were as follows: 94°C 5 min (1 cycle), 94°C 45 seconds followed by 55°C for 45 seconds followed by 72°C for 45 seconds (30 cycles), 72°C for 5 min (1 cycle). PCR product was

purified with QIAquick PCR Purification kit (Qiagen, #28104) and then sent for Sanger sequencing using the MD Anderson Sequencing Core facility.

Statistics

All experiments were repeated independently at least two times and the data (bar graphs) expressed as mean \pm s.d., unless noted otherwise. Statistical analysis was performed using Student's *t*-test (two-sample assuming unequal variances). Survival analysis was performed using the Kaplan-Meier method. The criterion for statistical significance was taken as $p < 0.05$ (two-sided).

CHAPTER 3

DIRAS family members inhibit Ras-driven transformation and interact directly with Ras.

Somatic mutation of proteins belonging to the rat sarcoma (Ras) family was the first genetic alteration documented to drive human oncogenesis. Oncogenic mutations in K-Ras, N-Ras, and H-Ras are found in nearly 30% of cancer cases, resulting in a constitutively active GTP-bound state. (Prior, Lewis et al. 2012) Active, GTP-loaded Ras recruits effector proteins which perpetuate the signaling cascade resulting in cell proliferation and survival. (Karnoub and Weinberg 2008) Of the three major isoforms, K-Ras which has two splice variants 4A and 4B, is most commonly affected in cancer and it is estimated that 90% of pancreatic adenocarcinomas and ~60% of low grade ovarian cancers are driven by K-Ras mutations. (Singer, Oldt et al. 2003, Prior, Lewis et al. 2012) Despite decades of research, targeting constitutively active Ras has remained elusive. Recent reports suggest the role of Ras dimerization in this process, however no natural inhibitors of Ras dimerization/multimerization have been reported to date. (Muratcioglu, Chavan et al. 2015, Nan, Tamguney et al. 2015) Previous studies document the requirement of the membrane-anchoring domain for Ras dimerization/multimerization. (Nan, Tamguney et al. 2015) However, the specific mechanism by which this occurs has not been fully elucidated.

DIRAS3 inhibits RasG12V-induced transformation of NIH3T3 murine fibroblasts and requires the N-terminal and CAAX domains of DIRAS3. Using a classical transformation assay to study the effects of mutant K-Ras on murine fibroblasts (NIH3T3), we observed that co-transfection of constitutively active (G12V) mutant Ras constructs with wild-type DIRAS family members resulted in significant ($p < 0.01$) inhibition of focus formation, compared to those co-transfected with an empty vector control. Previous studies from the Bast lab has demonstrated that the N-terminal extension of DIRAS3 which distinguishes it from other members of the Ras superfamily, is critical for its suppressor function. Co-transfection of mutant K-Ras constructs (**Figure 6A**) with the N-terminal deleted construct of DIRAS3 (Δ NT DIRAS3) produced a similar number of foci in NIH3T3 murine fibroblasts, as did co-transfection with an empty vector control, underlying the importance of the N-terminus in functional inhibition of Ras- induced

transformation. Additionally, a construct containing a single mutation in the CAAX membrane anchoring domain of DIRAS3 (C226S) was also unable to inhibit Ras transformation, demonstrating that localization of DIRAS3 to the membrane is important for functional inhibition of Ras. **(Figure 6B)**

DIRAS3 inhibits RasG12V-induced transformation of MCF10a partially transformed

breast epithelial cells

and also requires the

N-terminal and CAAX

domains of DIRAS3.

Importantly, the anti-

Ras role of DIRAS3

was confirmed using

MCF10a partially

transformed breast

epithelial cells.

Similarly, co-

transfection of different

DIRAS3 constructs with

mutant Ras (G12V)

significantly inhibit

($p < 0.01$) clonogenic

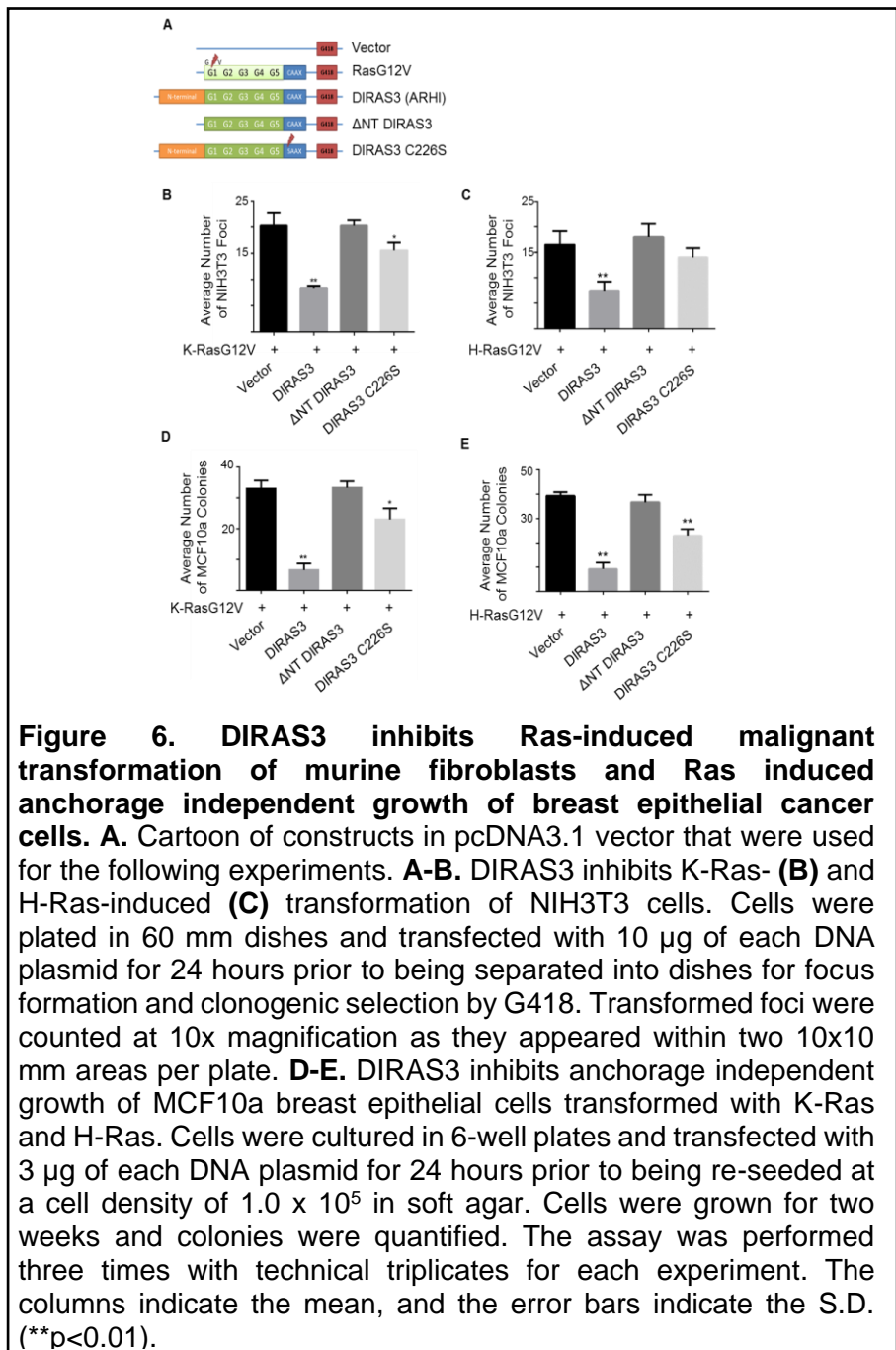
growth in soft agar

(Figure 10D) after 2

weeks following re-

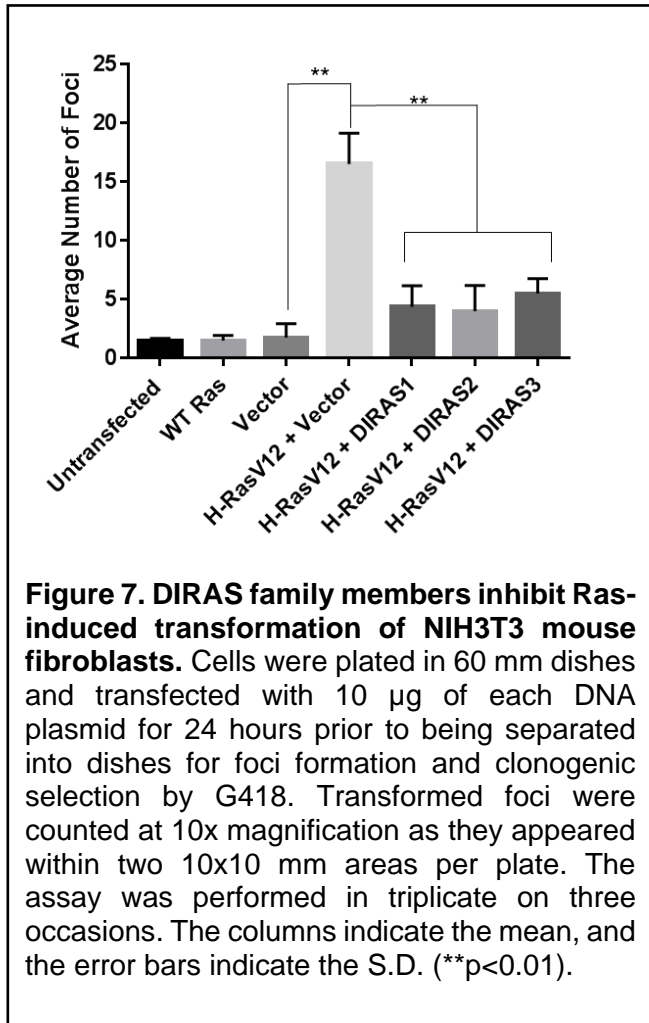
expression of DIRAS3,

but not Δ NT



DIRAS3 and less significantly C226S. Similar results were obtained for H-Ras (**Figure 6C and 6E**).

DIRAS1 and DIRAS2 inhibit H-RasG12V-induced transformation of NIH3T3 murine fibroblasts. DIRAS1 and DIRAS2 were also able to inhibit Ras-induced transformation of NIH3T3

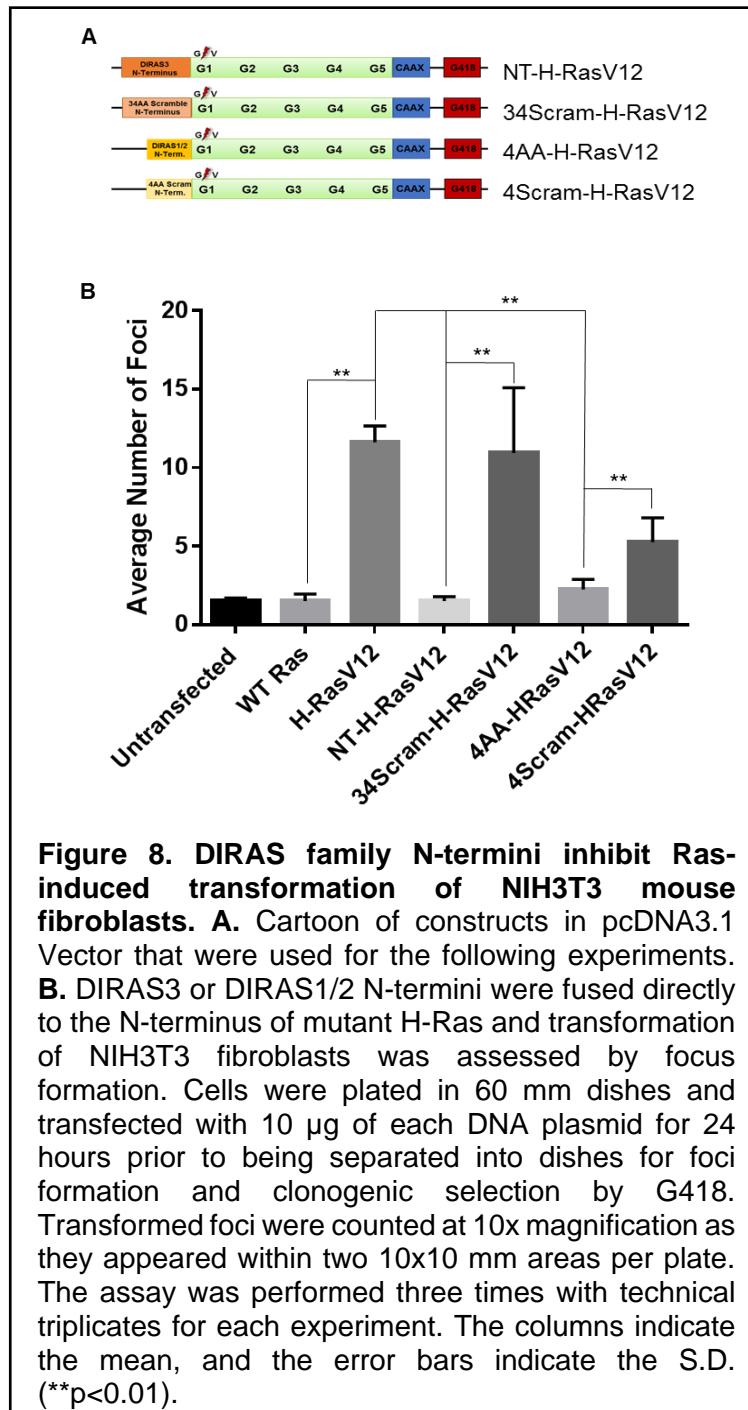


mouse fibroblasts (**Figure 7**), exhibiting activity similar to DIRAS3. Co-transfection of mutant H-RasG12V with an empty vector control increased foci formation ~5 fold compared to the empty vector alone, whereas co-transfection with the DIRAS family members inhibited the number of foci greater than 50%.

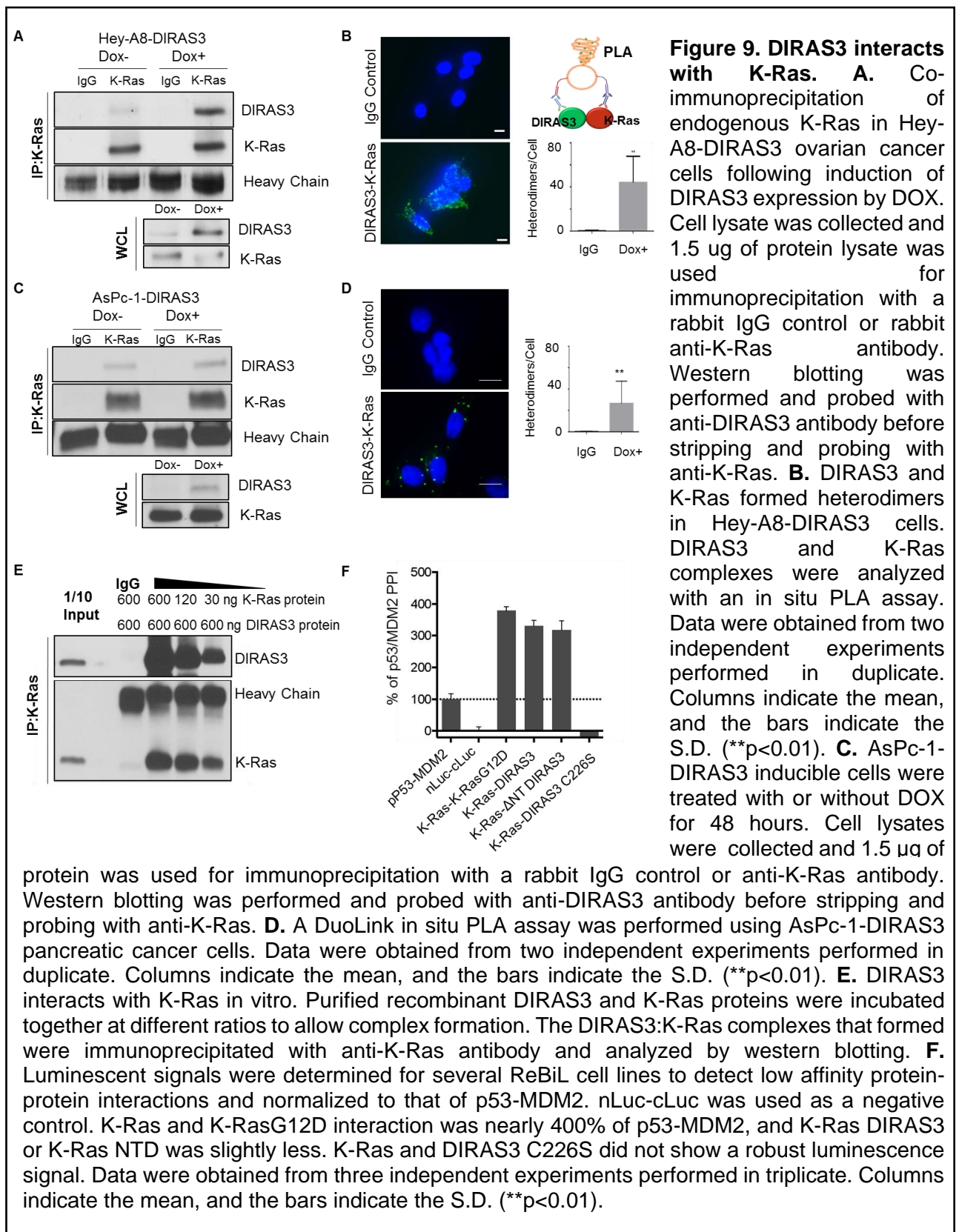
The N-terminal extensions of DIRAS1, 2, and 3 suppress the transforming activity of H-RasG12V. While DIRAS3 has a 34-amino acid N-terminal extension, DIRAS1 and DIRAS2 contain a 4-amino acid N-terminal extension. To assess the effect of the N-termini directly,

constructs were developed in which the N-terminal extension of DIRAS3 or DIRAS1/2 were fused directly to the N-terminus of mutant Ras. Compared to an empty vector control, or a 34- or 4-amino acid scrambled control, the N-termini of the DIRAS family members were able to suppress Ras driven transformation. (**Figure 8**)

DIRAS3 associates with K-Ras and requires the CAAX domain of DIRAS3. To delineate the role of DIRAS3 in Ras inhibition, we asked whether Ras associated with DIRAS3 as reported by Baljuls et. al.. (Baljuls, Beck et al. 2012) Using HeyA8-DIRAS3 ovarian cancer cell line, which harbors a K-Ras activating mutation and re-expression of DIRAS3 at near physiologic levels can be achieved by the addition of Doxycycline (DOX) in an inducible system, (Lu, Luo et al. 2008)



we performed immunoprecipitation and observed that DIRAS3 and K-Ras precipitated in the same complex (**Figure 9A**). Additionally, a DuoLink proximity ligation assay was performed, indicating close associates of DIRAS3 and K-Ras (**Figure 9C**). These results were confirmed using the AsPc-1-DIRAS3 pancreatic cancer cell line engineered to express DIRAS3 from a DOX-inducible promoter (**Figure 9B and Figure 9D**). Using purified recombinant protein, we observed a dose-dependent decrease in interaction between DIRAS3 and K-Ras, where the amount of DIRAS3 was held constant at 600 ng, and K-Ras was decreased from 600 ng to 30ng (**Figure 9E**). To quantify the



relative binding affinity of DIRAS3 to K-Ras, we created cell lines using the **Recombinase-enhanced BiL** system for detection of protein-protein interactions. (Li, Rodewald et al. 2014) U2OS, bone osteosarcoma cells with inducible expression of split luciferase complementing protein-protein interactions were generated. These lines included K-Ras-K-Ras, K-Ras-K-RasG12D, K-Ras-DIRAS3, K-Ras- ΔNT DIRAS3, and K-Ras-DIRAS3 C226S. Using p53-Mdm2 as a positive control, and nLuc-cLuc as a negative control, K-Ras-K-Ras and K-Ras-DIRAS3 interactions were approximately 3-fold that of p53-MDM2. I found that the interaction between K-Ras and DIRAS3 was not dependent upon the N-terminal extension of DIRAS3 as similar results to my immunoprecipitation studies were obtained using K-Ras- ΔNT DIRAS3; however, this interaction was dependent upon CAAX localization of DIRAS3 to the membrane as K-Ras-DIRAS3 C266S no longer showed a robust interaction as compared to the wild-type DIRAS3 construct (**Figure 9F**).

This membrane dependent co-localization was observed by confocal microscopy using the U2OS K-Ras-DIRAS3 cancer cells (**Figure 10A**). Additionally, stochastic optical reconstruction microscopy (STORM) imaging performed at total internal reflection (TIRF) confirmed the interaction between DIRAS3 and K-Ras on the membrane (**Figure 10B**). Using methods previously reported by Hancock et. al. (Prior, Muncke et al. 2003, Prior, Parton et al. 2003, Plowman, Muncke et al. 2005) we assessed the co-localization of K-RasG12V and DIRAS3 on the plasma membrane of Hey-A8-DIRAS3 ovarian cancer cells. Following infection of these cells with mGFP-K-RasG12V I harvested the plasma membrane and used anti-DIRAS3-2nm-gold particles and anti-GFP-6nm-gold particles to assess the clustering and spatial orientation of DIRAS3 and K-Ras. K-function analysis revealed a significant interaction between DIRAS3 and K-Ras on the plasma membrane (**Figure 10C-D**).

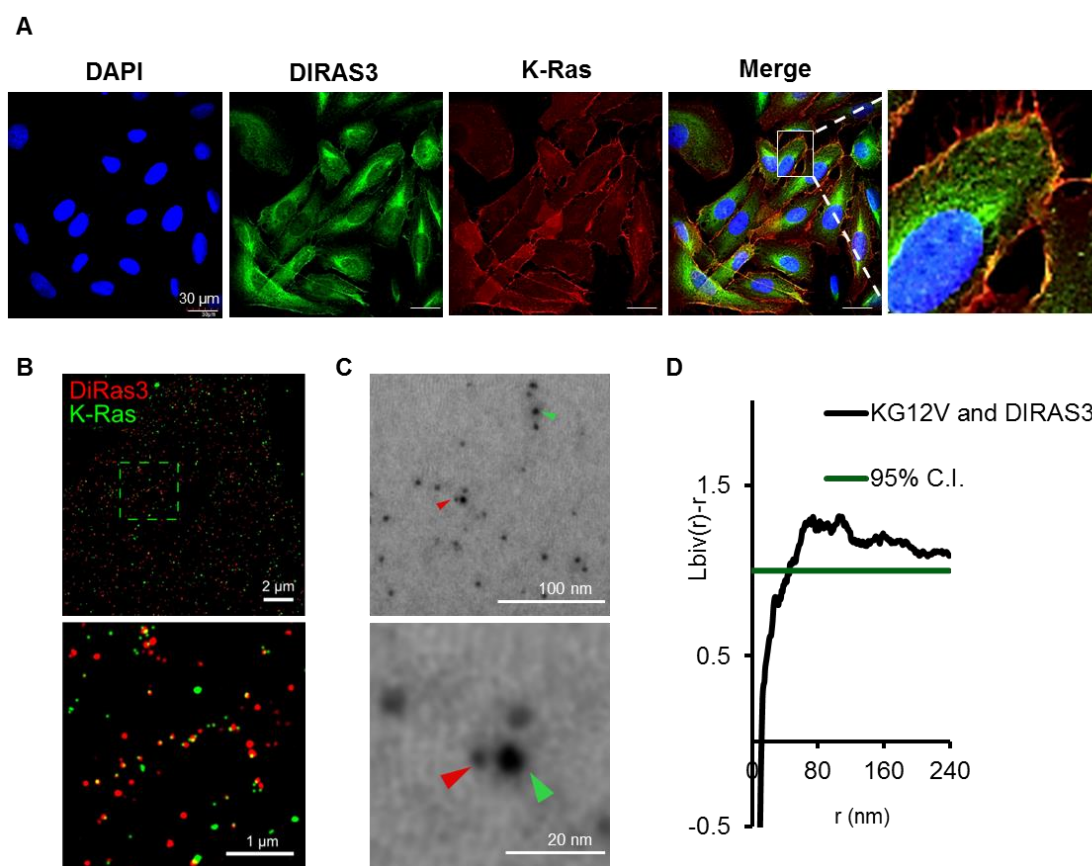
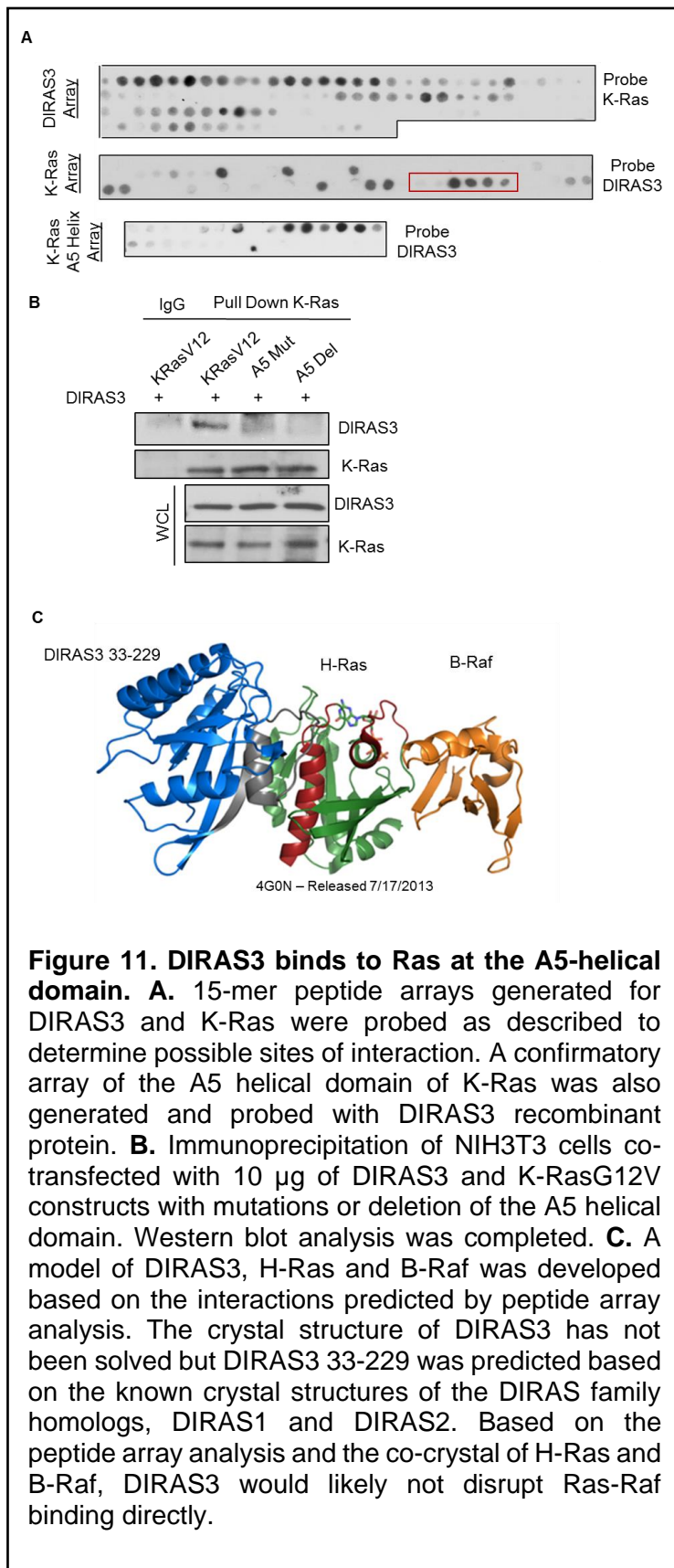


Figure 10. DIRAS3 interacts with K-Ras at the plasma membrane. **A.** DIRAS3 co-localized with K-Ras in U2OS-701 cells treated with DOX for 24 hours to induce K-RasG12D and DIRAS3 gene expression. Immunofluorescence staining of DIRAS3 and K-Ras was analyzed by confocal microscopy. Scale bars: 30 μm . **B.** U2OS TR2 cells were treated with DOX for 24 hours to induce K-Ras expression and simultaneously transfected with DIRAS3 pcDNA plasmid. STORM imaging at TIRF confirmed the interaction between DIRAS3 and K-Ras on the membrane. Scale bars: 2 μm and 1 μm for the higher magnification. DIRAS3 is labeled in red and K-Ras is labeled in green. **C.** TEM of DIRAS3- and K-Ras-labeled gold nanoparticles on the inner leaflet of the plasma membrane of Hey-A8-DIRAS3 ovarian cancer cells following induction of DIRAS3 by doxycycline for 24 hours. Scale bars: 100 nm and 20 nm for the higher magnification. DIRAS3 is labeled in red (2nm gold) and K-Ras is labeled in green (6nm gold). **D.** Bivariate K-function analysis of TEM documenting the extent of clustering and size of the clusters observed between K-Ras and DIRAS3 on the surface of the plasma membrane.

DIRAS3 binds to the A5 helical domain of H-Ras and K-Ras. To identify the specific regions necessary for K-Ras-DIRAS3 interaction, I used peptide arrays (15-mer polypeptide sequences that span the entire length of the protein shifting by 1-3 amino acids at each spot) which identified the A5 helical domain of both H- and K-Ras as the primary region of DIRAS3



binding (**Figure 11A**). This sequence was further confirmed using a single amino acid shift peptide array spanning from amino acids 151 to 171 (**Figure 11A**). To confirm this interaction site, K-RasG12V constructs harboring three point mutations (E153A, Y157A, and R161A) or deletion of the A5 helical domain (Δ 153-161) were used for immunoprecipitation. The interaction between DIRAS3 and K-RasG12V was interrupted with mutagenesis to the A5 helical domain (**Figure 11B**). Using crystal structures of H-Ras and BRaf released July 2013 (4G0N) (Fetics, Guterres et al. 2015), we were able to model the binding of DIRAS3 to Ras and Raf demonstrating that DIRAS3 does not interfere with the Raf binding domain based on the peptide array predictions and confirming the possibility that all three proteins could act in a single complex (**Figure 11C**). (Baljuls, Beck et al. 2012)

The binding pattern between full length DIRAS3 and Δ NT DIRAS3 were nearly identical for both H- and K-Ras (**Figure 12A**). Similarly, DIRAS1 and DIRAS2 also appear to bind to the C-terminus of K-Ras by peptide array analysis (**Figure 12B**). Interestingly, DIRAS2 has a more potent effect on growth inhibition and also has a larger extent of overlapping interaction with the A5 helical domain of K-Ras compared to DIRAS1. Using immunoprecipitation, I confirmed DIRAS1 and DIRAS2 are also found in the same complex as Ras (**Figure 12C-D**).

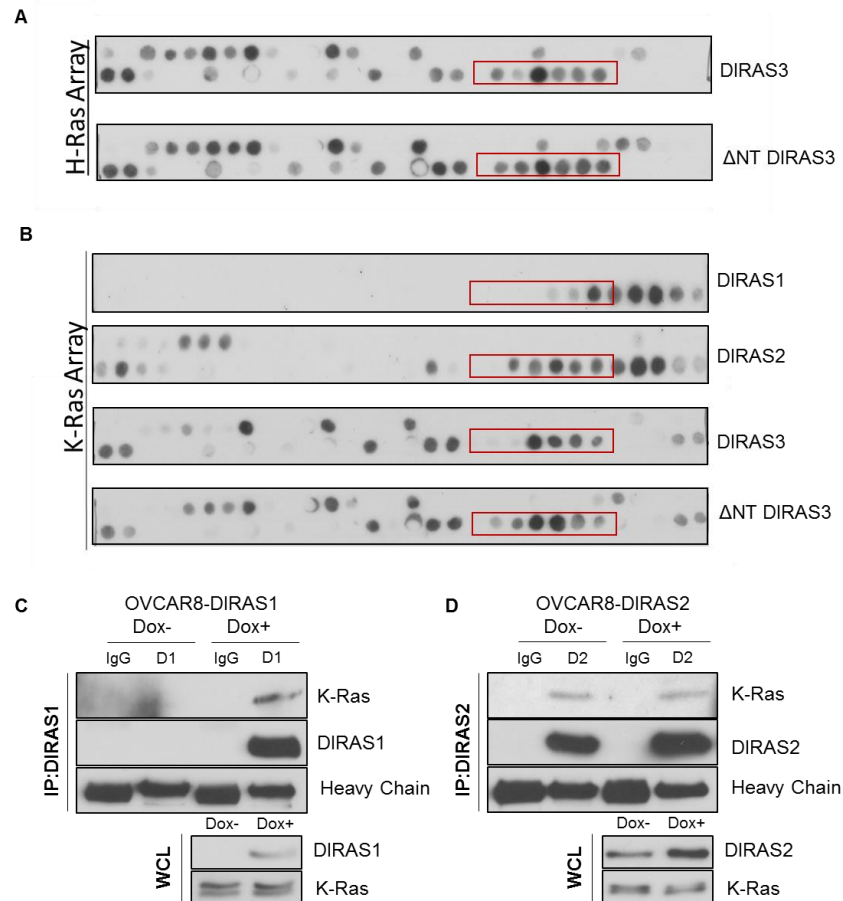
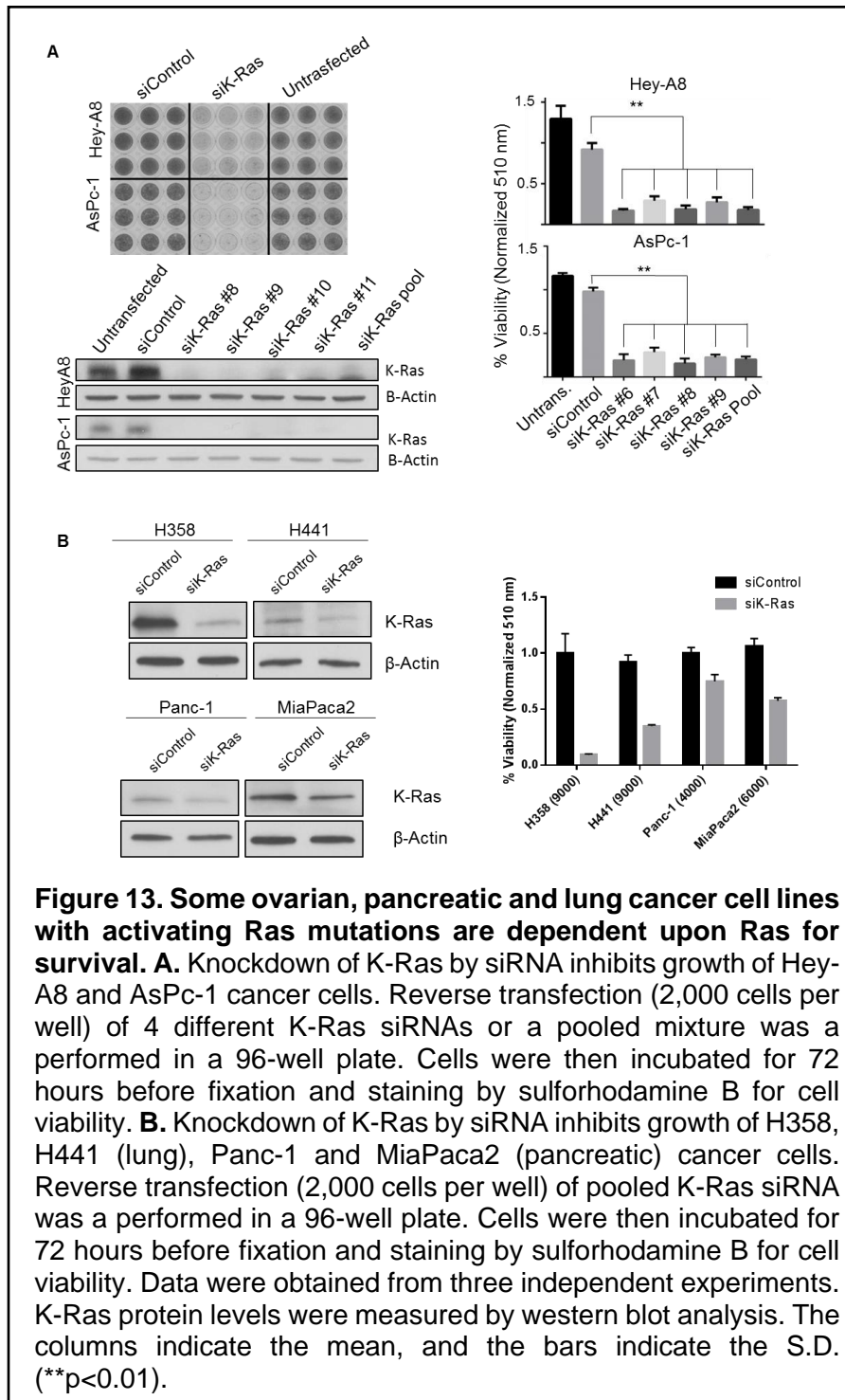


Figure 12. DIRAS family members share similar binding domains on Ras. **A.** 15-mer peptide arrays generated for H-Ras were probed with either full length DIRAS3 or Δ NT DIRAS3 as described to determine possible sites of interaction. **B.** 15-mer peptide arrays generated for K-Ras4b were probed with either full length DIRAS1, DIRAS2, DIRAS3 or Δ NT DIRAS3 as described to determine possible sites of interaction. The A5 helical domain is denoted by a red box. **C.** Co-immunoprecipitation of endogenous K-Ras in OVCAR8-DIRAS1 ovarian cancer cells following induction of DIRAS1 expression by doxycycline. Cell lysate was collected and 1.5 ug of lysate was used for immunoprecipitation with a mouse IgG control or anti-DIRAS1 antibody. Western blotting was performed and probed with anti-K-Ras antibody before stripping and probing with anti-DIRAS1. **D.** Co-immunoprecipitation of endogenous K-Ras in OVCAR8-DIRAS2 ovarian cancer cells following induction of DIRAS2 expression by DOX. Lysate was collected and probed as described above.

CHAPTER 4

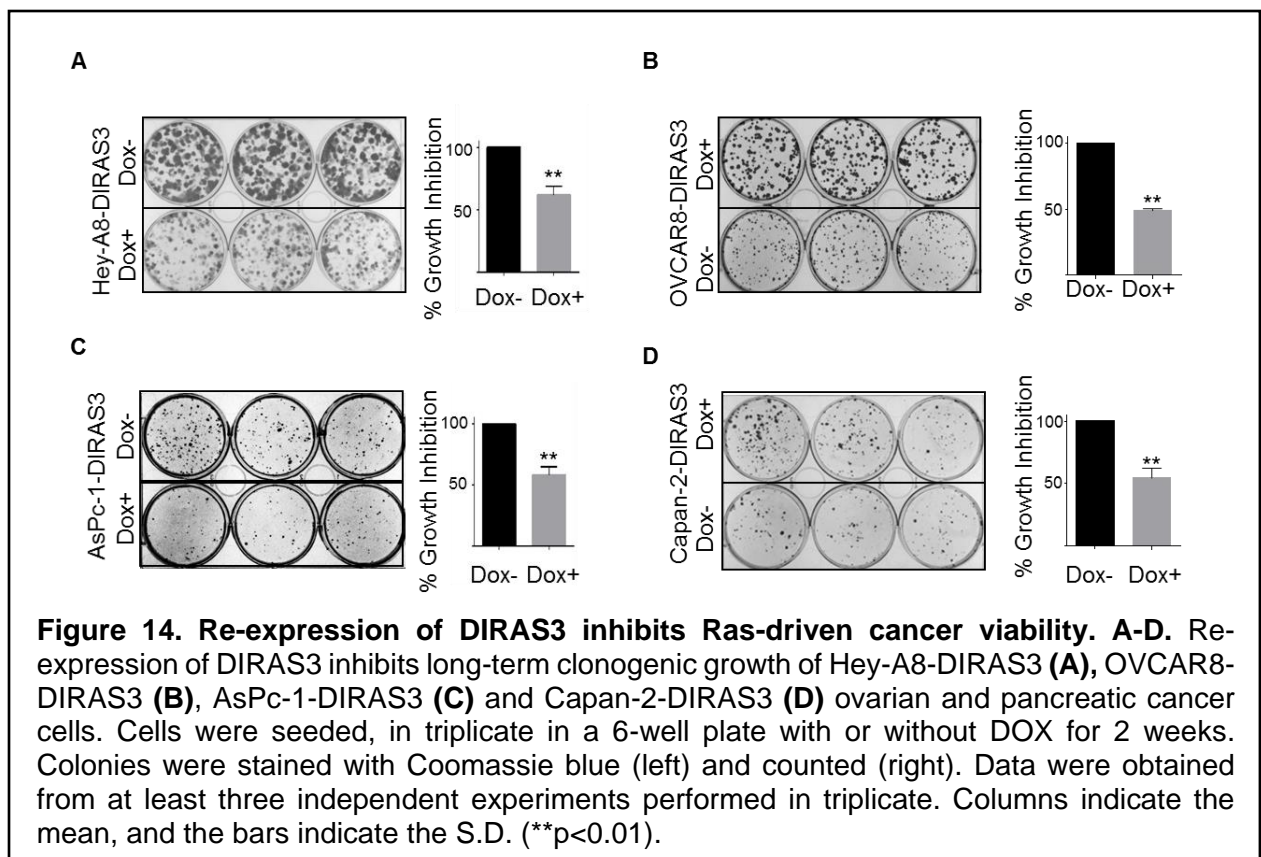
DIRAS3 inhibits Ras-driven cancer and downstream ERK signaling by disrupting Ras multimerization/clustering.

DIRAS3 inhibits growth of K-Ras dependent ovarian, pancreatic, and lung cancer cell lines. Activating mutations in Ras promote increased PI3K and Ras/MAPK signaling cascades which are often denoted by increased p-AKT and p-ERK protein expression and promote increased cell proliferation. Previous studies demonstrated that re-expression of DIRAS3 at

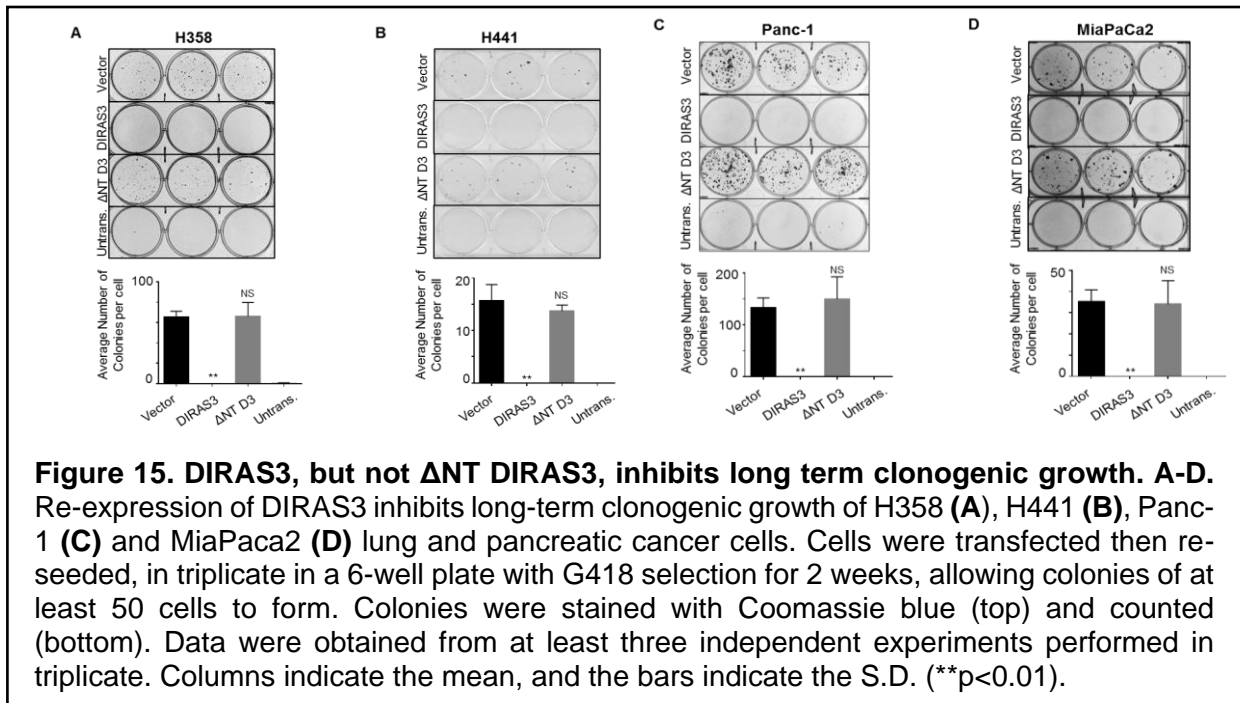


physiologic levels in ovarian cancer cell lines can inhibit clonogenic growth and the Ras/MAPK signaling pathway resulting in decreased p-ERK. (Lu, Luo et al. 2008) To examine the role of DIRAS3 in the regulation of K-Ras dependent cancer cell lines, I first tested the ability of several pancreatic and ovarian cancer cell lines, with a known activating K-Ras mutation, to grow following knockdown of K-Ras using four different small interfering RNAs

(siRNAs). Knockdown of K-Ras in AsPc-1 pancreatic cancer cells and HeyA8 high grade serous ovarian cancer cells significantly impaired cell viability in a 5 day sulforhodamine B (SRB) colorimetric assay of cytotoxicity, demonstrating the essential role of K-Ras in sustaining cell growth (**Figure 13A**). The same was true for Panc-1, MiaPaca2 (pancreatic), H358 and H441 (lung) cancer cell lines (**Figure 13B**). Interestingly, decreases in proliferation appeared to directly correlate with the knockdown efficiency of K-Ras, showing a dose-dependent effect of K-Ras inhibition. This observation is clinically important as it demonstrates the level at which the Ras/MAPK pathway must be inhibited to suppress growth of K-Ras dependent cancers. Re-expression of DIRAS3 using a tet-ON inducible system in AsPc-1-DIRAS3, Capan-2-DIRAS3, Hey-A8-DIRAS3 and OVCAR8-DIRAS3 inducible cancer cell lines inhibited clonogenic growth and downstream signaling driven by activated K-Ras (**Figure 14** and **Figure 16A-D**). Re-expression of DIRAS3 inhibited colony formation by approximately 50% at two weeks. Transient transfection of H358, H441 (lung), Panc-1 and MiaPaca2 (pancreatic), cancer cell lines

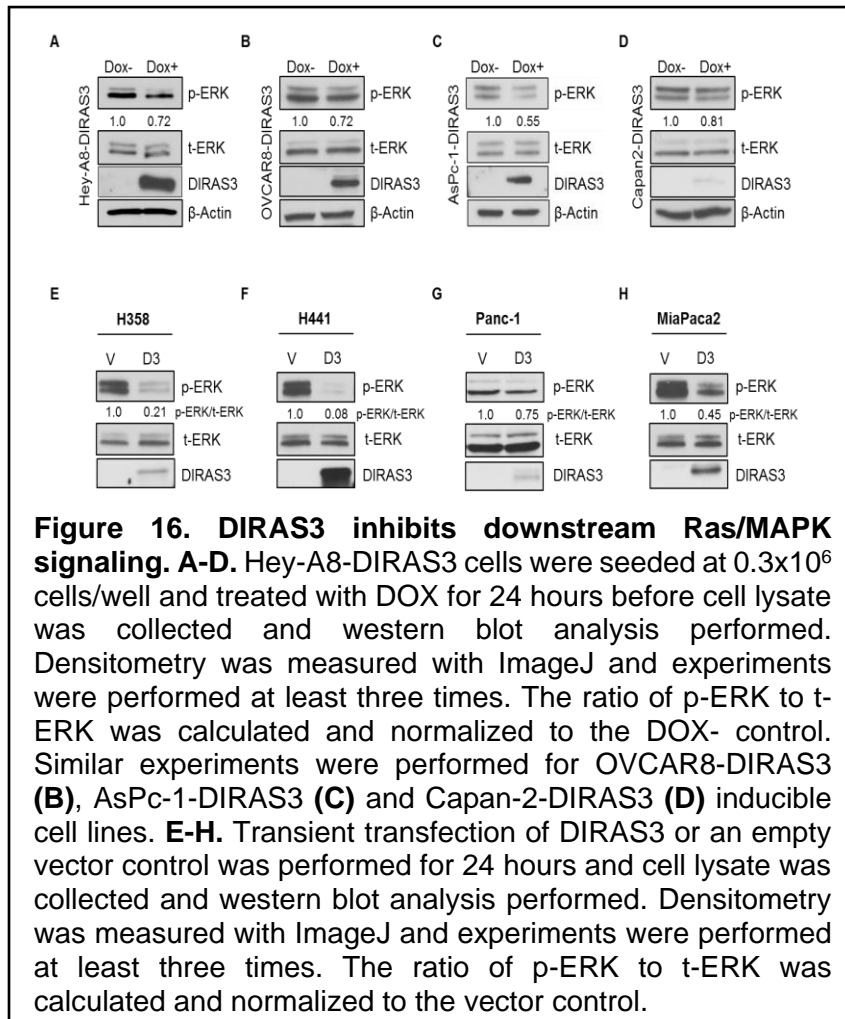


demonstrated similar long term growth inhibition and decreased MAPK signaling, while transfection of Δ NT DIRAS3 did not have the same effect (**Figure 15**). These results are in line with previously published data from the Bast laboratory, documenting the role of the N-terminus to inhibit long-term clonogenic growth of ovarian cancer cells. (Luo, Fang et al. 2003, Lu, Luo et



al. 2008) Using the complete panel of eight K-Ras dependent cancer cell lines from the pancreas, ovary and lung, the effect of re-expressing DIRAS3 on downstream Ras signaling was assessed. The MAPK/ERK signaling cascade is characterized by extracellular stimulation (growth factors, chemokines, hormones, integrins, receptor tyrosine kinases) which results in a series of sequential phosphorylation steps resulting in regulation of cytoplasmic proteins or transcription factors, based on the stimuli and effector bound to Ras. Once activated, GTP-bound Ras can recruit RAF to the plasma membrane where it can dimerize with a second Raf isoform before phosphorylating itself and then phosphorylating MAPK kinases/extracellular-signal-regulated kinases (MEK), which in turn phosphorylates and activates extracellular signal-regulated kinase (ERK). ERK phosphorylation is often assessed to determine downstream Ras pathway activation. In Hey-A8-DIRAS3, OVCAR8-DIRAS3 ovarian cancer cell lines and AsPc-1-DIRAS and Capan-2-DIRAS3 pancreatic cancer cell lines, re-expression of DIRAS3 was induced by the

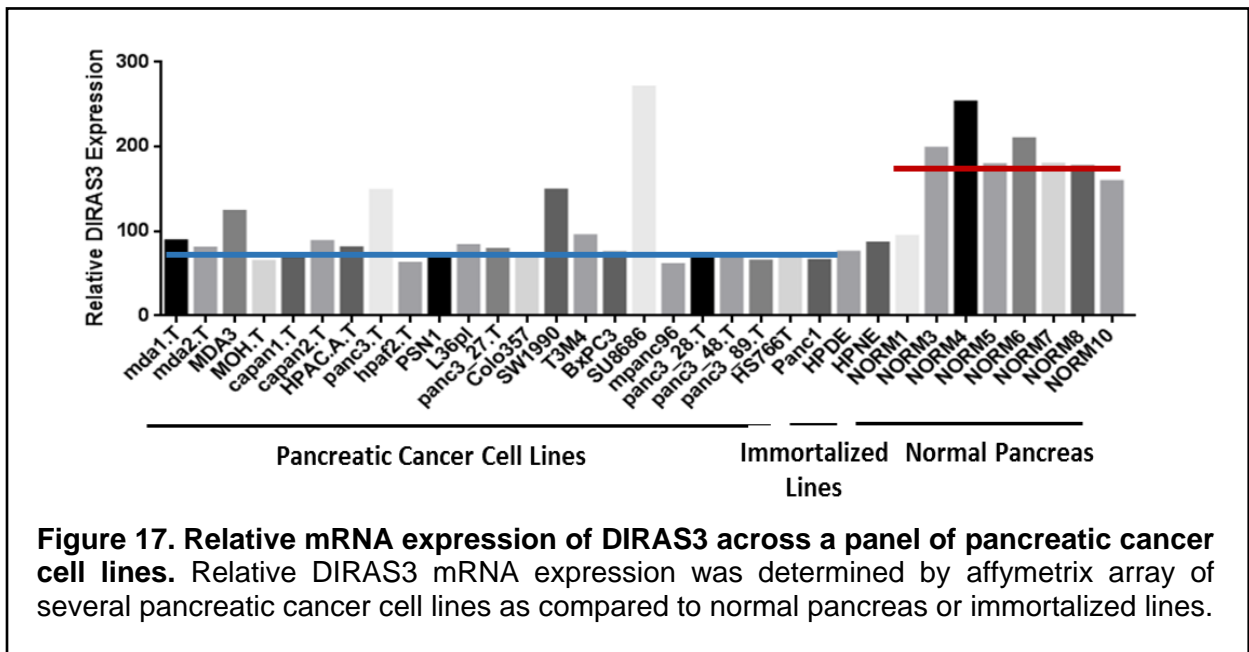
addition of DOX for 24 hours and western blot analysis of downstream ERK signaling was performed. A significant reduction was seen in p-ERK following re-expression of DIRAS3 for all



four cell lines, where the significance of inhibition appeared to correlate with the amount of DIRAS3 expression. (Figure 16A-D).

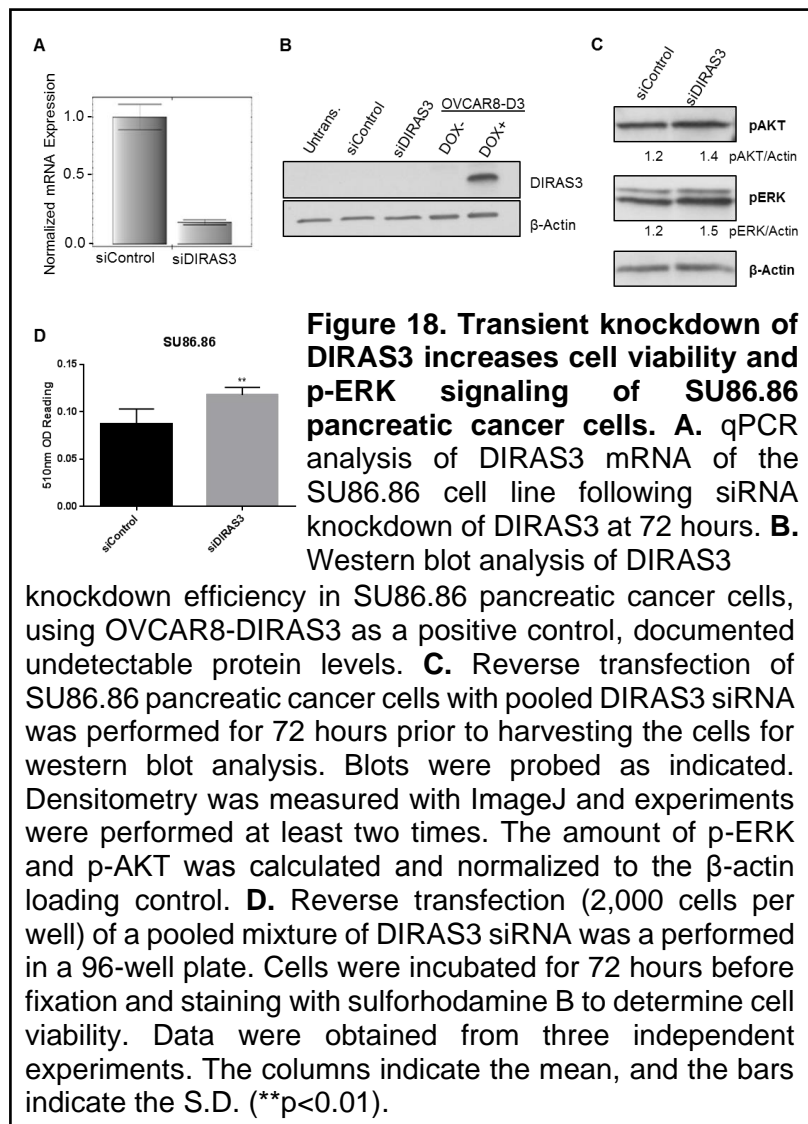
Transient overexpression of DIRAS3 in H358 and H441 lung cancer cell lines, and Panc-1 and MiaPaca2 pancreatic cancer cell lines also demonstrated a significant decrease in p-ERK compared to t-ERK for all four cell lines (Figure 16E-H).

Gene expression profiling allows mRNA expression levels to be measured for thousands of genes in a simultaneous fashion. This technique allows one to measure changes in expression levels following treatments, during development, or at a steady state across diseases, cell lines, tissues or organs. To gain a greater understanding of the expression profile of DIRAS3 across pancreatic cancer, we analyzed Affymetrix array data generated from a panel of pancreatic cancer cell lines, immortalized lines and normal pancreas controls in collaboration with Dr. Craig Logsdon. This analysis revealed that SU86.86 pancreatic cancer cell line had higher levels DIRAS3 mRNA expression (Figure 17). This data further demonstrated that DIRAS3 expression was likely downregulated in pancreatic cancer since the average relative expression of the



cancer cell lines was approximately one-third that of normal pancreas. Endogenous expression of DIRAS3 was not observed by western blot analysis, however qRT-PCR revealed decreased mRNA expression of DIRAS3 upon siRNA transfection (**Figure 18A-B**). To test they hypothesis that DIRAS3 can inhibit pancreatic cancer cell growth, we used small interfering RNAs (siRNAs) against DIRAS3 and observed increased pERK and pAKT signaling (**Figure 18C**) and increased short-term viability (**Figure 18D**). The low levels of endogenous DIRAS3 expression likely account for the minimal increases in proliferation and signaling following siRNA depletion of DIRAS3 (**Figure 18**).

DIRAS3, but not Δ NT DIRAS3, inhibits Ras multimerization. Recent studies have demonstrated a dimerization-dependent signaling mechanism of Ras. (Nan, Tamguney et al. 2015) Using the ReBiL system, as described above, to detect Ras-Ras interactions we investigated the role of DIRAS3 or Δ NT DIRAS3 to inhibit Ras multimerization. Re-expression of DIRAS3, but not Δ NT DIRAS3, resulted in decreased luminescence as seen when K-Ras clusters are present (**Figure 19A**). These results were confirmed by immunoprecipitation of the K-Ras oligomers, where K-Ras was labeled with either an HA-tag or a Flag-tag and each was



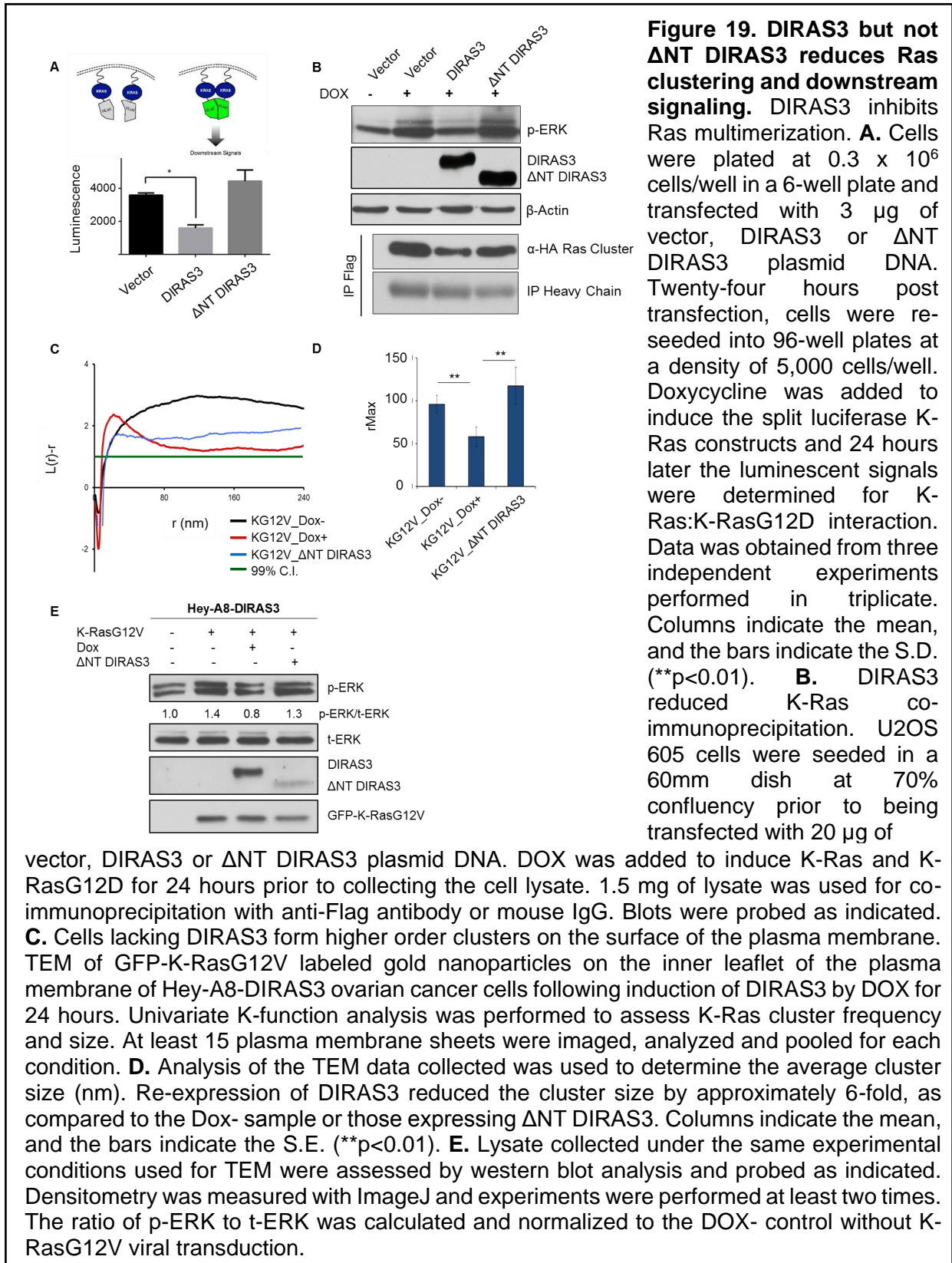
equally expressed using a bidirectional promoter following the addition of doxycycline.

Immunoprecipitation of α -Flag K-Ras showed decrease co-precipitation with HA-K-Ras when DIRAS3 was transiently introduced and then compared to an empty vector control or Δ NT DIRAS3. (Figure 19B) Similarly, DIRAS3 inhibited p-ERK activation upon the addition of DOX expressing the oligomerizable K-Ras constructs, suggesting that activation of the signaling

pathway is related to the multimerization/clustering (Figure 19B).

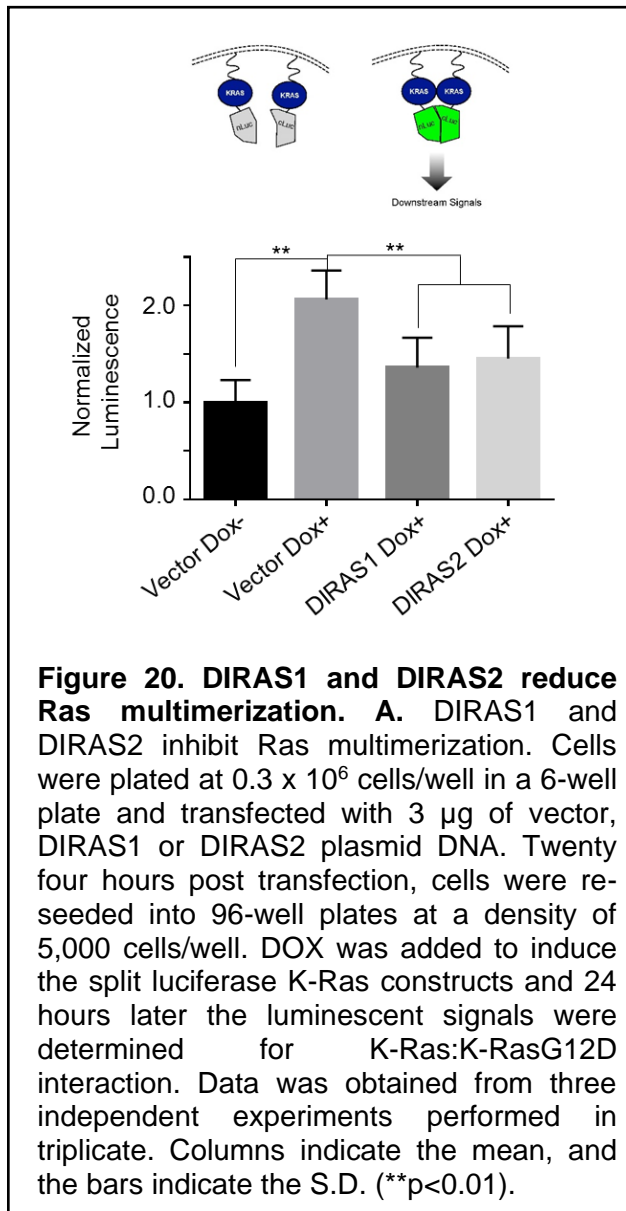
DIRAS3, but not Δ NT DIRAS3, reduces K-RasG12V clustering on the plasma membrane and downstream p-ERK signaling. We used electron microscopy to examine the clustering of K-RasG12V on the plasma membrane of Hey-A8-DIRAS3 ovarian cancer cells documents a striking difference in cluster size and extent of clustering with and without DIRAS3 expression. K-function analysis of the clustering documents that ovarian cancer cells without DIRAS3 expression have a significantly larger extent of clustering (~ two Fold), as determined by integration of the K-Function univariate curve, and approximately two fold larger radius of the

clusters, which corresponds to increased p-ERK signaling by western blot analysis (**Figure 19C-E**). As hypothesized, Δ NT DIRAS3 does not inhibit large K-RasG12V clustering on the plasma



membrane nor does it inhibit p-ERK signaling.

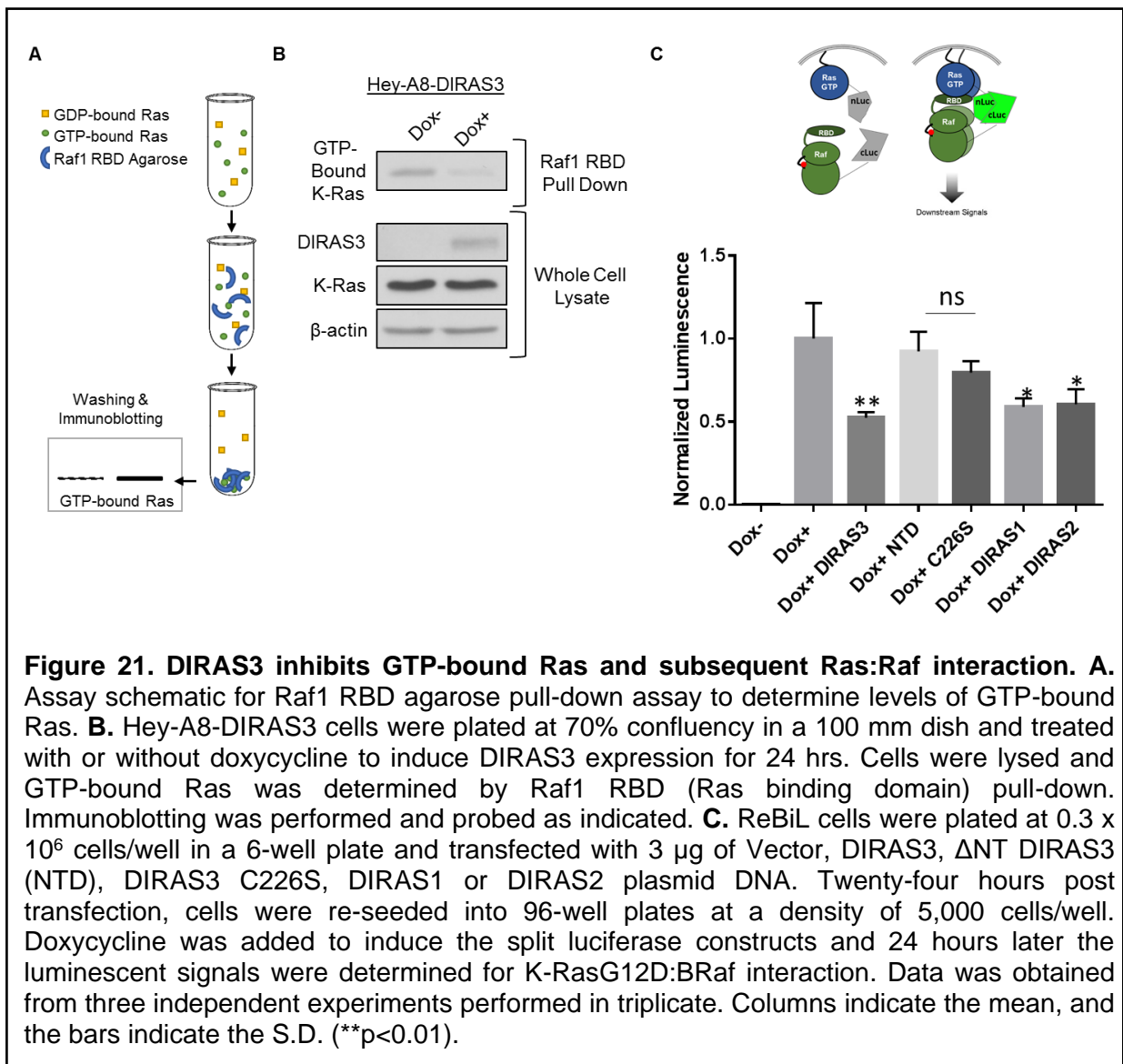
DIRAS1 and DIRAS2 reduce Ras multimerization. Similarly, re-expression of DIRAS1 or



DIRAS2 inhibited K-Ras multimerization dependent luminescence of the ReBiL U2OS cancer cells (**Figure 20**). DOX was added to induce n_Luc_K-Ras and c_Luc_K-RasG12D expression following transient transfection with DIRAS1, DIRAS2 or an empty vector control. Luminescence was measured as a surrogate for K-Ras multimerization, and upon normalization for cell viability we saw a statistically significant ($p < 0.01$) decrease in luminescence (approximately 60% decrease) following re-expression of DIRAS1 or DIRAS2.

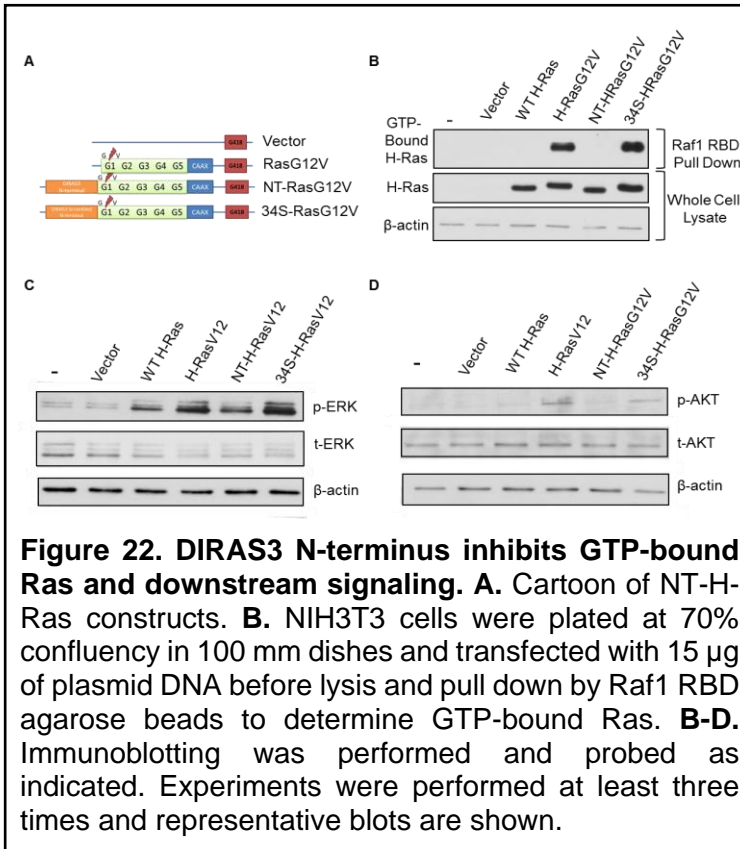
DIRAS3 reduces GTP binding by K-Ras and Ras/Raf interaction. Despite previous efforts to determine if GTP activation of Ras enhances Ras clustering, there has not been clear evidence that GTP-binding is

critical for multimerization. We have asked whether downstream Ras activation following dimerization, as determined by increased ERK signaling (Nan, Tamguney et al. 2015), might relate directly to GTP loading of Ras. To determine if decreased Ras dimerization by DIRAS3 was due to decreased “active” Ras, we examined the levels of GTP-bound Ras following re-expression of DIRAS3. Re-expression of DIRAS3 reduced GTP-bound Ras as determined by Ras binding domain (RBD) Raf immunoprecipitation. (**Figure 21A-B**) Using the ReBiL system to



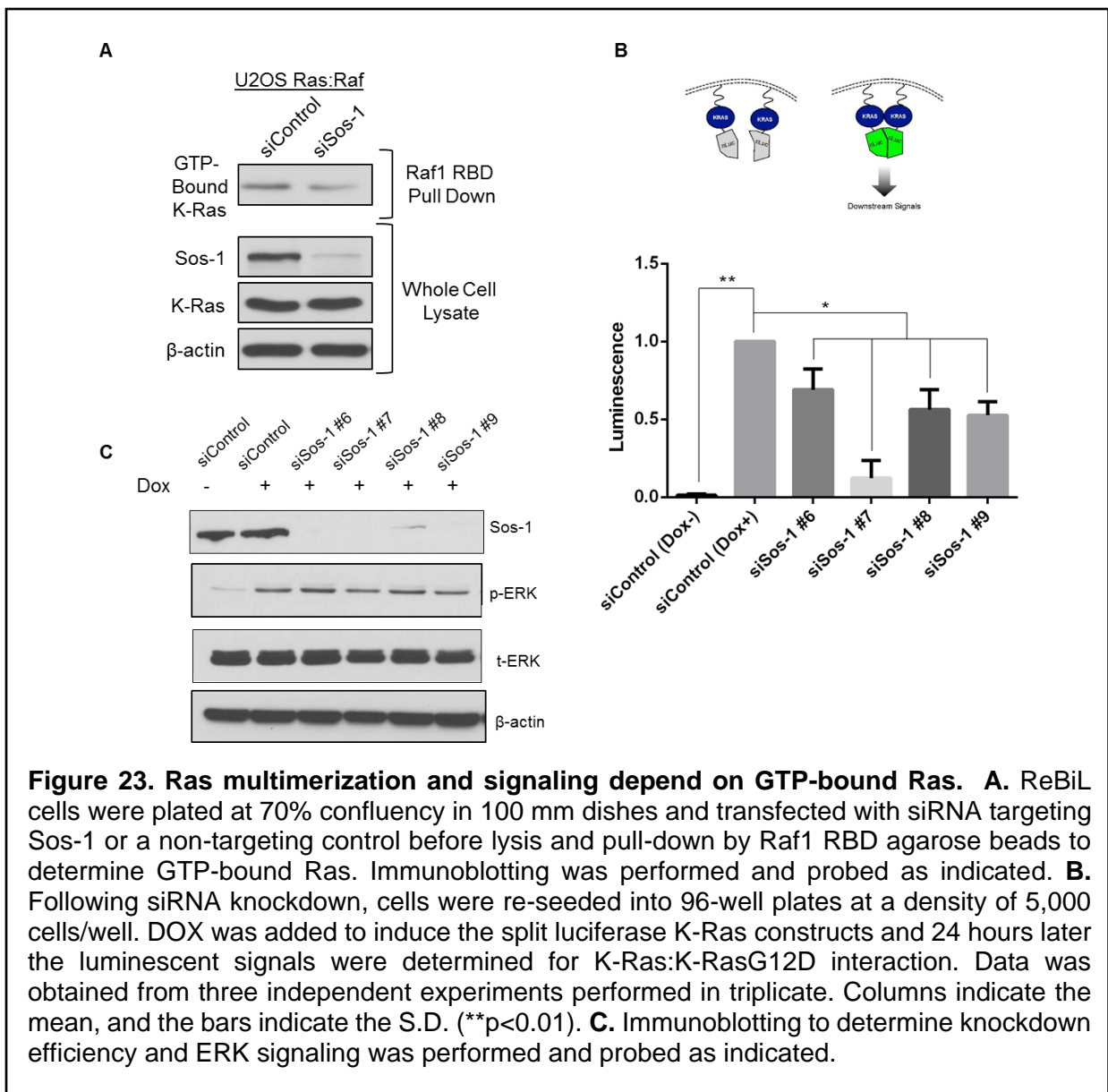
detect K-RasG12D:BRaf interaction, I also measured the effect of the DIRAS family members to inhibit this downstream interaction in the signaling cascade (**Figure 21C**). I found that re-expression of DIRAS1, DIRAS2 and DIRAS3 significantly reduced the K-RasG12D:B-Raf interaction, whereas ΔNT DIRAS3 (NTD) and DIRAS3 C226S constructs did not. These results were extended to determine if the N-terminus of DIRAS3 was responsible for this phenotype. Using DNA plasmids with the N-terminus of DIRAS3 (1-34 amino acids) added directly to the N-terminus of mutant Ras I observed that the addition of the N-terminus reversed the mutant Ras function compared to H-RasG12V or a 34-amino acid N-terminus scrambled control. (Previously

described in Figure 12) These constructs containing the N-terminus of DIRAS3 fused to mutant H-Ras resulted in decreased GTP-bound H-Ras, as well as downstream p-ERK and p-AKT signaling (**Figure 22**).



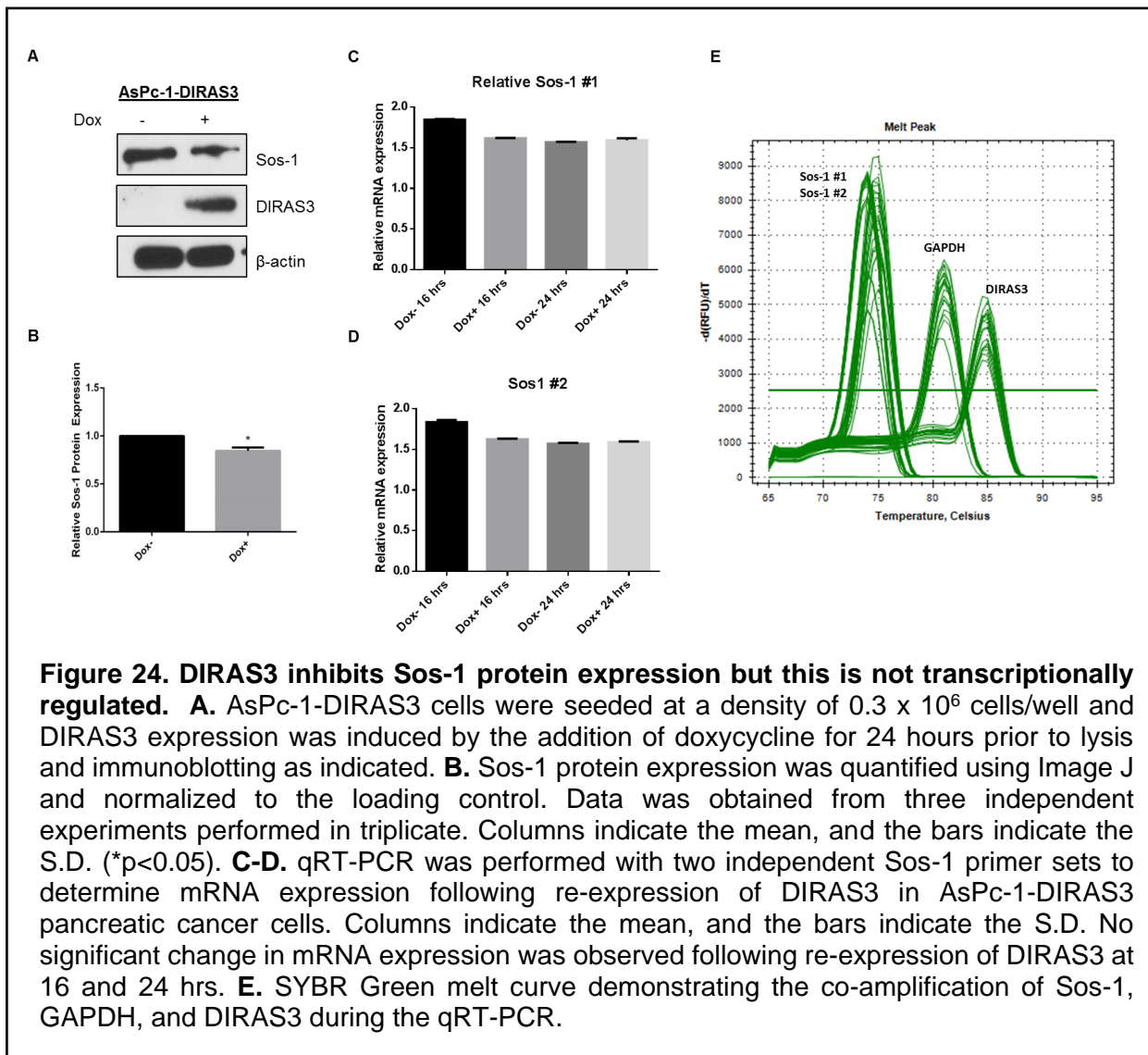
Son of Sevenless 1 (Sos-1) is one of the first identified Ras guanine exchange factors, that helps catalyze the exchange of GDP to GTP upon activation of Ras. Named for its discovery in *Drosophila melanogaster*, it was found to operate downstream of the *sevenless* gene, which when mutated results in dysfunctional development of the fly's eye when the seventh central photoreceptor fails to form. SOS1 and SOS2, the

mammalian orthologues of Sos function downstream of many growth factor receptors. To investigate the importance of GTP binding in Ras multimerization, I tested the hypothesis that knocking down Sos-1, a critical guanosine exchange factor (GEF) to facilitate GTP binding to Ras, would inhibit GTP bound Ras and subsequently Ras multimerization. Knockdown of Sos-1 by small interfering RNAs (siRNAs) significantly inhibits the GTP bound Ras (**Figure 23A**). Knockdown of Sos-1 also results in decreased multimerization of K-Ras and downstream signaling (**Figure 23B-C**). Taken together, this data suggests that activation of Ras could play a critical role in Ras multimerization/clustering. To determine if DIRAS3 was affecting Sos-1 to alter the GTP-bound state of Ras and could account for the significant decrease in Ras multimerization, I performed western blot analysis following re-expression of DIRAS3. Using



AsPc-1-DIRAS inducible cells, re-expression of DIRAS3 was achieved by adding doxycycline to the culture media for 16-24 hours. Upon re-expression, DIRAS3 slightly reduced Sos-1 protein expression (**Figure 24A-B**), however this was not transcriptionally regulated (**Figure 24C-D**) as determined by qRT-PCR analysis with two independent sets of Sos-1 primers (**Figure 24E**). While this decrease in Sos-1 likely does not account for the more dramatic decrease in GTP-bound Ras and Ras multimerization following re-expression of DIRAS3, this might provide a secondary mechanism by which DIRAS3 inhibits activated Ras signaling. Additionally, these data

suggest that DIRAS3 reduced GTP-bound Ras may be more related to the overall state of Ras, when bound to DIRAS3, rather than the effect of DIRAS3 on Ras GEFs or GAPs.



Taken together my data suggest a membrane associated mechanism by which DIRAS3 regulates Ras clustering and decreased binding with downstream activators of the signaling cascade resulting in decreased p-ERK signaling which is depicted in **Figure 25**.

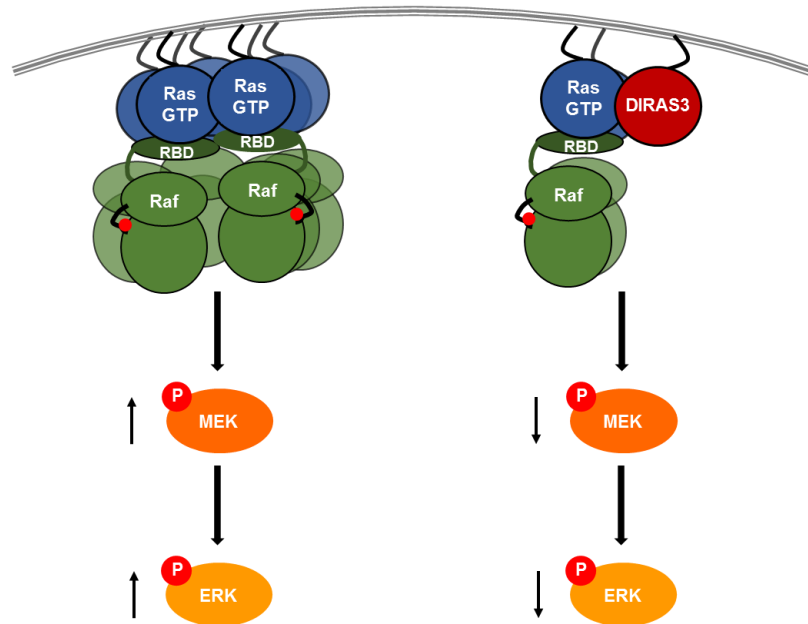


Figure 25. Model of DIRAS3 inhibition of Ras clustering. Without DIRAS3 present in the cancer cells, Ras can form higher order clusters, resulting in increased Raf effector binding and subsequent downstream signaling activation. When DIRAS3 associates with Ras at the plasma membrane, the N-terminus regulates Ras multimerization, limiting the output of Ras effector signaling.

CHAPTER 5

DIRAS family members are conserved small GTPases with differential expression across multiple organs.

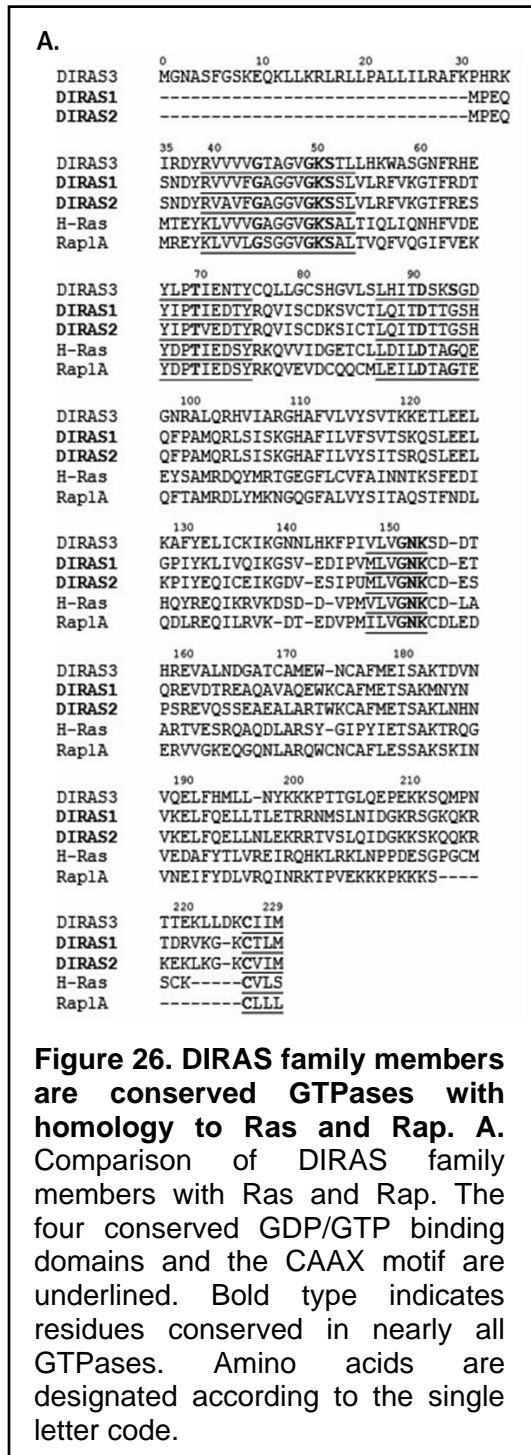
Throughout much of the last century our understanding of oncogenesis has deepened on many fronts, but the development of model systems, molecular and biochemical techniques, and large-scale data analysis in particular have been driving factors. From early work it was understood that oncogenesis occurs when either an oncogene is activated or through the loss of tumor suppressors, in which both alleles must be inactivated or silenced, allowing for uncontrolled cell division, invasion and metastasis.

DIRAS3 (DIRAS family GTPase3, Distinct Subgroup of the Ras family member 3, also known as Aplasia Ras Homology I (ARHI) and Normal Ovarian Epithelial Yinhu Yu 2 (NOEY2)) is a particularly interesting maternally imprinted tumor suppressor gene that is downregulated in a majority of ovarian cancers and several other tumor types. (Yu, Xu et al. 1999, Luo, Peng et al. 2001, Wang, Hoque et al. 2003, Rosen, Wang et al. 2004) As described above, *DIRAS3* was identified as the most downregulated gene in high grade serous ovarian cancers compared to normal ovarian epithelial cells. More recent studies have focused on the molecular mechanisms whereby *DIRAS3* regulates cell growth, motility, autophagy and tumor dormancy. Reports suggest that *DIRAS3* is downregulated in ovarian cancer by several mechanisms including loss of heterozygosity (~40%), transcriptional regulation by E2F1/E2F4 or regulation by microRNAs (~10%), and hypermethylation of the paternal allele (~20%). (Lu, Luo et al. 2006, Lu, Luo et al. 2006, Yu, Luo et al. 2006)

Previous work from the Bast lab and others demonstrated the functional significance of *DIRAS3* re-expression documenting the inhibition of growth, motility, and invasion, as well as the induction of autophagy and tumor dormancy. Much of this work has focused on the mechanisms by which *DIRAS3* plays an essential role in the induction of autophagy by inhibiting the PI3K/AKT/mTOR signaling pathway, participating directly in the autophagy initiation complex by forming a heterodimer with Beclin1, and regulating the nuclear localization of the master autophagy-related transcription factor, FOXo3a. (Yu, Luo et al. 2006, Lu, Luo et al. 2008, Lu, Baquero et al. 2014, Lu, Yang et al. 2014) *DIRAS3*-induced autophagy can also sustain survival

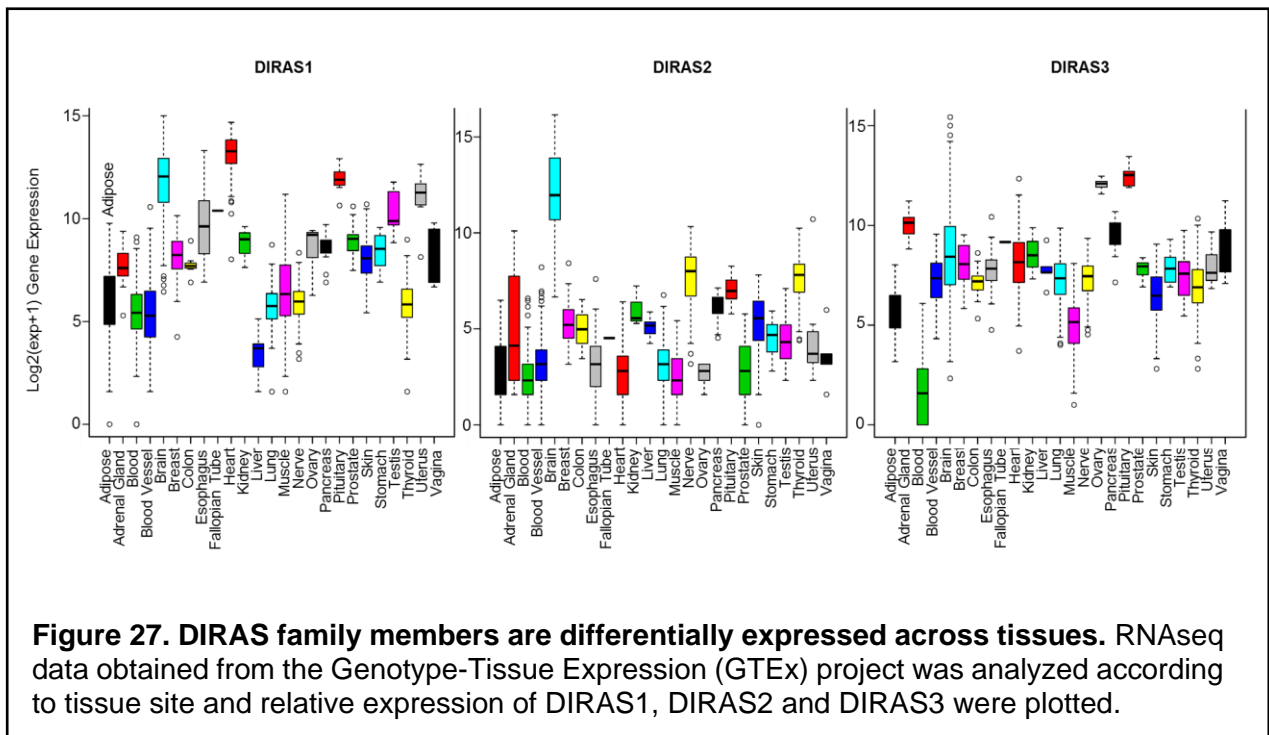
of dormant ovarian cancer xenografts, and disruption of autophagy with chloroquine, a functional inhibitor, significantly delayed outgrowth of tumors following downregulation of DIRAS3. (Lu, Luo et al. 2008)

The DIRAS family small GTPases are highly conserved members of the Ras-superfamily.

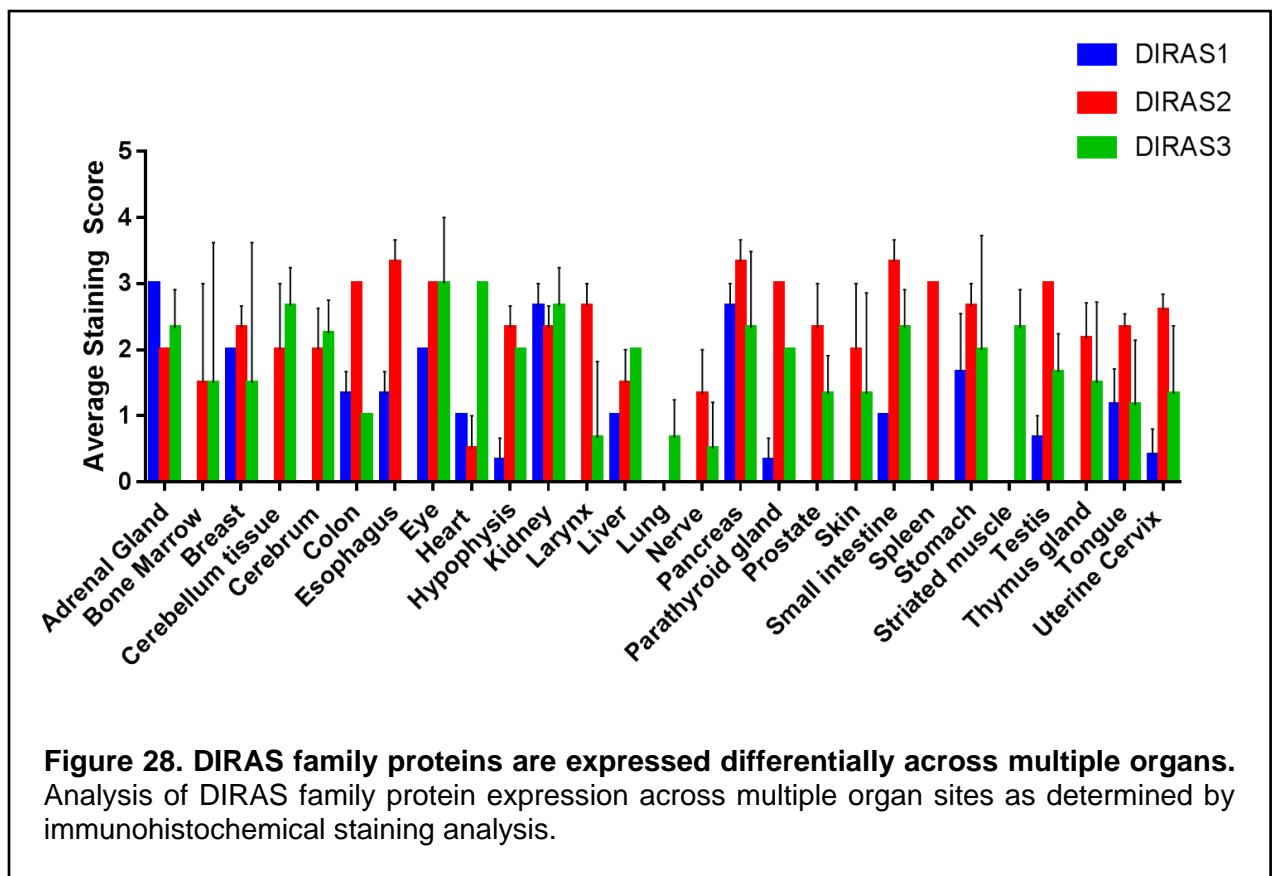


The DIRAS family of small GTPases belong to the Ras superfamily of proteins. This family is made up of three family members known as DIRAS1 (Rig), DIRAS2 and DIRAS3 (ARHI, NOEY2). As with other small GTPases, this family of proteins are most notably characterized by their homology (40-60%) to Ras and Rap, and their ability to serve as a molecular switch binding GTP and GDP. *DIRAS1* and *DIRAS2* have not been studied extensively and only few reports have indicated their function in tumor progression. (Ellis, Vos et al. 2002, Zhu, Fu et al. 2013) Most recently, Bergom and colleagues described a tumor-suppressive role for DIRAS1, documenting that its interaction with SmgGDS, antagonizes the guanine nucleotide exchange factor and inhibits its binding to other small oncogenic GTPases. (Bergom, Hauser et al. 2016, Bergom, Hauser et al. 2016) These 22 kDa conserved GTPases have 50-60% homology with *DIRAS3* where the only major difference is the truncation of the N-terminal extension from 34-amino acids to 4-amino acids (**Figure 26**).

DIRAS family expression is differentially expressed across tissues. DIRAS3 has been the most extensively studied of the three family members. To determine the expression of the DIRAS family members in normal tissue analysis of messenger RNA expression was performed in collaboration with Dr. Keith Baggerly and Shelley Herbrich across a panel of normal tissues in the Genotype-Tissue Expression (GTEx) database. GTEx was launched by the National Institutes of Health (NIH) in September 2010, and serves as a resource to study how inherited changes in gene expression can contribute to common human diseases. This database and tissue bank contains multiple human tissues from over 900 donors and has an accompanying online portal where genetic variation can be matched within their genomes. Using this data, I found that each DIRAS family member was differentially expressed across tissues, but, as hypothesized, those tissues known to have higher basal levels of autophagy (e.g. heart, brain) had relatively higher messenger RNA expression of DIRAS1, DIRAS2 and DIRAS3 (**Figure 27**).

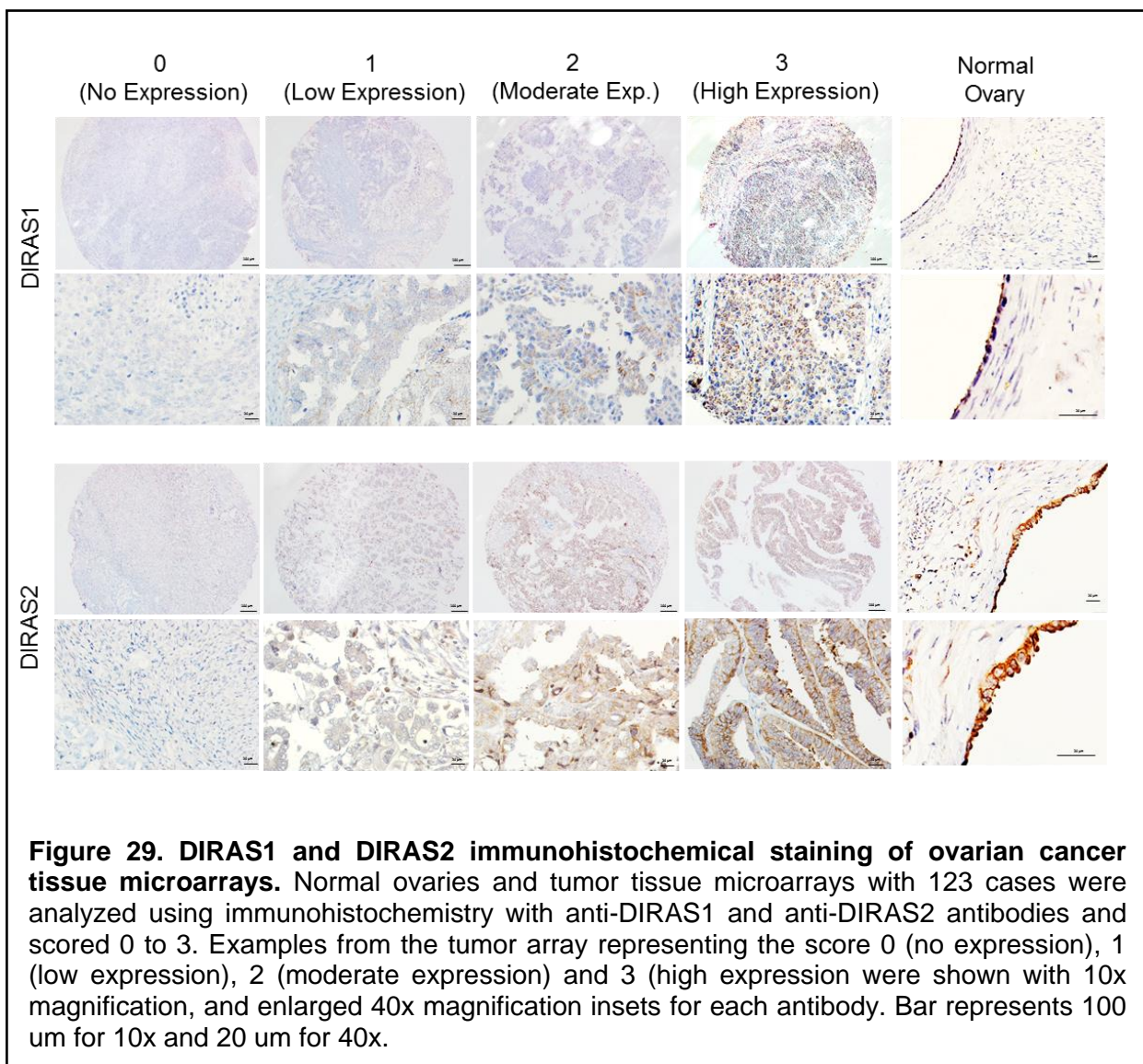


To determine if the messenger RNA expression levels correlated with protein expression, we performed immunohistochemical staining of normal organ tissue arrays. The arrays contained 2-6 samples per tissue site, and included samples from 27 different organ sites. I found that DIRAS1 was expressed the least frequently of the DIRAS family members and that similar patterns of expression were observed when compared to the mRNA expression obtained from the GTEx analysis (**Figure 28**). All three family members were strongly expressed in adrenal gland, eye, kidney, pancreas and stomach. DIRAS2 and DIRAS3 were both highly expressed in cerebellum, cerebrum, hypophysis (pituitary gland), liver, parathyroid gland, prostate, small intestine, testis, thymus, and uterine cervix.

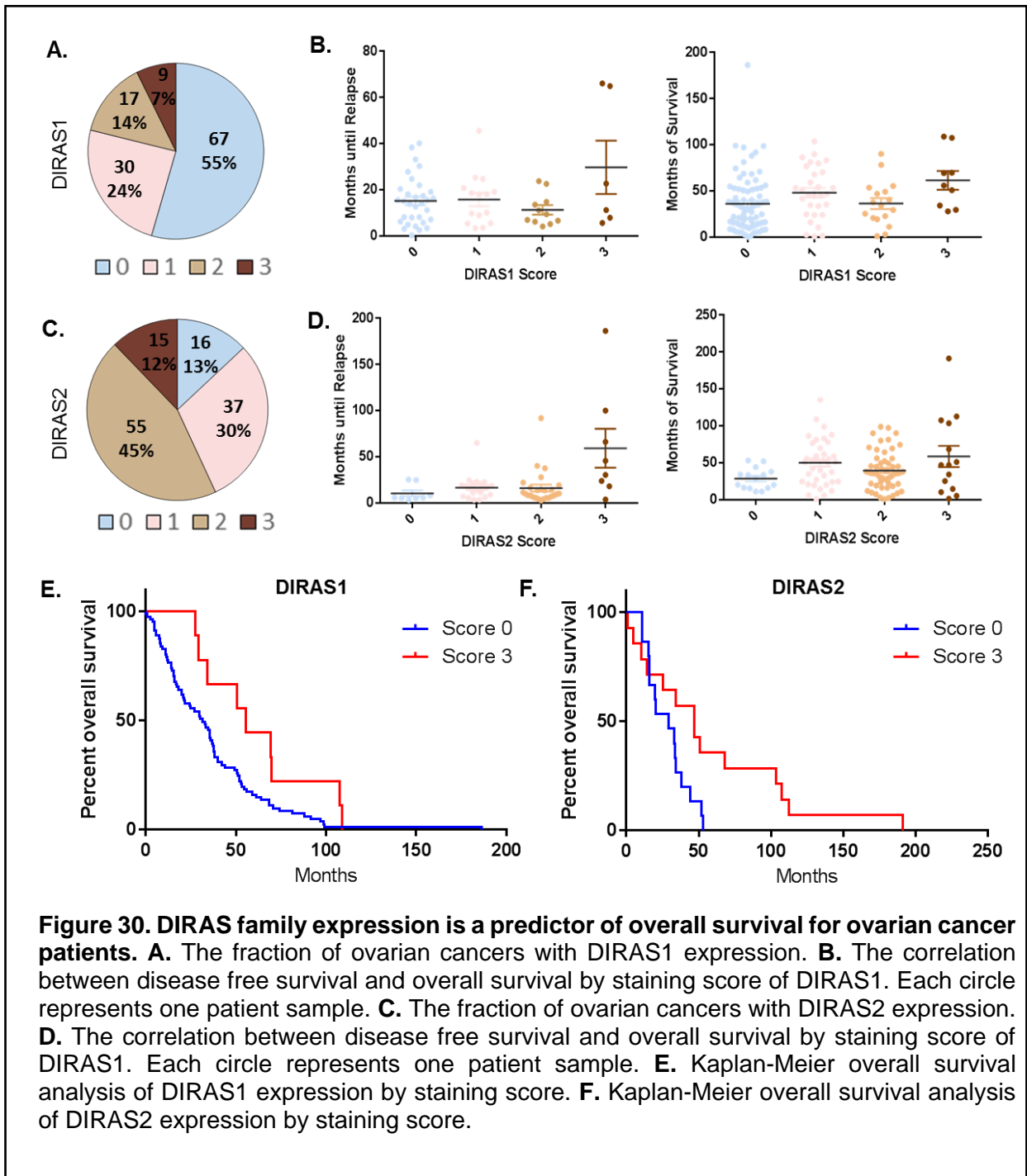


DIRAS1 and DIRAS2 are downregulated in ovarian cancer. To determine the expression of DIRAS1 and DIRAS2 in ovarian cancer, immunohistochemical staining of tumor microarrays

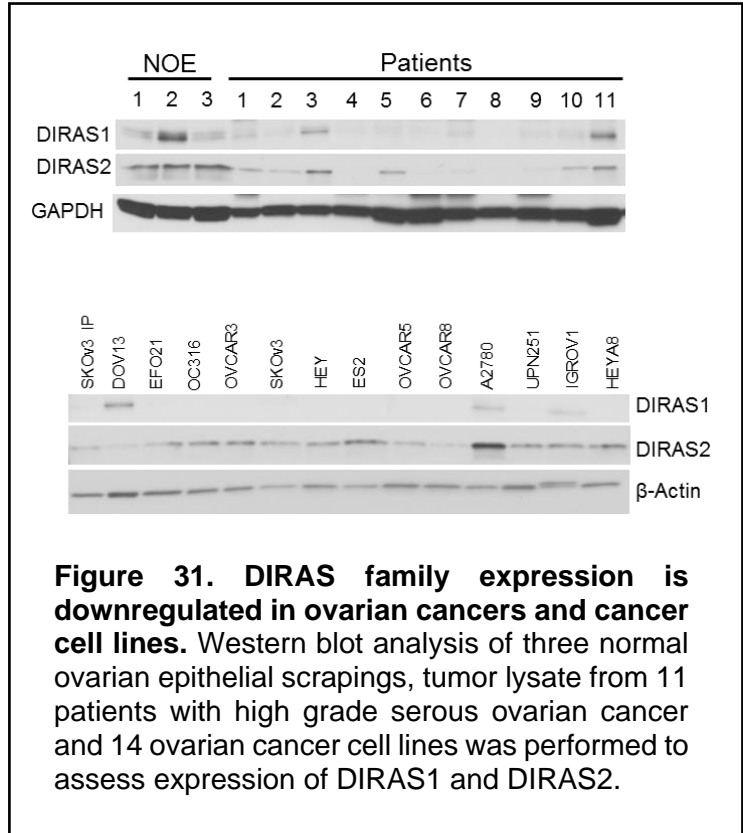
was performed. Of 123 cases, 67 cases did not express DIRAS1 (55%) and 16 cases did not express DIRAS2 (13%), and were scored 0. Those cases with definite, but low expression in the tumor, were scored as 1, whereas those with moderate expression were scored as 2. High expression was scored as 3, and this occurred in 9 cases for DIRAS1 (7%) and 15 cases for DIRAS2 (12%). Representative images of the scoring for each group are shown in **Figure 29**. Survival analysis revealed a significantly longer progression-free and overall survival for patients that had high (Score 3) DIRAS1 or DIRAS2 expression compared to those who did not have any expression (Score 0) (**Figure 30**).



The median overall survival for those patients who did not have any DIRAS1 expression was 31.4 months compared to 55.7 months for those with high expression. Likewise, patients whose tumors had high DIRAS2 expression has a median overall survival of 46.7 months compared to 29.4 months when no expression was present (**Figure 30A-F**).



Western blot analysis of three normal ovarian epithelial scrapings, tumor lysate from 11 patients with high grade serous ovarian cancer and 14 ovarian cancer cell lines was performed to assess expression of DIRAS1 and DIRAS2. Based on the average densitometry of the normal ovarian epithelial scrapings, I found that DIRAS1 was downregulated in 10 of 11 patient tumor samples (91%) and 12 of 14 ovarian cancer cell lines (86%) whereas DIRAS2 was downregulated in 8 of 11 patient tumor samples (73%) and 9 of 14 ovarian cancer cell lines (64%) (Figure 31).

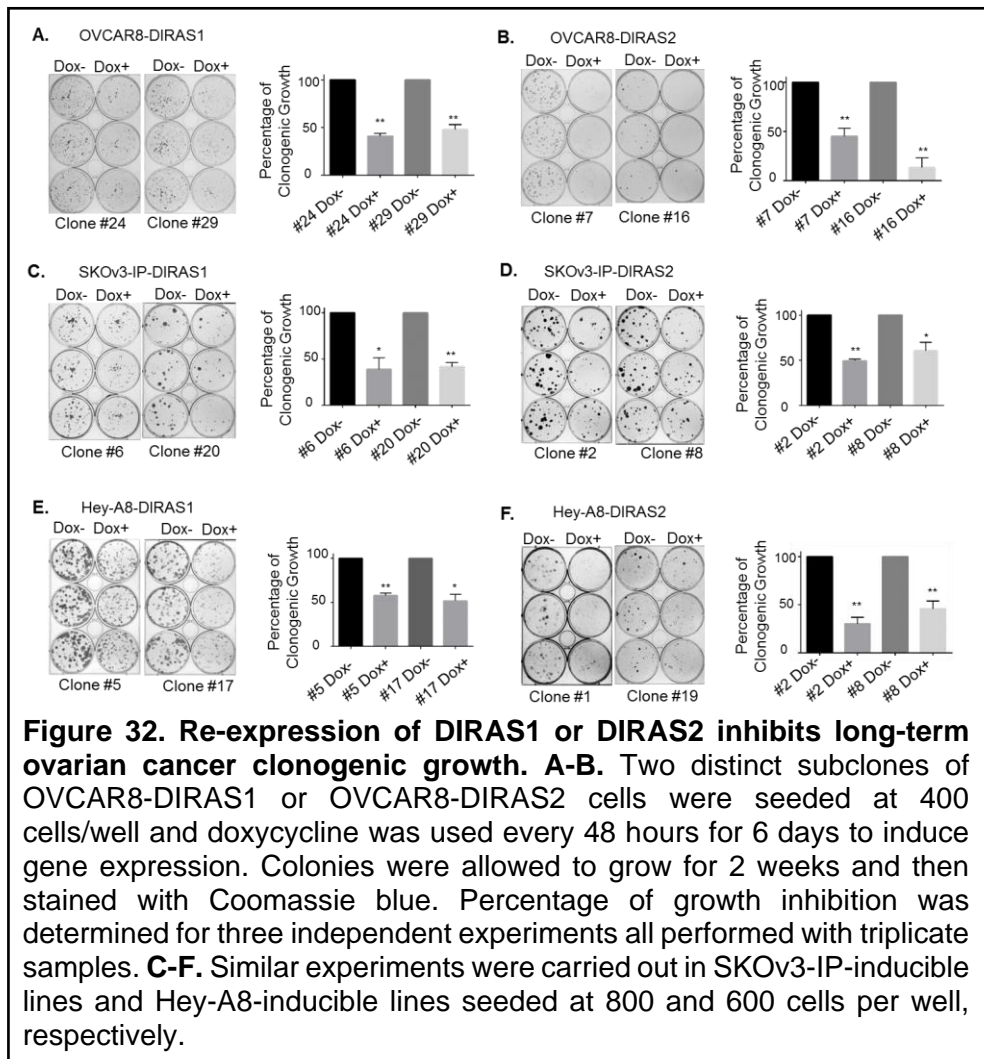


CHAPTER 6

DIRAS1 and DIRAS2 inhibit ovarian cancer cell growth by inducing autophagic cell death.

DIRAS3 (ARHI) is a known tumor suppressor of ovarian cancer, and has been shown to inhibit long term and short cell viability, which is dependent upon its N-terminal extension. Although DIRAS1 and DIRAS2 only have a 4-amino acid N-terminal extension compared to Ras, I sought out to determine if DIRAS1 or DIRAS2 would also have a tumor suppressive role. Using stable sublimes of OVCAR8, SKOV3-IP and Hey-A8 ovarian cancer cell lines with Tet-on inducible expression of DIRAS1 or DIRAS2 as well as transient transfection of DIRAS1 or DIRAS2 I determined their effect on long term and short-term cell viability.

DIRAS1 and DIRAS2 suppress growth of ovarian cancer cell lines. Induction of DIRAS1 or DIRAS2 expression following incubation of each subline with 1 ng/mL DOX produced stable expression of each gene and long term and short term cell viability was measured. Re-expression



of both DIRAS1 and DIRAS2 resulted in inhibited cancer cell clonogenic growth. Two subclones were used for each inducible subline to ensure the effect observed was not just selected for upon subcloning (Figure 32 and Figure 33).

Short Term Growth SRB Assay

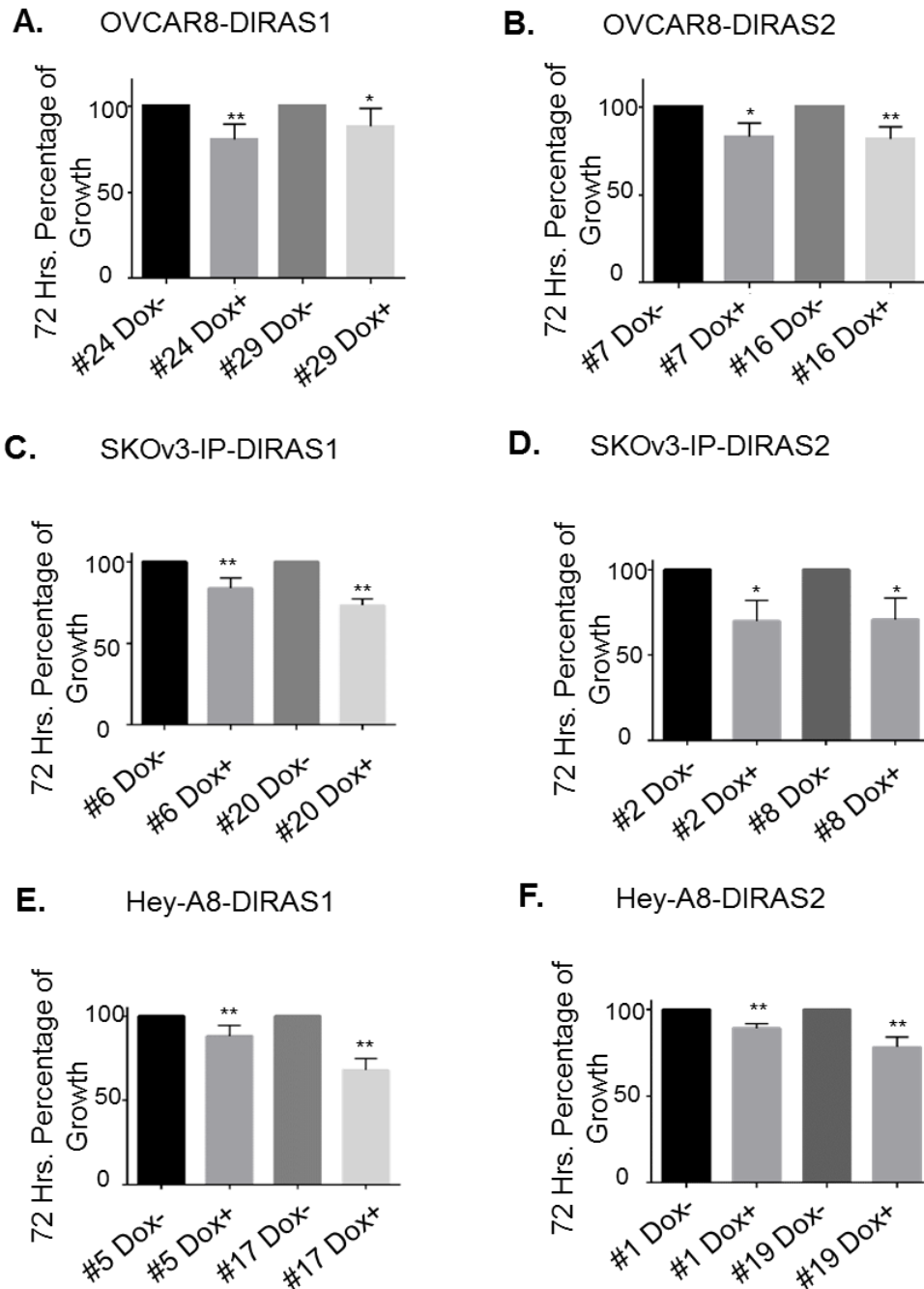
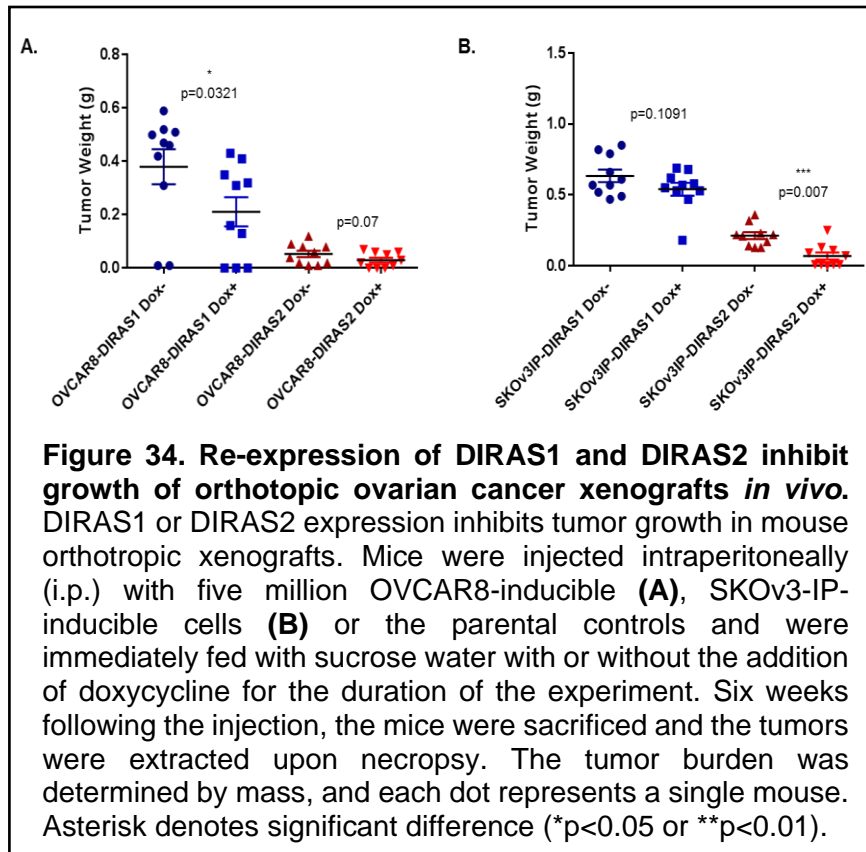


Figure 33. Re-expression of DIRAS1 or DIRAS2 inhibits short-term cell viability. A-B. Two distinct subclones of OVCAR8-DIRAS1 or OVCAR8-DIRAS2 cells were seeded at 1,000 cells/well in a 96-well format and doxycycline was added every 24 hours for a total of 72 hrs. Plates were then fixed with 30%TCA. Percentage of growth inhibition was determined for three independent experiments all performed with triplicate samples. **C-F.** Similar experiments were carried out in SKOV3-IP-inducible lines and Hey-A8-inducible lines seeded at 800 and 600 cells per well, respectively.

DIRAS1 and DIRAS2 inhibit human ovarian cancer xenograft growth. To determine whether growth inhibition was observed *in vivo*, 5 million OVCAR8- or SKOV3-IP-inducible cells, and their parental controls were injected intraperitoneally into 6-week old athymic nude mice. Doxycycline



was added to the drinking water to induce DIRAS1 or DIRAS2 gene expression, and tumor burden was assessed 4-6 weeks post injection. In both cases re-expression of DIRAS1 or DIRAS2 inhibited tumor burden and the parental cell lines were not affected by the addition of doxycycline to the drinking water (Figure 34A-B).

Neither DIRAS1 nor DIRAS2 induce apoptosis, cell cycle arrest or senescence. Using the previously described inducible ovarian cancer cell lines, we next sought to identify the mechanism(s) by which DIRAS1 and DIRAS2 might contribute to growth inhibition. Using cisplatin as a positive control, I measured Annexin V/Propidium Iodide (PI) staining to determine the percentage of apoptotic cells following re-expression of DIRAS1 and DIRAS2 over a time period of 72 hours, by flow cytometry. Neither DIRAS1 (Figure 35A) nor DIRAS2 (Figure 35C) upregulation produced significantly different levels of apoptosis judged by immunostaining for Annexin V/PI, but apoptosis was readily induced in the same three inducible cell lines by treatment with cisplatin. Western blot analysis of cleaved caspase 3 confirmed these results

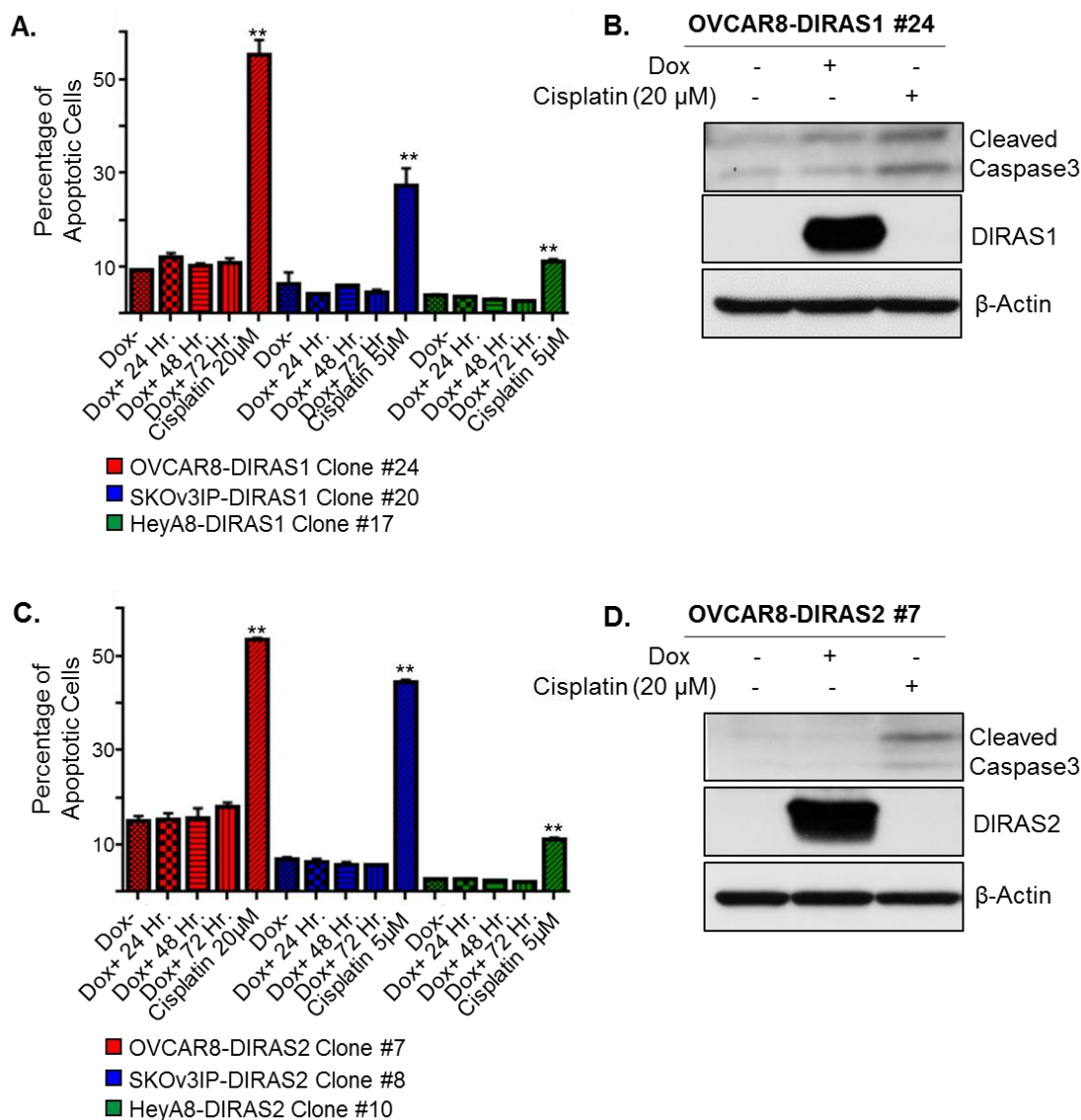


Figure 35. Growth inhibition of ovarian cancer cells following re-expression of DIRAS family members is not due to apoptosis. A-D. OVCAR8-inducible, SKOv3-IP-inducible and Hey-A8-inducible ovarian cancer cell lines were treated with or without doxycycline for 24, 48, and 72 hours. An additional plate was treated with cisplatin (5-20 µM) for 72 hours and used as a positive control. Cells were stained with Annexin V/PI and analyzed by flow cytometry, or western blot analysis of cleaved caspase 3, no significant change was overserved in the level of apoptotic cells following re-expression of DIRAS1 or DIRAS2. Data was collected over three independent experiments with technical duplicates for each. Asterisk denotes significant difference (* $p < 0.05$ or ** $p < 0.01$).

(Figure 35B and 35D). Cell cycle analysis was performed using flow cytometry of PI stained inducible ovarian cancer cells. While slight changes were observed no significant increases in

cell cycle arrest were noted across G 1, S, or G2/M for both DIRAS1 and DIRAS2 in the three inducible cell lines (**Figure 36**). These results suggest that cell cycle arrest is not the main

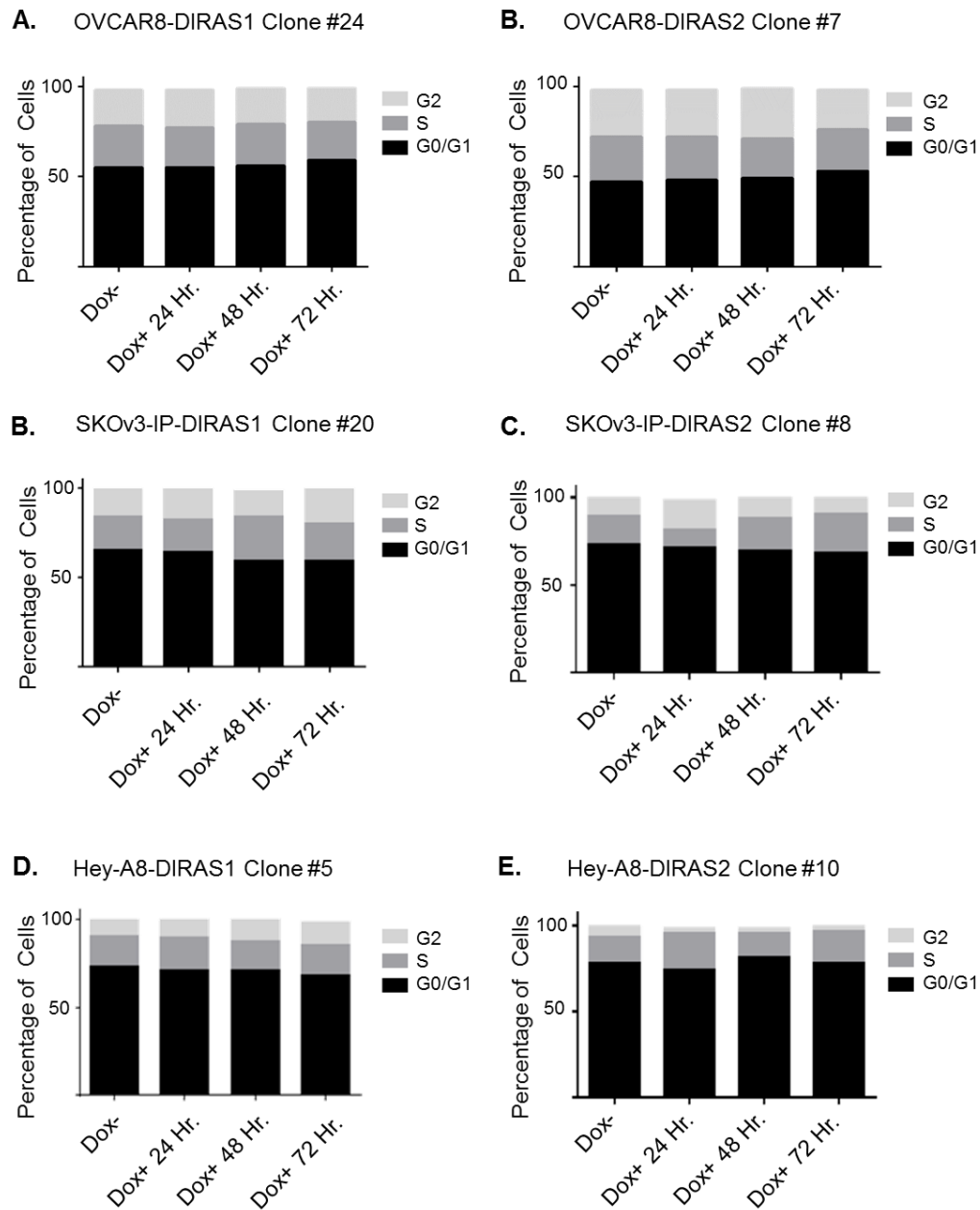


Figure 36. Growth inhibition of ovarian cancer cell following re-expression of DIRAS family members is not due to cell cycle arrest. A-E. OVCAR8-inducible, SKOV3-IP-inducible and Hey-A8-inducible ovarian cancer cell lines were treated with or without doxycycline for 24, 48, and 72 hours. Cells were collected and stained with propidium iodide and analyzed for cell cycle using flow cytometry. No significant changes were observed in cell cycle at G0/G1, S, or G2/M phase. Data was collected over three independent experiments with technical duplicates for each. Asterisk denotes significant difference (* $p < 0.05$ or ** $p < 0.01$).

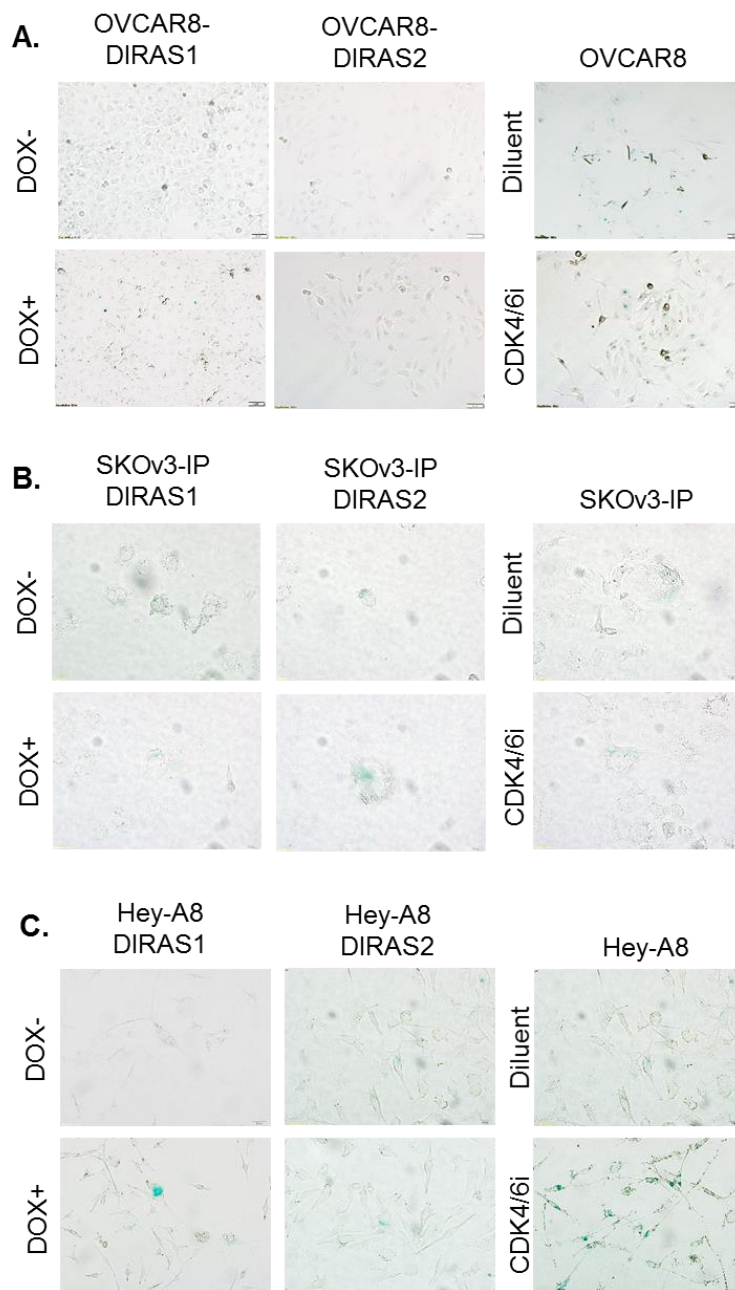
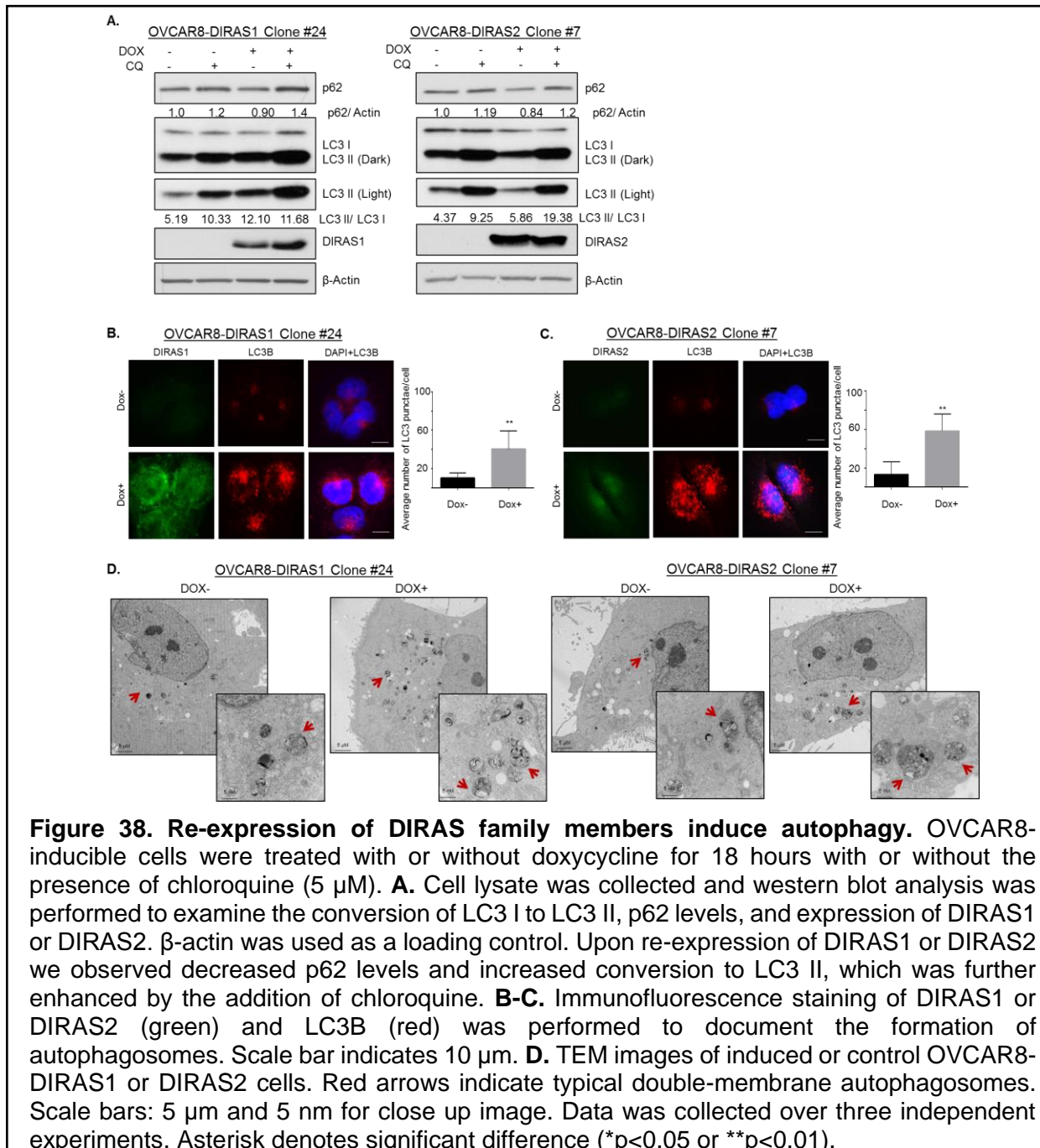


Figure 37. Growth inhibition of ovarian cancer cell following re-expression of DIRAS family members is not due to senescence. A-C. Senescence of OVCAR8-inducible, SKOV3-IP-inducible and Hey-A8-inducible ovarian cancer cell lines was analyzed by SA-β-Gal staining following treatment with or without doxycycline for 72 hours. 5μM palbociclib, a CDK4/6 inhibitor was used as a positive control. No significant increase in senescence was observed following re-expression of DIRAS1 or DIRAS2. Data was collected over three independent experiments with technical duplicates for each. Asterisk denotes significant difference (*p<0.05 or **p<0.01).

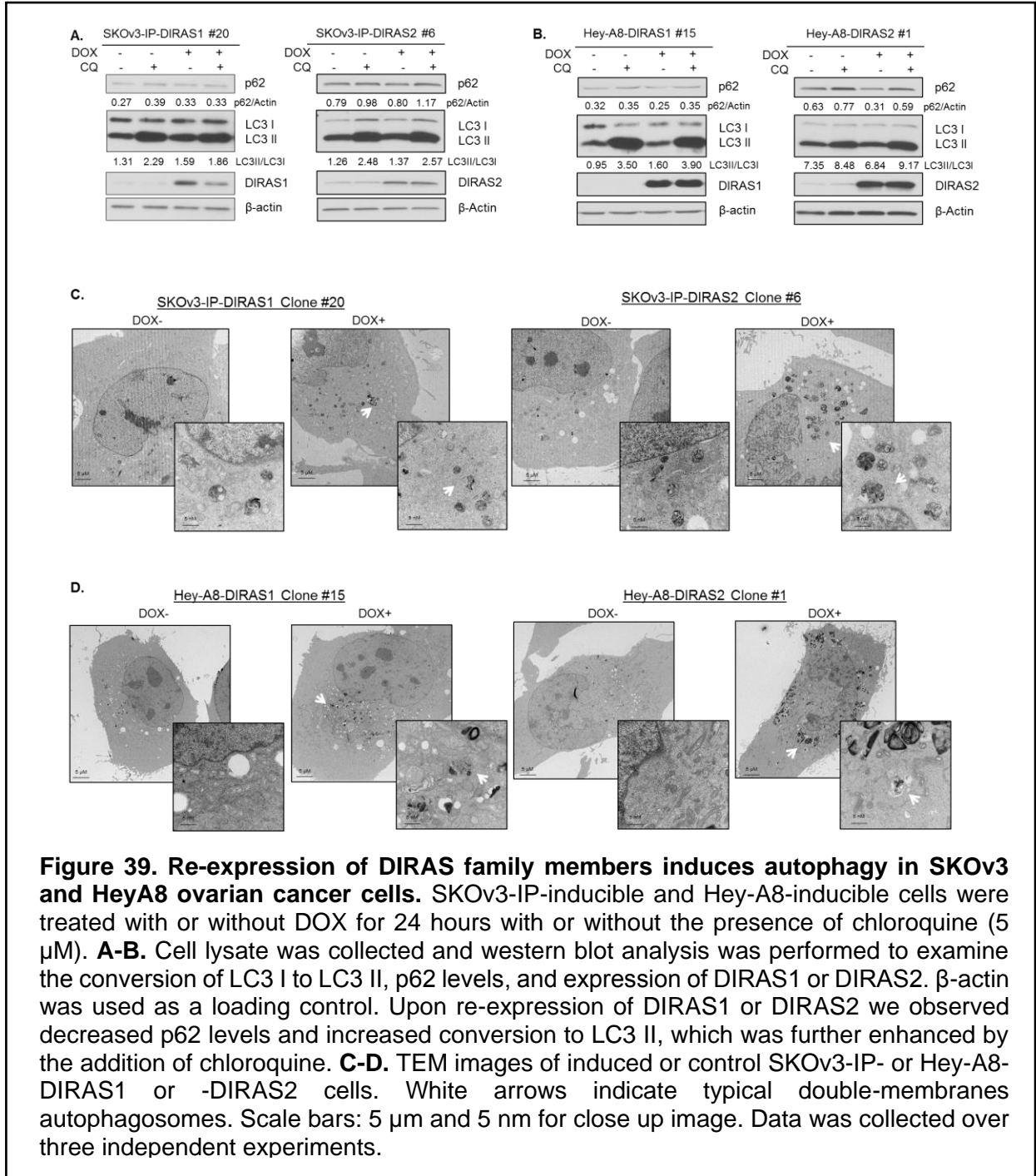
mechanism by which DIRAS1 or DIRAS2 inhibit ovarian cancer cell growth. Next I investigated the induction of cellular senescence by SA-β-Gal staining. Cellular senescence or cellular aging is a normal phenomenon where diploid cells cease to divide, adopting a permanent state of cell-cycle arrest. Senescence markers include lack of DNA replication (which cannot be distinguished from quiescence), or staining with the senescence-associated β-galactosidase (SA-β-gal). Similarly, re-expression of DIRAS1 or DIRAS2 did not produce a significant increase in positively stained cells, but treatment with the CDK4/6 inhibitor palbociclib did, providing a positive control (Figure 37). SA-β-Gal staining

was extremely faint in the p53 null SKOV3 cell line, as would be predicted based on the role of p53 to activate this pathway.

DIRAS1 and DIRAS2 induce autophagy. LC3-I conversion to its cleaved product LC3-II generated by ATG4, a cysteine protease, is a key process during the elongation and formation of the autophagosome membrane, and frequently used to document the induction of autophagy. (Asanuma, Tanida et al. 2003) Using the previously described OVCAR8-inducible, SKOV3-

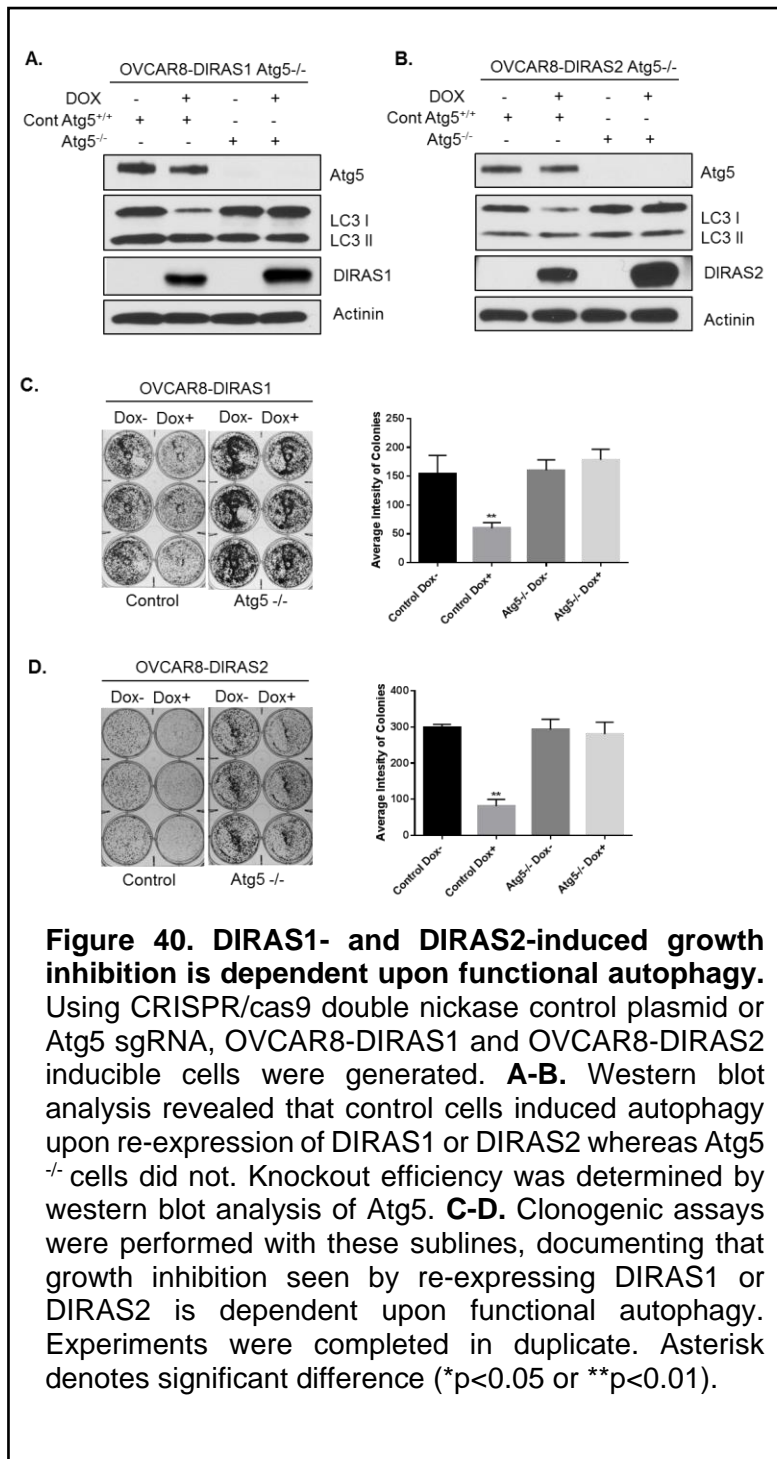


inducible and HeyA8-inducible sublines of ovarian cancer, I induced DIRAS1 or DIRAS2 expression for 18-24 hours with the addition of doxycycline. Upon re-expression I observed an increased LC3-II to LC3-I ratio, that could be further enhanced by using chloroquine, a functional inhibitor of autophagy (**Figure 38**). The same was true in both SKOv3-inducible and Hey-A8-inducible ovarian cancer cell lines (**Figure 39**). Using immunofluorescence I was able to confirm these results by staining for MAP-LC3B, where the formation of punctae demonstrate the



presence of autophagosomes and represents the accumulation of a membrane-bound form of LC3 on autophagic vesicles (Kabeya, Mizushima et al. 2000, Takahashi, Coppola et al. 2007) **(Figure 38B-C)**. Interestingly, neither DIRAS1 nor DIRAS2 does co-localized with LC3B by immunofluorescence staining, differing from DIRAS3 in this regard. Transmission electron microscopy (TEM) is the gold standard for detection of autophagosome formation and the characteristic feature is the presence of intracellular contents that are enclosed by a double-membrane vacuolar structure. TEM performed on OVCAR8-inducible, SKOV3-inducible and HeyA8-inducible cells with and without the re-expression of DIRAS1 or DIRAS2 confirmed my previously documented results and demonstrated autophagosomes, which contained multiple lamellae, intact cytoplasmic structures and residual digested materials **(Figure 38D and Figure 39C-D)**. Although basal autophagy and autophagosome formation was observed in the samples without DOX, there was a significant increase, not only in number but also size of the autophagosomes once DIRAS1 or DIRAS2 was re-expressed.

Inhibition of autophagy by knockdown of Atg5 prevents DIRAS1 and DIRAS2 inhibition of ovarian cancer cell growth. Autophagy protein 5 (Atg5) is a well-characterized E3 ubiquitin ligase that is essential for the elongation of the autophagosome. Following activation by Atg7, Atg5 forms a complex with ATG12 which is necessary for conjugation of phosphatidylethanolamine to LC3-I, allowing for cleavage to the LC3-II form. Using the CRISPR/Cas9 gene editing technique I developed Atg5 ^{-/-} cells and their paired controls for the OVCAR8-DIRAS1 and OVCAR8-DIRAS2 inducible cell lines. Following development of these lines I determined if knockdown of Atg5 would inhibit DIRAS1 or DIRAS2-induced autophagy as determined by LC3 II conversion **(Figure 40A-B)**. The growth inhibition observed following re-expression of DIRAS1 or DIRAS2 was also dependent upon functional autophagy, as seen by clonogenic long-term growth assays **(Figure 40C-D)**. These results suggest that induction of autophagy is a key mechanism by which DIRAS1 and DIRAS2 inhibit ovarian cancer cell growth and survival.



DIRAS1 and DIRAS2
inhibit ovarian cancer cell migration. In addition, re-expression of DIRAS1 and DIRAS2 significantly inhibited ovarian cancer cell migration. SKOV3 and Hey ovarian cancer cells were transiently transfected with pLoc-DIRAS family plasmids, and seeded in a 96-well format using the Oris Cell migration assay. A round wound was formed by the stopper which was subsequently removed and cell migration was tracked for 20 hours. GFP-positive cells were quantified and used to control for transfection efficiency. I documented a significant decrease in migration upon re-expression of all three DIRAS family members (**Figure 41**).

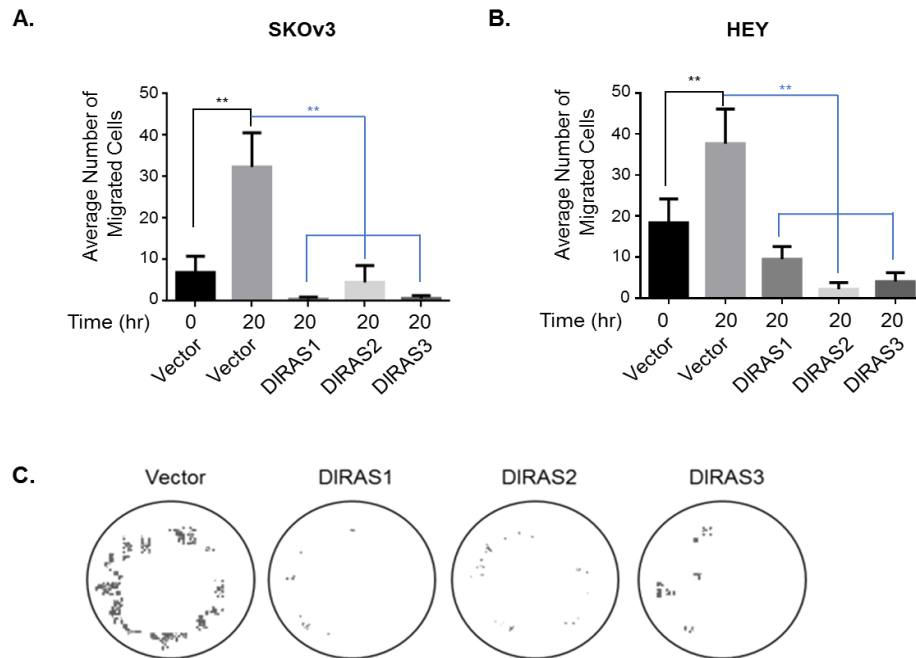


Figure 41. DIRAS family members inhibit ovarian cancer cell migration. **A.** SKOv3 ovarian cancer cells transfected with pLoc-DIRAS family member plasmids and an empty vector control were assessed for migration potential 20 hours after the removal of a rubber boundary. GFP-positive (transfected) cells were imaged and quantified. **B.** Similar studies were conducted with Hey-A8 ovarian cancer cells. **C.** Representative image following quantification of migration into the center well space. Each experiment was completed with technical triplicates and performed at least three times. Asterisk denotes significant difference (* $p < 0.05$ or ** $p < 0.01$).

CHAPTER 7

DIRAS1 and DIRAS2 induce autophagy by inhibiting the PI3K and Ras/MAPK signaling pathways resulting in nuclear localization of autophagy-related transcription factors FOXO3a and TFEB.

Under nutrient poor or stressful conditions including hypoxia and DNA damage, autophagy is induced to maintain cellular homeostasis. One of the mechanisms by which autophagy is induced involves upregulation of transcription factors forkhead box O3 (FOXo3a) and transcription factor EB (TFEB) that regulate expression of several autophagy related proteins. When FOXo3a is phosphorylated by AKT, it is shuttled out of the nucleus where it is bound by 14-3-3 and degraded. Inhibition of the PI3K/AKT signaling pathway results in increased nuclear accumulation of FOXo3a and increased transcription of MAPLC3, Gabarap, Atg5 and Atg12, VPS34, Beclin1, BNIP3 and Rab7. (Miranda, Mickle et al. 2009, Vellai 2009, Zhou,

Deng et al. 2009, Mukherjee, Ray et al. 2010) In starved cells, TFEB becomes dephosphorylated and translocated to the nucleus where it initiates transcription of key autophagy-related genes including MAPLC3, SQSTM1, UVRAG and LAMP1a (Figure 42). (Settembre and Ballabio 2011)

Re-expression of DIRAS1 or DIRAS2 inhibits phosphorylation of AKT, mTOR, and ERK. To determine the mechanism by which DIRAS1 and DIRAS2 induce autophagy I first observed the effect of re-

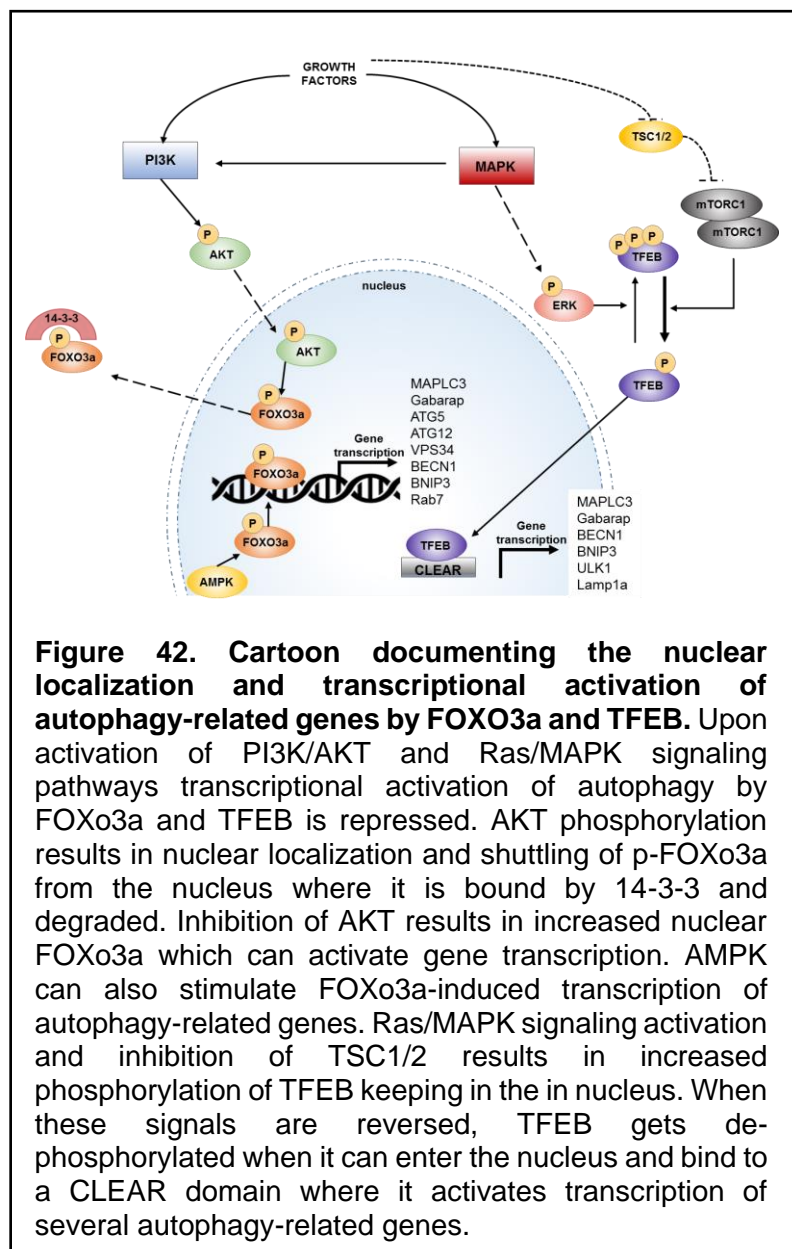
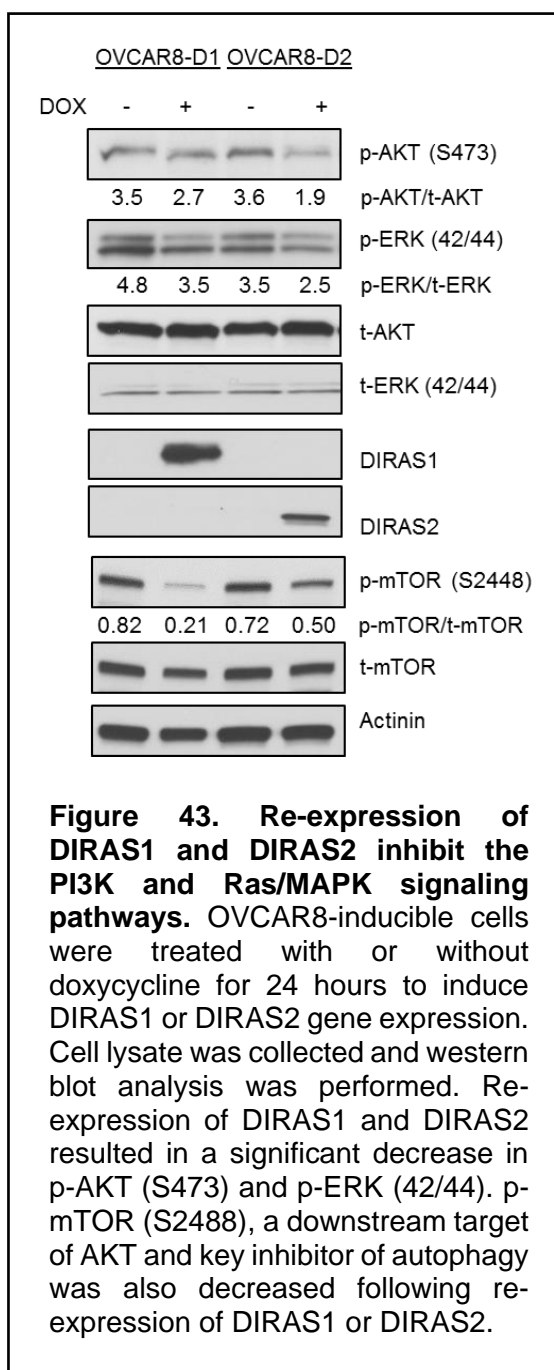


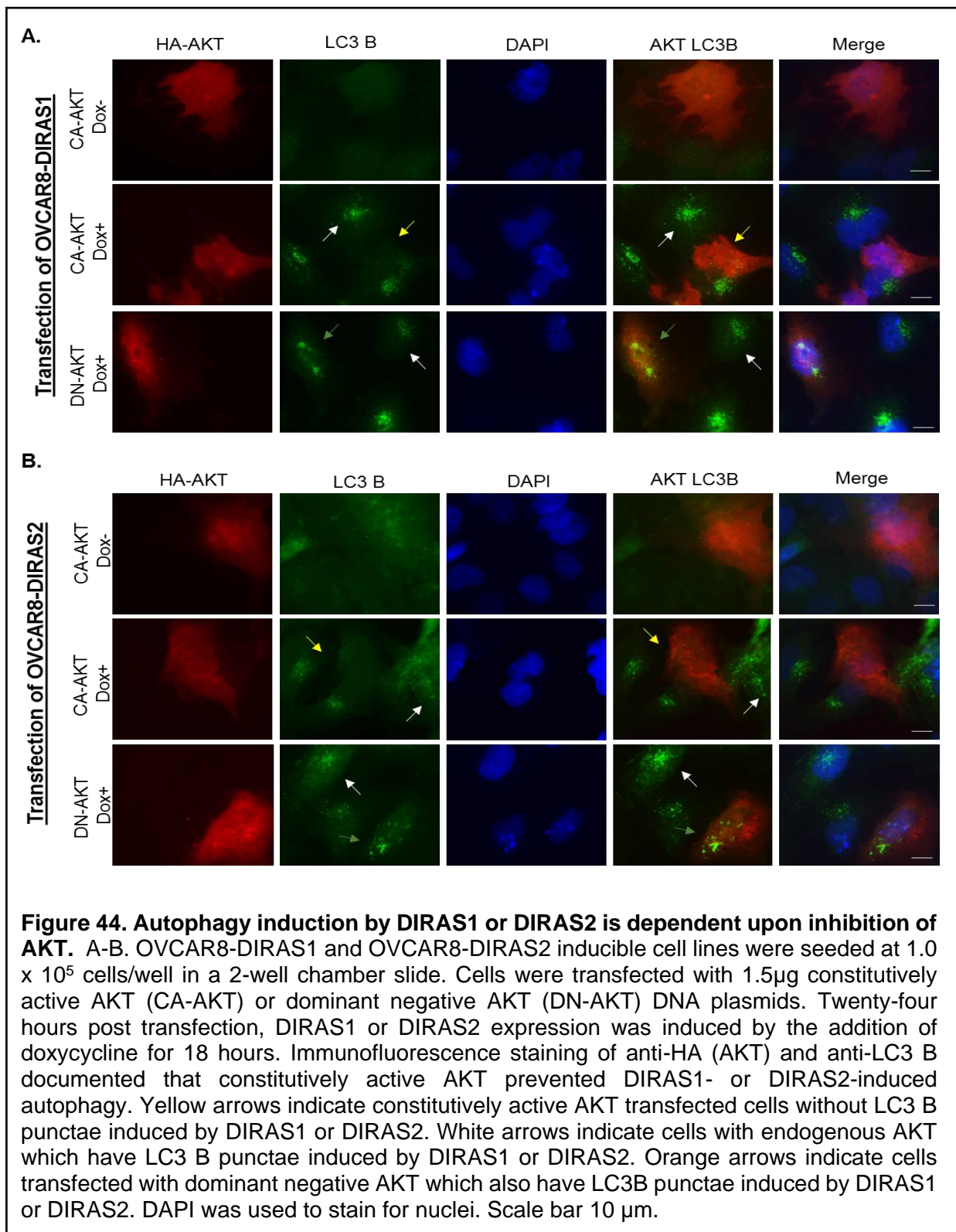
Figure 42. Cartoon documenting the nuclear localization and transcriptional activation of autophagy-related genes by FOXO3a and TFEB. Upon activation of PI3K/AKT and Ras/MAPK signaling pathways transcriptional activation of autophagy by FOXO3a and TFEB is repressed. AKT phosphorylation results in nuclear localization and shuttling of p-FOXo3a from the nucleus where it is bound by 14-3-3 and degraded. Inhibition of AKT results in increased nuclear FOXO3a which can activate gene transcription. AMPK can also stimulate FOXo3a-induced transcription of autophagy-related genes. Ras/MAPK signaling activation and inhibition of TSC1/2 results in increased phosphorylation of TFEB keeping in the in nucleus. When these signals are reversed, TFEB gets dephosphorylated when it can enter the nucleus and bind to a CLEAR domain where it activates transcription of several autophagy-related genes.



expressing DIRAS1 and DIRAS2 on both the phosphoinositide 3-kinase (PI3K) and Ras/MAP kinase signaling pathways. Re-expression of DIRAS1 and DIRAS2 significantly inhibited S473 AKT phosphorylation, S2448 mTOR phosphorylation and 42/44 ERK phosphorylation 24 hours after gene expression (**Figure 43**).

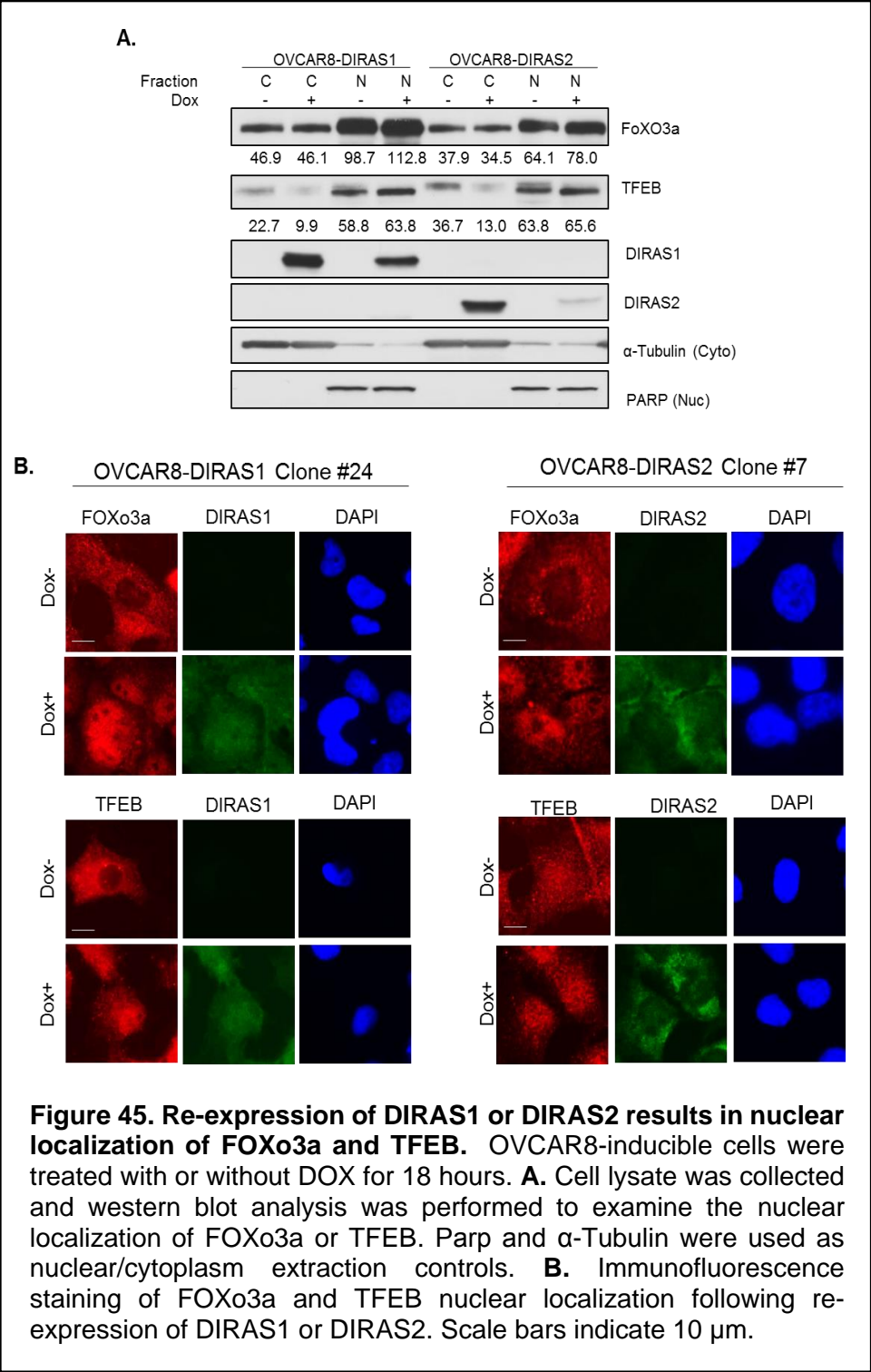
Constitutively active AKT inhibits the induction of autophagy which is induced upon re-expression of DIRAS1 or DIRAS2. The phosphoinositide 3-kinase/AKT/mTOR signaling pathway is a critical signaling node which impacts the induction of autophagy. To examine the functional interaction of DIRAS1 and DIRAS2 with the PI3K/AKT/mTOR signaling pathway, dominant-negative AKT (AKT-DN) which contains three point mutations, S473A, T308A and K179A and constitutively active (AKT-CA) which contains two point mutations, S473D and T308D plasmids were transfected into OVCAR8-inducible cells. Re-

expression of DIRAS1 or DIRAS2 increased LC3 punctae as determined by immunofluorescence staining, and this could be inhibited in cells transfected with constitutively active AKT (**Figure 44**). Transfection of dominant negative AKT had no effect on DIRAS1- or DIRAS2-induced autophagy as determined by LC3 punctae formation (**Figure 44**), which is consistent with the conclusion that autophagy induced by re-expressing the DIRAS family members was, in part, regulated by the PI3K pathway.



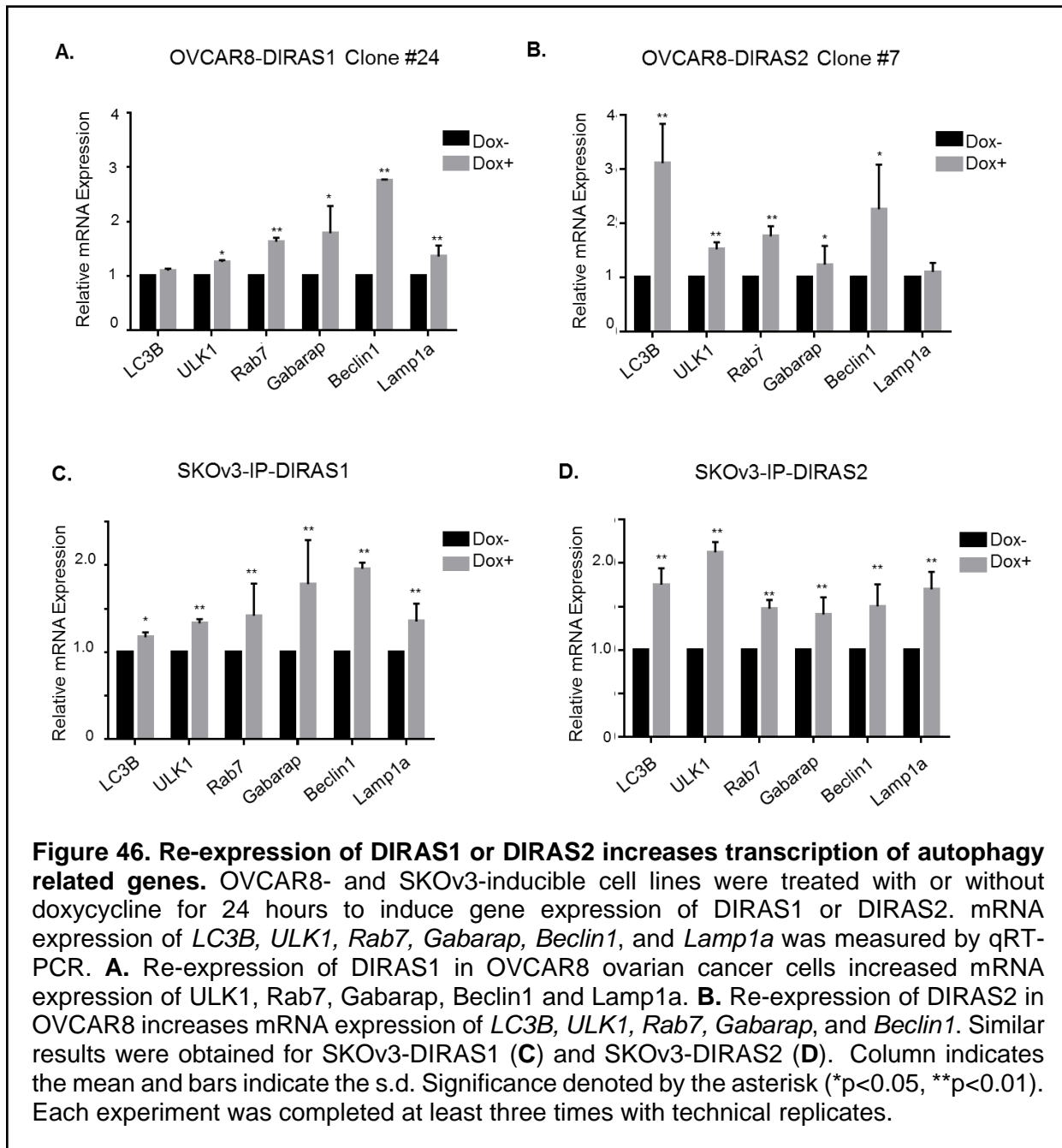
DIRAS1 or DIRAS2 enhance nuclear localization of FOXo3a and TFEB. Re-expression of DIRAS1- or DIRAS2-increased nuclear localization of autophagy-related transcription factors.

Increased nuclear localization of FOXo3a and TFEB was observed by western blot analysis (Figure 45A) and immunofluorescence staining following re-expression of the DIRAS family members (Figure 45B). Alpha-tubulin and PARP were used as cytoplasm and nuclear extract



controls, respectively, for the western blot analysis. Using quantitative real time polymerase chain reaction (qRT-PCR) I observed significant transcriptional upregulation of several key autophagy-related genes including: MAP-LC3 B, ULK1, Rab7, Gabarap, Beclin1 and Lamp1a (Figure 46A-B) at 24 hours post re-expression of DIRAS1 or DIRAS2. The same

was true using SKOv3-IP-inducible ovarian cancer cells (**Figure 46C-D**). However, I did not observe a consistent increase in transcriptional regulation for *Rab11a*, *Atg4*, *Atg12* or *Bnip1* (data not shown). Knockdown of FOXo3a or TFEB by transient siRNA transfection resulted in



decreased autophagy following re-expression of DIRAS1 and DIRAS2 compared to cells transfected with control siRNA, as observed by western blot analysis of p62 and LC3B (**Figures 47A-B**). Similarly, I observed that knockdown of FOXo3a or TFEB in OVCAR8-inducible ovarian

cancer cell lines inhibited the transcription-mediated upregulation of several key autophagy-related proteins (**Figure 47C-D**). Interestingly, knockdown of FOXo3a and TFEB had differential effects suggesting that some compensatory mechanisms might facilitate survival following loss of these regulators of autophagy.

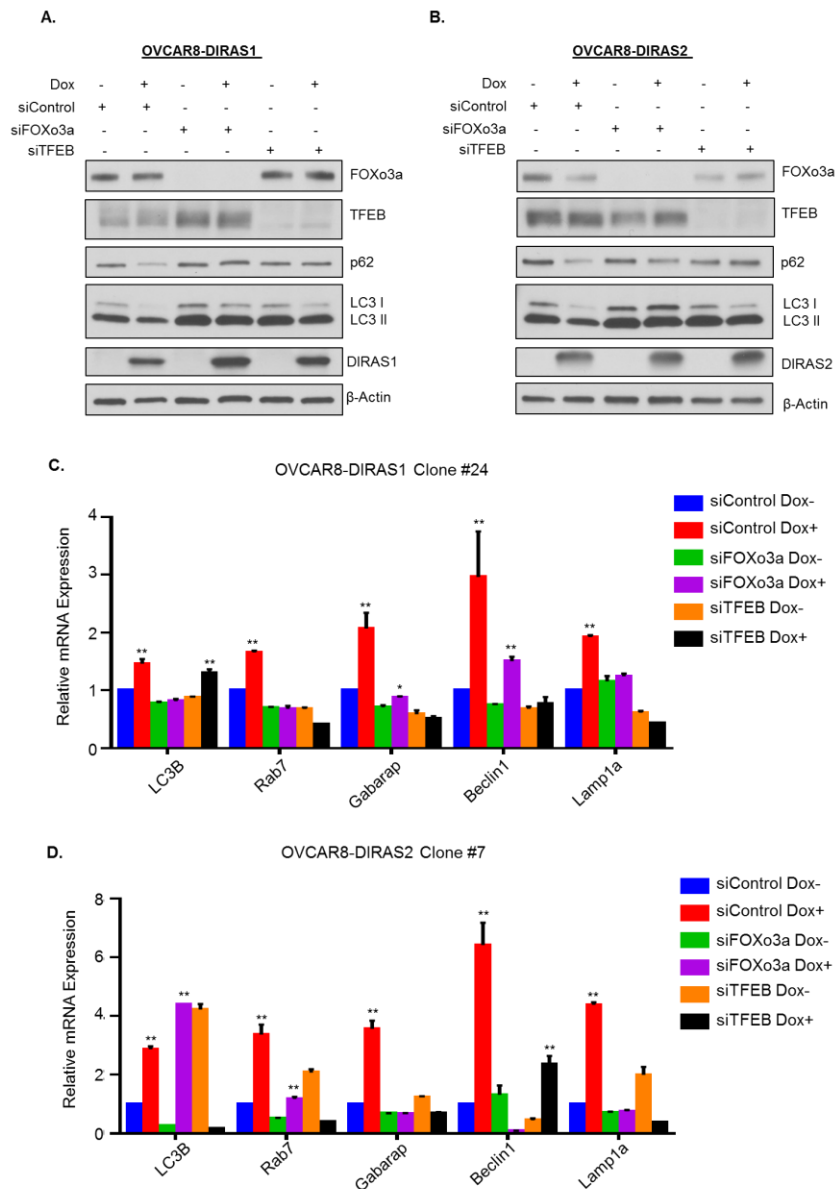
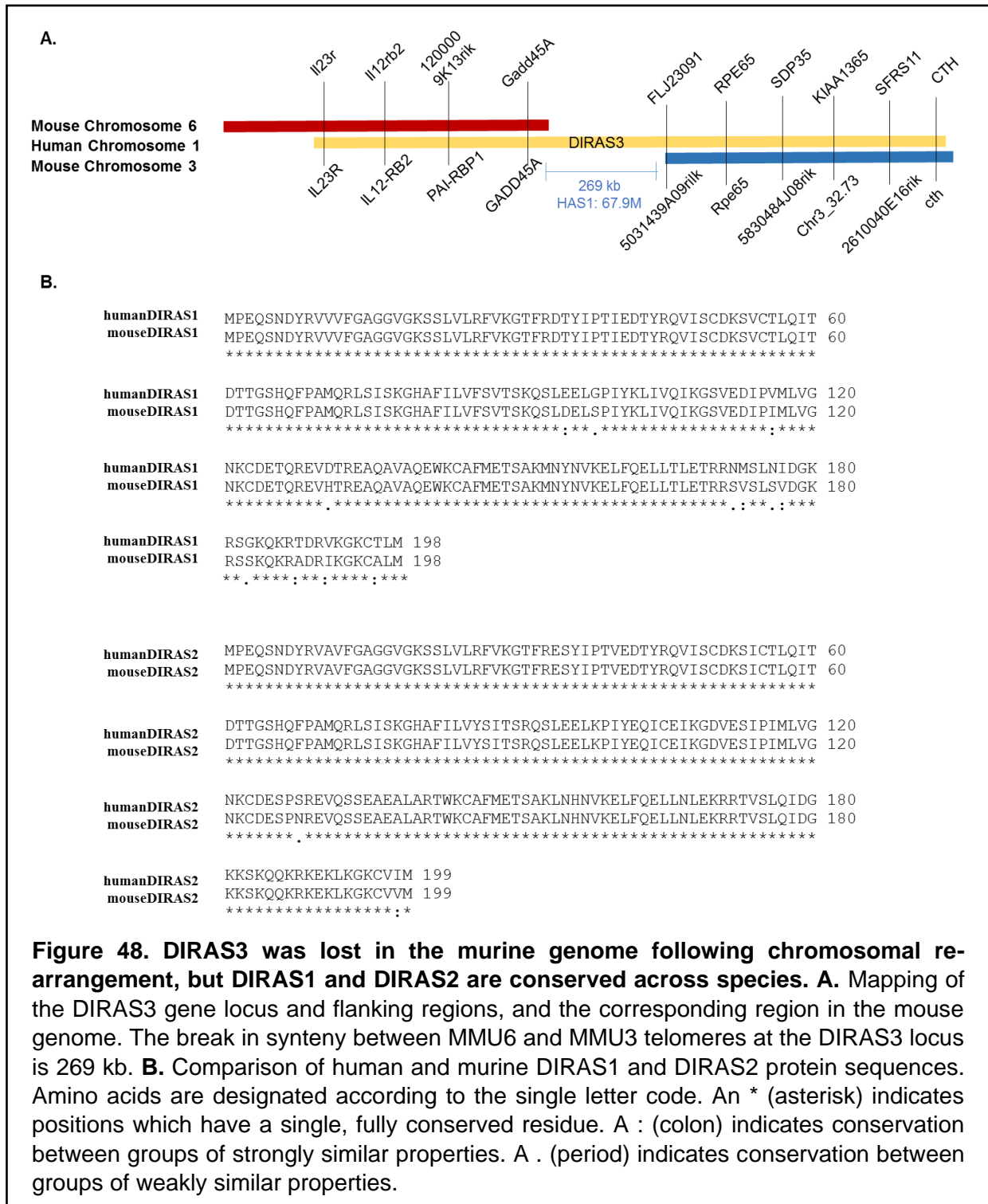


Figure 47. Knockdown of FOXo3a or TFEB inhibits autophagy induced by re-expression of DIRAS1 and DIRAS2. OVCAR8-inducible cells were transfected with siRNA against FOXo3a and TFEB for 18 hours prior to treatment with or without DOX for 18 hours to induce gene expression. **A-B.** Western blot analysis documents the knockdown efficiency, autophagic flux and re-expression of DIRAS1 or DIRAS2. **C-D.** Quantitative RT-PCR quantification of mRNA expression of autophagy-related genes. Column indicates the mean and bars indicate the s.d. Significance denoted by the asterisk (* $p < 0.05$, ** $p < 0.01$). Each experiment was completed at least three times with technical duplicates.

CHAPTER 8

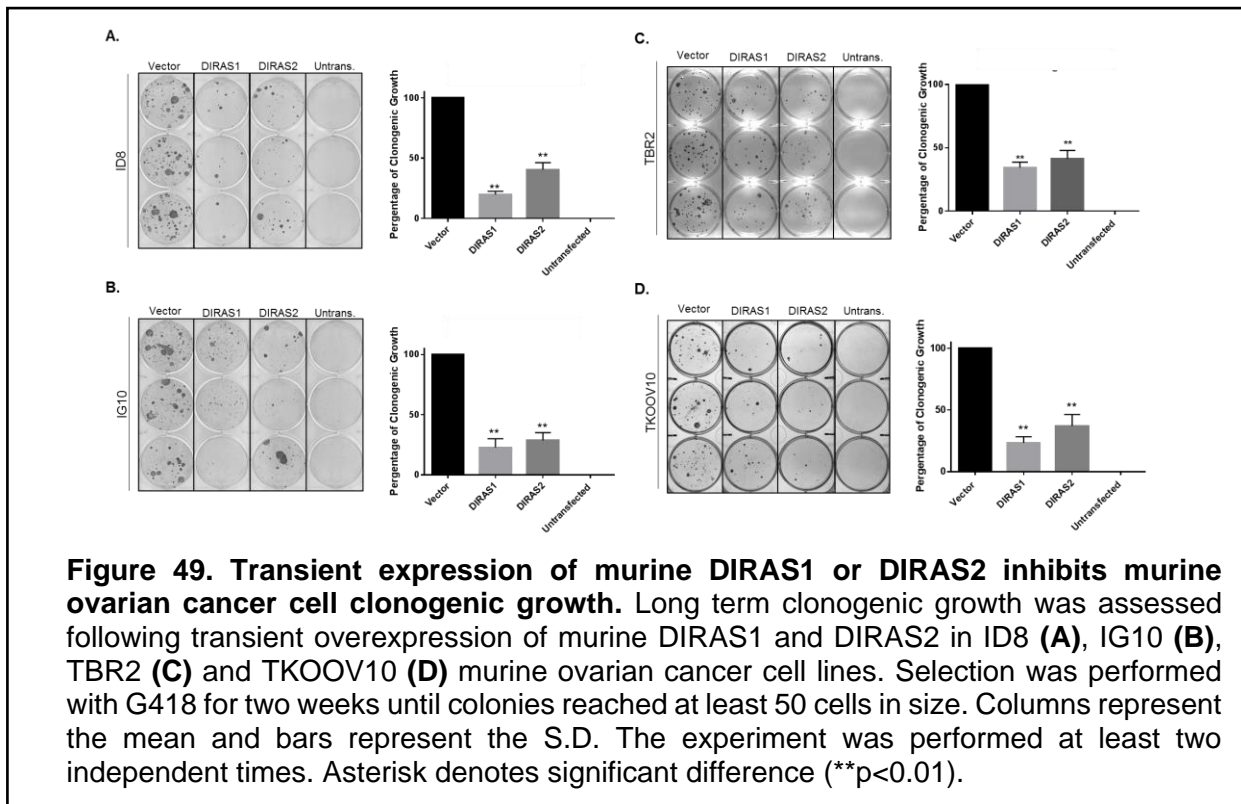
DIRAS1 and DIRAS2 serve as surrogates for DIRAS3 in the murine genome.

Since DIRAS3 was lost during telomeric chromosomal rearrangement (**Figure 48A**) in the murine genome (Fitzgerald and Bateman 2004), some 60 million years ago, we hypothesized that DIRAS1 or DIRAS2 may serve as surrogates for DIRAS3, playing an essential role in the induction of autophagy. DIRAS3 maps to an apparent evolutionary breakpoint in which the



murine genome was re-arranged relative to humans, and is one of several genes in the human but not in the murine genome, including *COL21A1*, *STK17A* and *GPF145*. (Fitzgerald and Bateman 2004) Mapping of the DIRAS3 locus and flanking regions compared to the corresponding region of the mouse genome identified that murine chromosomes 6 and 3 align with genes on either side of DIRAS3. The break in synteny between MMU6 and MMU3 telomeres at the DIRAS3 locus is 269 kb. Murine DIRAS1 and DIRAS2 are 94% and 99%, respectively, homologous to the *homo sapien* proteins, mainly differing at the C-terminus (**Figure 48B**).

Re-expression of DIRAS1 or DIRAS2 induces growth inhibition and autophagy in murine ovarian cancer cells. To determine whether DIRAS1 and DIRAS2 have some of the functions of DIRAS3, I measured the ability of DIRAS1 and DIRAS2 to inhibit cell growth and to induce autophagy in murine ovarian cancer cells. Transient overexpression of murine DIRAS1 and DIRAS2 resulted in long term growth inhibition of TBR2, ID8, IG10 and TKOOV10 murine ovarian cancer cell lines (**Figure 49**). A similar result was obtained using NIH3T3 murine fibroblasts (data



not shown) documenting that growth inhibition following overexpression of DIRAS1 and DIRAS2 is true for both normal and malignant murine cell lines. Transient overexpression of murine DIRAS1 or DIRAS2 resulted in reduction of p62 and increased conversion of LC3 I to LC3 II, which was further confirmed by the addition of chloroquine (**Figure 50**) in a panel of four murine

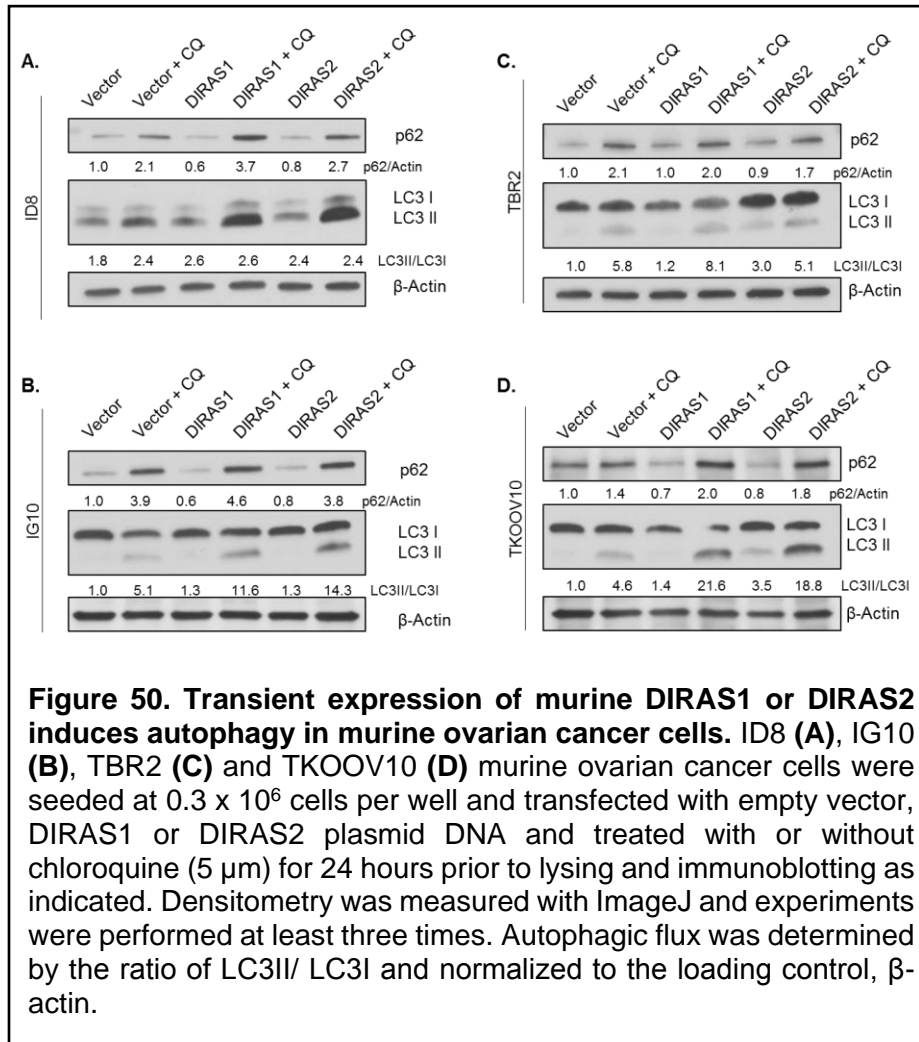


Figure 50. Transient expression of murine DIRAS1 or DIRAS2 induces autophagy in murine ovarian cancer cells. ID8 (A), IG10 (B), TBR2 (C) and TKOOV10 (D) murine ovarian cancer cells were seeded at 0.3×10^6 cells per well and transfected with empty vector, DIRAS1 or DIRAS2 plasmid DNA and treated with or without chloroquine (5 μ M) for 24 hours prior to lysing and immunoblotting as indicated. Densitometry was measured with ImageJ and experiments were performed at least three times. Autophagic flux was determined by the ratio of LC3II/ LC3I and normalized to the loading control, β -actin.

ovarian cancer cell lines. This data is consistent with the previously described increase in autophagic flux observed in human ovarian cancer cell lines following re-expression of DIRAS1 or DIRAS2. Induction of autophagy was confirmed using ultrastructural studies with transmission electron microscopy

(TEM) where I detected scattered classical double membrane vacuolar structures at 18 hours post transfection of murine DIRAS1 or DIRAS2. Typical autophagosomes containing multiple lamellae, intact cytoplasmic structures and residual digested materials were also identified. (**Figure 51**). Previous work from the Bast lab documented the essential role of DIRAS3 in autophagy. Knockdown of DIRAS3 expression in ovarian cancer cells or normal ovarian epithelial

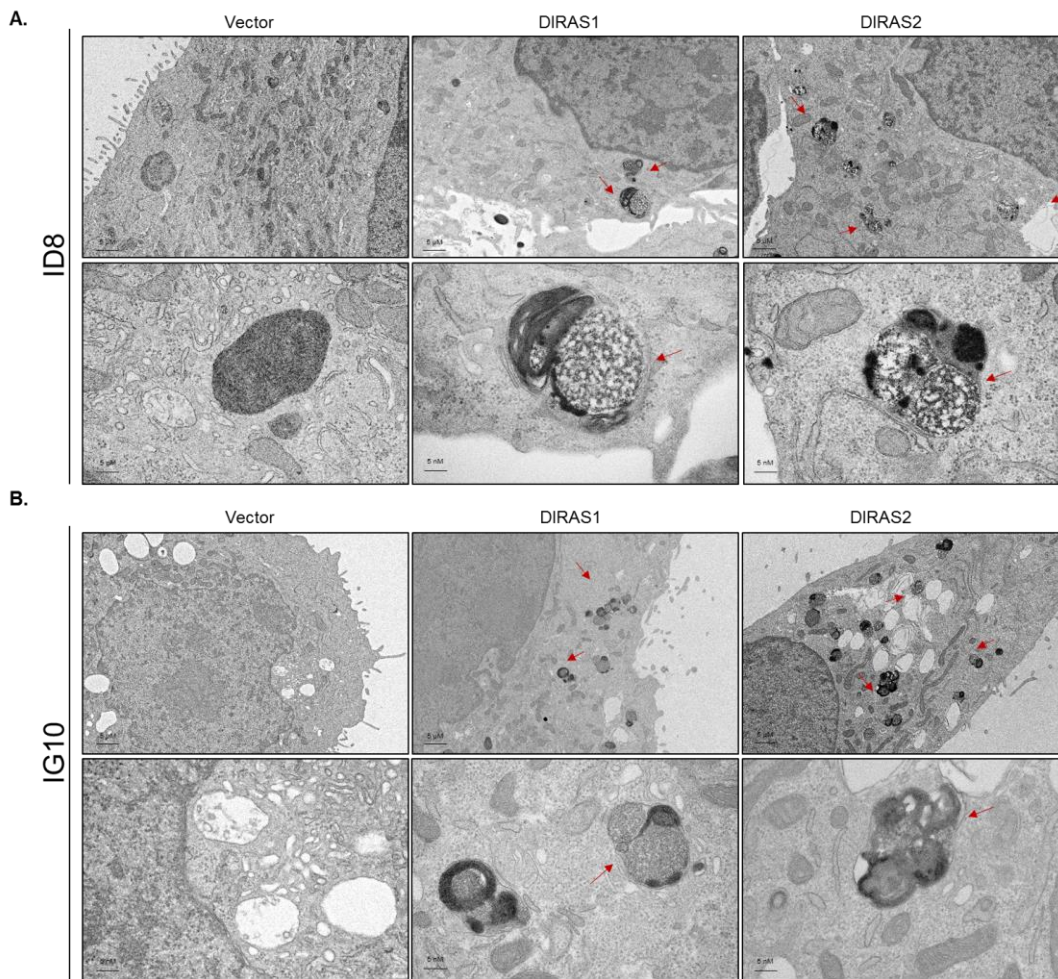
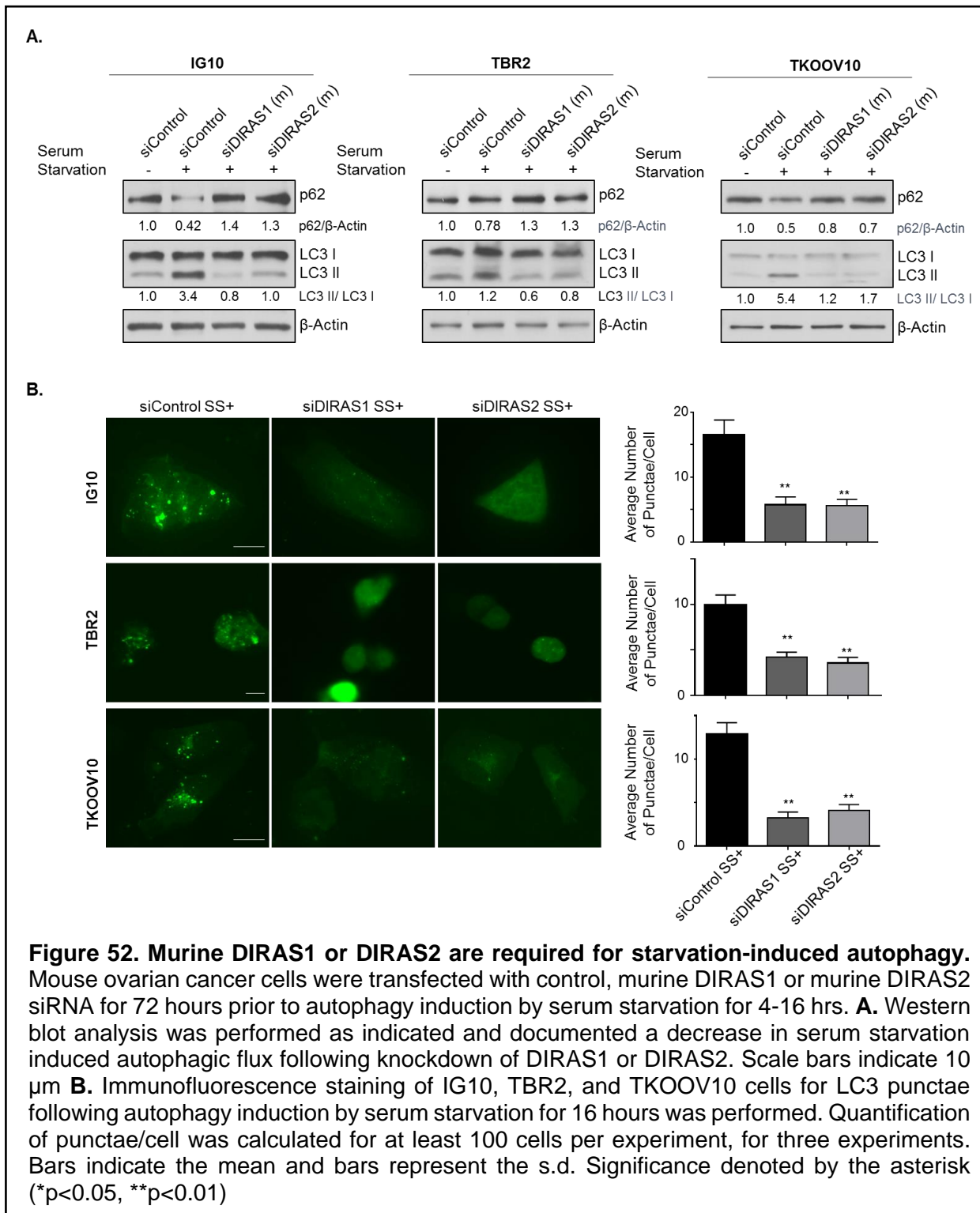


Figure 51. Transient expression of murine DIRAS1 or DIRAS2 induces classical double membrane autophagosomes by electron microscopy. TEM images of ID8 **(A)** and IG10 **(B)** murine ovarian cancer cells were transfected with murine DIRAS1 or DIRAS2 plasmid DNA for 18 hours before fixation. **A-B.** TEM images of ID8 and IG10 cells. Red arrows indicate typical double-membrane autophagosomes. Scale bars: 5 μm and 5 nm for close up image.

scrapings dramatically reduced autophagy and the formation of autophagic vesicles with or without rapamycin treatment to induce autophagy. To determine if DIRAS1 and DIRAS2 were required for murine autophagy, I performed similar experiments on cells that were starved of amino acids for a period of 2-16 hours. I found that autophagy induced by amino acid starvation was inhibited when murine DIRAS1 or murine DIRAS2 was knocked down by siRNA transfection. Upon knockdown I saw decreased conversion LC3 I to LC3 II as compared to siRNA control cells

by western blot analysis (**Figure 52A**) and immunofluorescent staining of LC3 punctae, which represent the membrane-bound form of LC3 on autophagic vesicles, suggesting an essential role for murine DIRAS1 and DIRAS2 in autophagy (**Figure 52B**).



Manipulation of the genetic code to parse out gene function has been a longstanding interest of the scientific community since the discovery of the double helix. Since then, many techniques and technologies have been used to induce, overexpress or knockdown genes, and subsequently their protein products. Early approaches to introduce site-specific modifications depended on the recognition of the DNA by oligonucleotides, self-splicing introns, zinc-finger nucleases and TAL effector nucleases or small molecules. Most recently, a discovery of an RNA-programmable genome engineering system came from understanding the protection mechanisms by which bacteria evade phage. Known as CRISPR-Cas9, this technology originates from type II CRISPR-Cas systems, where the endonuclease, Cas9, introduces site-specific double-strand breaks in the DNA based on a guide sequence within an RNA duplex. This system has been further simplified, where a single guide RNA (sgRNA) can be engineered, replacing the dual tracrRNA:crRNA complex, such that it can bind to DNA at the 5' side, providing specificity to the DNA target site, and it can bind Cas9 at the 3' side. (Doudna and Charpentier 2014) This technology is still being developed to better elucidate the homology-directed repair mechanisms, which are triggered by the double strand break, with the hypothesis that its applications could provide an avenue to successfully revitalize the field of gene therapy. Using the CRISPR-Ca9 gene editing system, I created whole genome knockout of DIRAS1 or DIRAS2 murine embryos (**Figure 53**) and implanted them into surrogate females. Following several backcross generations to eliminate off-target effects, I evaluated the F2 generation offspring for genetic and phenotypic effects. I observed that in both cases, germline incorporation had occurred but the offspring did not follow Mendelian order, and no homozygous offspring were birthed (**Figure 53**). To determine if the pups were dying in early infancy due to the lack of autophagy sustaining life prior to colostrum production, I performed C-sections at gestational day 18.5 and placed the liter with a surrogate mother, but still no homozygous knockout offspring were seen. To determine the day of embryonic lethality, I euthanized pregnant females at several

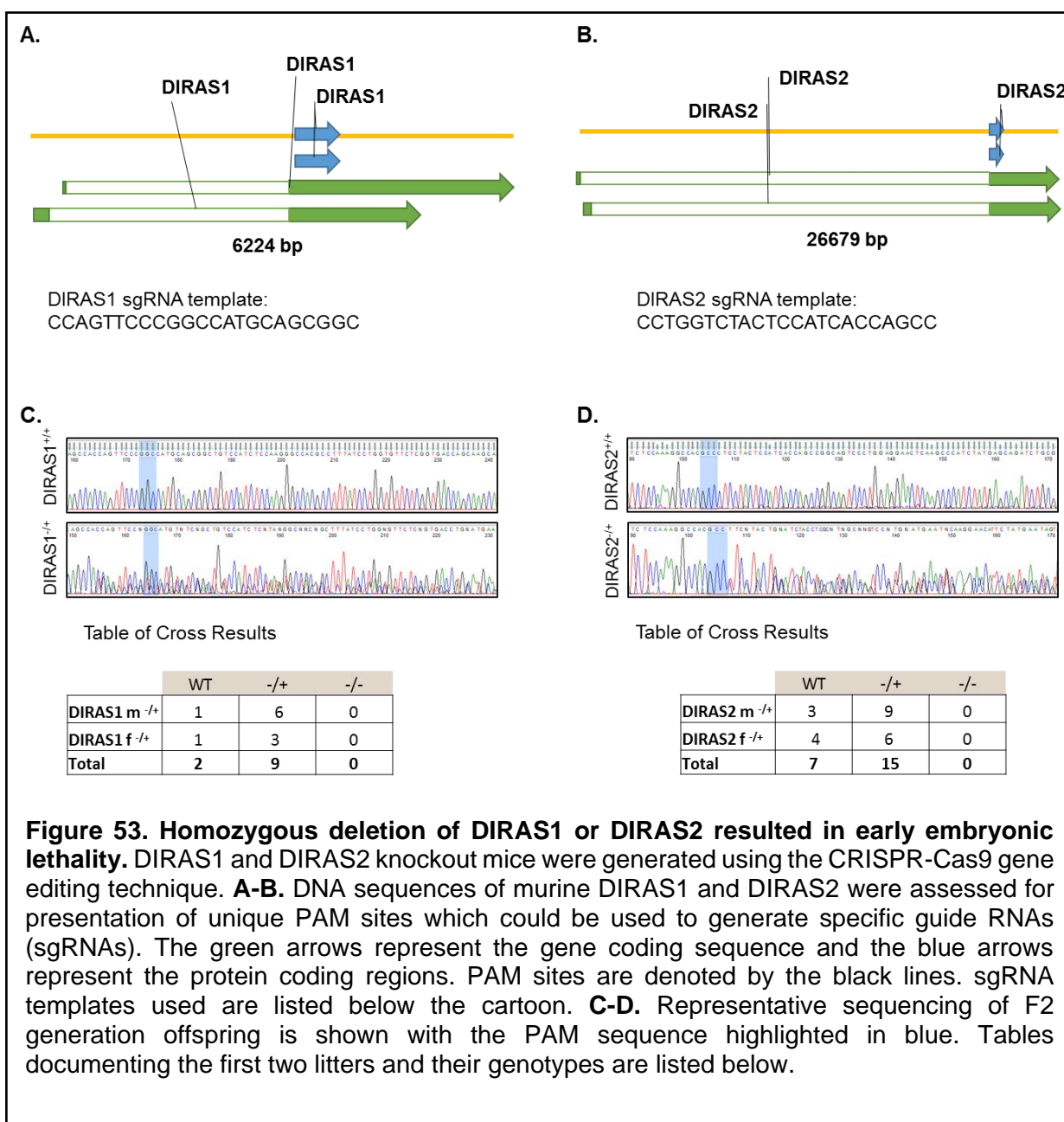


Figure 53. Homozygous deletion of DIRAS1 or DIRAS2 resulted in early embryonic lethality. DIRAS1 and DIRAS2 knockout mice were generated using the CRISPR-Cas9 gene editing technique. **A-B.** DNA sequences of murine DIRAS1 and DIRAS2 were assessed for presentation of unique PAM sites which could be used to generate specific guide RNAs (sgRNAs). The green arrows represent the gene coding sequence and the blue arrows represent the protein coding regions. PAM sites are denoted by the black lines. sgRNA templates used are listed below the cartoon. **C-D.** Representative sequencing of F2 generation offspring is shown with the PAM sequence highlighted in blue. Tables documenting the first two litters and their genotypes are listed below.

gestational time points, critical for organ development. No homozygous knockout pups were seen at 10.5 days or later, suggesting likely early embryonic lethality. As others have previously reported, autophagy is increased following fertilization of the egg resulting in stalled development of preimplantation mouse embryos which are autophagy deficient. (Tsukamoto, Kuma et al. 2008) Further analysis of blasts will be necessary to determine if homozygous loss of DIRAS1 or DIRAS2 results in an arrested blast phenotype and whether the ability to induce autophagy is impaired.

CHAPTER 9

Discussion and Future Directions

The *DIRAS* family members have been identified as ovarian cancer tumor suppressors and inhibitors of Ras-induced transformation. These Ras-related small GTPases have an N-terminal extension, which distinguishes them from other members of the Ras superfamily. Previous studies report that DIRAS3, the best characterized of the DIRAS family, is downregulated in multiple tumor types including lung, pancreatic, thyroid, breast and ovarian cancer where its expression is associated with increased progression-free survival. (Weber, Aldred et al. 2005, Yu, Luo et al. 2006, Dalai, Missiaglia et al. 2007, Huang, Lin et al. 2009, Lin, Cui et al. 2011, Wu, Liang et al. 2013) As DIRAS3 was lost from the murine genome ~60 million years ago, classical knockout experiments have not been feasible to demonstrate its function as a murine tumor suppressor. (Fitzgerald and Bateman 2004) Experiments performed above have documented, for the first time, that DIRAS3, as well as DIRAS1 and DIRAS2, can suppress transformation of NIH3T3 murine fibroblasts and partially transformed MCF10a breast epithelial cells by RasG12V.

DIRAS1, DIRAS2 and DIRAS3 serve as natural antagonists of Ras/MAPK signaling, likely by direct binding and disruption of Ras-Ras association and multimerization. While many tumor suppressors have been shown to regulate oncogenesis through mechanisms including cell cycle arrest, programmed cell death, repairing DNA damage and inhibiting metastasis, to my knowledge this is the first instance where a tumor suppressor protein binds directly to an oncogene protein to reverse oncogenic function. In this dissertation, I demonstrate that re-expression of DIRAS3 inhibits clonogenic growth of Ras-dependent cancer cells across multiple cancer types, including cancers that originate in the pancreas, lung and ovary. Growth inhibition is associated with decreased p-ERK signaling and knockdown of endogenous DIRAS3 can reverse this phenotype. As Ras mutations are found in approximately 30% of all cancer cases and increased reports describe downregulation of DIRAS3 across multiple tumor sites, these data suggest that greater understanding of this signaling axis may provide novel therapeutic opportunities to target mutant Ras. My observations revealed that the 34-amino acid N-terminal

extension of DIRAS3 is not required for binding, but is critical for inhibiting transformation, for disrupting Ras clusters, as well as for the tumor suppressive functions previously reported. I documented that this antagonistic relationship may be related to the interaction of DIRAS3 and K-Ras on the plasma membrane. Using immunoprecipitation, Duo-link in-situ hybridization, peptide-array analysis, split-luciferase complementation, immunofluorescence, STORM and gold-labeled EM, we identified co-localization of DIRAS3 and K-Ras on the plasma membrane. While blocking of transformation, inhibition of clonogenic growth and induction of autophagy required both the N-terminus and CAAX membrane anchoring domain of DIRAS3, binding of DIRAS3 to Ras was dependent upon the CAAX membrane anchoring domain of DIRAS3, but did not require the N-terminus or the myristolation site found in the N-terminal extension. Addition of the N-terminus from DIRAS3 directly to the N-terminal end of mutant Ras can inhibit oncogenic function and downstream effector signaling, highlighting the importance of the N-terminus for suppressor function. Using murine fibroblasts and human epithelial cells, I demonstrated that DIRAS3 can suppress transformation driven by mutant H- or K-Ras, and both the N-terminal extension and CAAX membrane anchoring domains are necessary for the suppression. Although the precise mechanism by which this N-terminal region antagonizes Ras function remains unclear, my data suggest several potential possibilities including increased stabilization of the protein-protein interactions, trafficking to an alternative location on the plasma membrane, disruption of Ras-effector binding, or altering the GTP-bound state of Ras, through GEFs, GAPs, or by altering intrinsic GTPase activity. Future work to determine the membrane localization dynamics following nucleoside exchange, and other Ras-protein interactions will be critical to determine the therapeutic potential of targeting mutant Ras.

My studies demonstrate for the first time that DIRAS3 can disrupt Ras multimerization and clustering, associated with decreased Ras signaling through ERK. Although recent work has indicated GTP activation following Ras dimerization and many previous reports have shown increased signaling with constitutively active Ras, it is not clear whether the number of Ras

multimers is directly correlated with the amount of GTP-bound Ras within the cell. (Harmon, Nielsen et al. 1985, Nan, Tamguney et al. 2015) Additional evidence is mounting to suggest that oligomerization of Ras at different regions within the plasma membrane results in differential functions, suggesting that other effector molecules likely cooperate in the trafficking and spatial orientation resulting in activation of this critical signaling axis. (Zhou, Prakash et al. 2017) As previously documented, H-Ras or K-Ras increased cluster size when stimulated by EGF, Gal-1, mutations of the Ras switch II region, or changes in Ras S181 phosphorylation, associated with increased signal output as determined by increased Raf and pErk activity. (Zhou, Liang et al. 2014, Solman, Ligabue et al. 2015, Zhou, Wong et al. 2015) My data suggest that the inhibition of Sos-1 and GTP-bound Ras by DIRAS3 may serve as a critical step in the membrane clustering assembly which results in increased effector signaling.

Distinguishing effectors that regulate Ras-driven signaling in tumors remains a great challenge. The interaction between DIRAS3 and Ras provides a novel approach to target this signaling axis, which drives multiple malignancies, however, future work to determine the mechanism by which DIRAS3 regulates Ras clustering on the plasma membrane is critical to the success of translating these findings to clinical therapies. Peptides or small molecules that mimic DIRAS3 activity could target the function of mutant Ras directly and specifically, filling a significant unmet clinical need for Ras inhibitors.

In addition to affecting Ras clustering, I found that DIRAS1 and DIRAS2 also induce autophagy at several levels and likely serve as surrogates to DIRAS3 in the murine genome. Knockdown of DIRAS1 or DIRAS2 prevents induction of starvation induced autophagy, consistent with their being required for murine autophagy, similar to the requirement for DIRAS3 to induce autophagy in human cells. Under nutrient poor or stressful conditions such as hypoxia and DNA damage, autophagy is elicited to help maintain cellular homeostasis. These conditions result in a transcriptional response of FOXo3a and TFEB, which trigger transcriptional expression of autophagy-related proteins. Re-expression of DIRAS1 or DIRAS2 alters intracellular signaling

pathways that favor autophagy. Expression of DIRAS1 or DIRAS2 downregulates both the PI3K/AKT and Ras/MAPK pathways, as observed by decreased p-AKT and p-ERK protein expression, both of which have downstream effects on mTOR. (He and Klionsky 2010)

The significance of this inhibition is underlined by the ability of DIRAS1 or DIRAS2 to regulate autophagy by modulating nuclear localization of FOXO3a and TFEB, two master regulators of autophagy-related transcription. The dual role of these pathways to maintain cellular homeostasis through autophagy regulation is highlighted as upregulation of one pathway occurs following reciprocal knockdown with siRNA. In response to DIRAS1 or DIRAS2 expression, I observed increased transcription of *LC3B*, *ULK1*, *Rab7*, *Gabarap*, *Beclin1* and *Lamp1a*, which was dependent upon FOXo3a and TFEB nuclear localization. While DIRAS3 has been shown to regulate FOXo3a-mediated upregulation of ATG4, LC3 and Rab7, (Lu, Yang et al. 2014) DIRAS1 and DIRAS2 increase several additional autophagy-related genes, most notably those involved in lysosomal fusion. This is in line with my experimental results which show rapid progression through autophagy that is highlighted by a large increase in LC3 II conversion following the addition of chloroquine, a lysosomotropic agent which inhibits lysosomal hydrolases and prevents autophagosomal fusion and degradation LC3 and the contents of the autophagosome. All three members of the DIRAS family have multiple LC3-interacting regions (LIR) domains (Kalvari, Tsompanis et al. 2014), but based on my immunofluorescence staining of LC3II and DIRAS1 or DIRAS2, there does not seem to be significant co-localization between the two proteins, unlike the co-localization of DIRAS3 with LC3II. (Lu, Luo et al. 2008) Co-localization with LC3II does not seem to be the only difference between DIRAS1/DIRAS2 and DIRAS3. DIRAS3 has been well characterized as a member of the AIC (Lu, Baquero et al. 2014) but immunoprecipitation of DIRAS1 or DIRAS2 did not show co-localization with Beclin1 (data not shown). While the effect of DIRAS1 and DIRAS2 on Beclin1 homodimerization remains to be tested, this direct interaction may account for the weaker induction of autophagy as seen following re-expression of DIRAS1 or DIRAS2 compared to DIRAS3, in ovarian cancer cells. As

members of the Bast lab previously reported that the N-terminus of DIRAS3 may be important for the disruption of Beclin1-Bcl2 interaction, the shorter N-termini of DIRAS1 and DIRAS2 lacking the leucine-rich, hydrophobic domain might account for the differences in the mechanisms by which DIRAS1 and DIRAS2 induce autophagy compared to DIRAS3.

Genetically engineered mouse models generated by multiple approaches targeting autophagy-related genes have been used to better understand mammalian development and adult tissue homeostasis. Homozygous depletion of Ambra1, Atg5, and Beclin1, just to name a few, resulted in early embryonic lethality, suggesting a key developmental role for autophagy. (Qu, Yu et al. 2003, Fimia, Stoykova et al. 2007, Tsukamoto, Kuma et al. 2008) Tsukamoto et. al. used mice expressing green fluorescent protein (GFP)-fused LC3 (mammalian Atg8 homology), to document the induction of autophagy following fertilization, demonstrating how maternal proteins in oocytes can be degraded permitting expression of the zygote genome. (Tsukamoto, Kuma et al. 2008) Homozygous deletion of murine DIRAS1 or DIRAS2 resulted in early embryonic lethality. While these complex phenotypes may not only represent the role of autophagy, but also gene specific functions, they emphasize the importance of DIRAS1 and DIRAS2 in murine development. Future studies to determine the long-term phenotypes associated with heterozygous loss of DIRAS1 or DIRAS2 are underway. As others have previously reported, autophagy is increased following fertilization of the egg resulting in stalled development of preimplantation mouse embryos which are autophagy deficient. Based on these findings, observation of DIRAS1^{-/-} or DIRAS2^{-/-} embryos from the 2-cell stage and beyond should be completed to determine if knockdown of either of these two genes results in halted cell division or decreased cellular autophagy.

Although mutations in key autophagy-related genes are not seen widely across cancers, the role of autophagy to suppress tumorigenesis was discovered through loss of Beclin1 in breast, ovary and prostate cancers. (Liang, Jackson et al. 1999) In a mouse model, homozygous loss of Beclin1 resulted in prenatal lethality and heterozygous loss of Beclin1 resulted in

premature death, reduced autophagy and an increased incidence of lung carcinomas, hepatocellular carcinomas and lymphomas. (Yue, Jin et al. 2003) These data provide evidence that autophagy could serve as a tumor suppressive mechanism. Similarly, many other well characterized tumor suppressors, such as *PTEN*, *AMPK*, *LKB1* and *TSC1/2* all negatively regulate the protein kinase target of rapamycin (mTOR) and induce autophagy. The overlap in signaling cascades between regulation of autophagy and the control of cancer, provide mechanisms by which tumor suppressors and oncogenes can participate in this process, and adds to the complexity of the role of autophagy in oncogenesis. On the one hand, inhibition of autophagy has been shown to promote oxidative stress, genomic instability and oncogenesis, while on the other, autophagy protects the cancer cell from hypoxia and nutrient starvation which can promote resistance to chemotherapy in established tumors. (Avalos, Canales et al. 2014) In all cases, the induction of autophagy by mTOR inhibition seems to be a pivotal step leading to the digestion of cytoplasmic contents.

Consistent with the role of autophagy as a tumor suppressive mechanism, DIRAS1 and DIRAS2 protein expression correlated with both increased overall and progression-free survival in a cohort of ovarian cancer patients, whereas DIRAS3 downregulation was only associated with progression-free survival. Unlike DIRAS3, DIRAS1 and DIRAS2 are not imprinted genes, so the extent of downregulation may be less frequent where two hits are required. Future studies of the mechanisms by which DIRAS1 and DIRAS2 are downregulated needs to be performed. To this extent, sequence predictions document that miR221 and miR222 would likely recognize all three DIRAS family members and therefore one would hypothesize that those cases where DIRAS3 is downregulated by this mechanism might also show downregulation of DIRAS1 and DIRAS2. Immunohistochemical staining analysis of DIRAS1 and DIRAS2 across normal organs suggest differential expression, however all three DIRAS family members had relatively strong expression in normal pancreas, breast, kidney and adrenal gland. As DIRAS3 is downregulated in multiple tumor types, there may be a potential tumor suppressive role for DIRAS1 and DIRAS2

in other cancers, providing another avenue worth future exploration. DIRAS3-induced autophagy has been implicated in the induction of tumor dormancy *in vivo*, further studies to characterize the role of DIRAS1 or DIRAS2 as they relate to tumor dormancy could provide additional models and greater understanding of this process which often results in untreatable, resistant disease.

In conclusion, the data presented tested the hypothesis that the DIRAS family members inhibit Ras activity by binding directly to Ras and disrupting Ras multimerization. More specifically documenting that the N-terminus and CAAX membrane anchoring domain of DIRAS3 are essential for the suppressive function observed, highlighting a novel mechanism of tumor suppression which depends on direct interaction and antagonism of an oncogene. The N-terminus of DIRAS3 also plays a critical role in the mechanism(s) by which DIRAS3 induces autophagy. I also tested the hypotheses that DIRAS1 and DIRAS2 share some of the function(s) of DIRAS3, serving as ovarian cancer tumor suppressors by inhibiting proliferation and motility and inducing autophagic cell death and that they can serve as surrogates for DIRAS3 in the murine genome, playing an essential role in murine autophagy. This work establishes the role of DIRAS1 and DIRAS2 as tumor suppressors and highlights their importance in the murine genome. DIRAS1, 2, and 3, share the ability to inhibit cell proliferation and Ras-driven transformation while inducing autophagic cell death *in vitro*. Mechanistically, DIRAS1 and DIRAS2 induce autophagy by inhibition of the Ras/MAPK and PI3K/AKT/mTOR signaling pathways and inducing transcriptional activation of autophagy-related genes by FOXo3a and TFEB. Differing from DIRAS3, DIRAS1 and DIRAS2 do not appear to be critical members of the AIC nor do they co-localize with LC3B by immunofluorescence. Homozygous loss of DIRAS1 or DIRAS2 resulted in early embryonic lethality in mice and knockdown of murine DIRAS1 and DIRAS2 reduced starvation-induced autophagy in murine ovarian cancer cells. These studies demonstrate the importance of the N-terminal and CAAX domains of the DIRAS family members and provide novel insight into their tumor suppressive function, as well as their essential role in murine autophagy.

BIBLIOGRAPHY

- Aletti, G. D., S. C. Dowdy, K. C. Podratz and W. A. Cliby (2007). "Relationship among surgical complexity, short-term morbidity, and overall survival in primary surgery for advanced ovarian cancer." Am J Obstet Gynecol **197**(6): 676 e671-677.
- An, L., X. Zhao, J. Wu, J. Jia, Y. Zou, X. Guo, L. He and H. Zhu (2012). "Involvement of autophagy in cardiac remodeling in transgenic mice with cardiac specific over-expression of human programmed cell death 5." PLoS One **7**(1): e30097.
- Asanuma, K., I. Tanida, I. Shirato, T. Ueno, H. Takahara, T. Nishitani, E. Kominami and Y. Tomino (2003). "MAP-LC3, a promising autophagosomal marker, is processed during the differentiation and recovery of podocytes from PAN nephrosis." FASEB J **17**(9): 1165-1167.
- Ashworth, A., F. Balkwill, R. C. Bast, J. S. Berek, A. Kaye, J. A. Boyd, G. Mills, J. N. Weinstein, K. Woolley and P. Workman (2008). "Opportunities and challenges in ovarian cancer research, a perspective from the 11th Ovarian cancer action/HHMT Forum, Lake Como, March 2007." Gynecol Oncol **108**(3): 652-657.
- Avalos, Y., J. Canales, R. Bravo-Sagua, A. Criollo, S. Lavandero and A. F. Quest (2014). "Tumor suppression and promotion by autophagy." Biomed Res Int **2014**: 603980.
- Baker, S. J., E. R. Fearon, J. M. Nigro, S. R. Hamilton, A. C. Preisinger, J. M. Jessup, P. vanTuinen, D. H. Ledbetter, D. F. Barker, Y. Nakamura, R. White and B. Vogelstein (1989). "Chromosome 17 deletions and p53 gene mutations in colorectal carcinomas." Science **244**(4901): 217-221.
- Baker, S. J., S. Markowitz, E. R. Fearon, J. K. Willson and B. Vogelstein (1990). "Suppression of human colorectal carcinoma cell growth by wild-type p53." Science **249**(4971): 912-915.
- Baljuls, A., M. Beck, A. Oenel, A. Robubi, R. Kroschewski, M. Hekman, T. Rudel and U. R. Rapp (2012). "The tumor suppressor DiRas3 forms a complex with H-Ras and C-RAF proteins and

regulates localization, dimerization, and kinase activity of C-RAF." J Biol Chem **287**(27): 23128-23140.

Benedict, W. F., A. L. Murphree, A. Banerjee, C. A. Spina, M. C. Sparkes and R. S. Sparkes (1983). "Patient with 13 chromosome deletion: evidence that the retinoblastoma gene is a recessive cancer gene." Science **219**(4587): 973-975.

Bergom, C., A. D. Hauser, A. Rymaszewski, P. Gonyo, J. W. Prokop, B. C. Jennings, A. J. Lawton, A. Frei, E. L. Lorimer, I. Aguilera-Barrantes, A. C. Mackinnon, Jr., K. Noon, C. A. Fierke and C. L. Williams (2016). "The tumor-suppressive small GTPase DiRas1 binds the noncanonical guanine nucleotide exchange factor SmgGDS and antagonizes SmgGDS interactions with oncogenic small GTPases." J Biol Chem **291**(20): 10948.

Bergom, C., A. D. Hauser, A. Rymaszewski, P. Gonyo, J. W. Prokop, B. C. Jennings, A. J. Lawton, A. Frei, E. L. Lorimer, I. Aguilera-Barrantes, A. C. Mackinnon, K. Noon, C. A. Fierke and C. L. Williams (2016). "The Tumor-suppressive Small GTPase DiRas1 Binds the Noncanonical Guanine Nucleotide Exchange Factor SmgGDS and Antagonizes SmgGDS Interactions with Oncogenic Small GTPases." J Biol Chem **291**(12): 6534-6545.

Bieging, K. T. and L. D. Attardi (2012). "Deconstructing p53 transcriptional networks in tumor suppression." Trends Cell Biol **22**(2): 97-106.

Buhrman, G., G. Holzapfel, S. Fetics and C. Mattos (2010). "Allosteric modulation of Ras positions Q61 for a direct role in catalysis." Proc Natl Acad Sci U S A **107**(11): 4931-4936.

Cavenee, W. K., T. P. Dryja, R. A. Phillips, W. F. Benedict, R. Godbout, B. L. Gallie, A. L. Murphree, L. C. Strong and R. L. White (1983). "Expression of recessive alleles by chromosomal mechanisms in retinoblastoma." Nature **305**(5937): 779-784.

Cecconi, F. and B. Levine (2008). "The role of autophagy in mammalian development: cell makeover rather than cell death." Dev Cell **15**(3): 344-357.

- Cherfils, J. and M. Zeghouf (2013). "Regulation of small GTPases by GEFs, GAPs, and GDIs." Physiol Rev **93**(1): 269-309.
- Clark, G. J., A. D. Cox, S. M. Graham and C. J. Der (1995). "Biological assays for Ras transformation." Methods Enzymol **255**: 395-412.
- Cooper, G. M. and P. E. Neiman (1980). "Transforming genes of neoplasms induced by avian lymphoid leukosis viruses." Nature **287**(5783): 656-659.
- Crum, C. P., R. Drapkin, A. Miron, T. A. Ince, M. Muto, D. W. Kindelberger and Y. Lee (2007). "The distal fallopian tube: a new model for pelvic serous carcinogenesis." Curr Opin Obstet Gynecol **19**(1): 3-9.
- Cuervo, A. M. and E. Wong (2014). "Chaperone-mediated autophagy: roles in disease and aging." Cell Res **24**(1): 92-104.
- Dalai, I., E. Missiaglia, S. Barbi, G. Butturini, C. Doglioni, M. Falconi and A. Scarpa (2007). "Low expression of ARHI is associated with shorter progression-free survival in pancreatic endocrine tumors." Neoplasia **9**(3): 181-183.
- Der, C. J., T. G. Krontiris and G. M. Cooper (1982). "Transforming genes of human bladder and lung carcinoma cell lines are homologous to the ras genes of Harvey and Kirsten sarcoma viruses." Proc Natl Acad Sci U S A **79**(11): 3637-3640.
- Doudna, J. A. and E. Charpentier (2014). "Genome editing. The new frontier of genome engineering with CRISPR-Cas9." Science **346**(6213): 1258096.
- Edelstein, A., N. Amodaj, K. Hoover, R. Vale and N. Stuurman (2010). "Computer control of microscopes using microManager." Curr Protoc Mol Biol **Chapter 14**: Unit14 20.
- Ellis, C. A., M. D. Vos, H. Howell, T. Vallecorsa, D. W. Fults and G. J. Clark (2002). "Rig is a novel Ras-related protein and potential neural tumor suppressor." Proc Natl Acad Sci U S A **99**(15): 9876-9881.

Espey, D. K., X. C. Wu, J. Swan, C. Wiggins, M. A. Jim, E. Ward, P. A. Wingo, H. L. Howe, L. A. Ries, B. A. Miller, A. Jemal, F. Ahmed, N. Cobb, J. S. Kaur and B. K. Edwards (2007). "Annual report to the nation on the status of cancer, 1975-2004, featuring cancer in American Indians and Alaska Natives." Cancer **110**(10): 2119-2152.

Feng, W., R. T. Marquez, Z. Lu, J. Liu, K. H. Lu, J. P. Issa, D. M. Fishman, Y. Yu and R. C. Bast, Jr. (2008). "Imprinted tumor suppressor genes ARHI and PEG3 are the most frequently down-regulated in human ovarian cancers by loss of heterozygosity and promoter methylation." Cancer **112**(7): 1489-1502.

Fetics, S. K., H. Guterres, B. M. Kearney, G. Buhrman, B. Ma, R. Nussinov and C. Mattos (2015). "Allosteric effects of the oncogenic RasQ61L mutant on Raf-RBD." Structure **23**(3): 505-516.

Fimia, G. M., A. Stoykova, A. Romagnoli, L. Giunta, S. Di Bartolomeo, R. Nardacci, M. Corazzari, C. Fuoco, A. Ucar, P. Schwartz, P. Gruss, M. Piacentini, K. Chowdhury and F. Cecconi (2007). "Ambra1 regulates autophagy and development of the nervous system." Nature **447**(7148): 1121-1125.

Finlay, C. A., P. W. Hinds and A. J. Levine (1989). "The p53 proto-oncogene can act as a suppressor of transformation." Cell **57**(7): 1083-1093.

Fitzgerald, J. and J. F. Bateman (2004). "Why mice have lost genes for COL21A1, STK17A, GPR145 and AHRI: evidence for gene deletion at evolutionary breakpoints in the rodent lineage." Trends Genet **20**(9): 408-412.

Frank, R. (2002). "The SPOT-synthesis technique. Synthetic peptide arrays on membrane supports--principles and applications." J Immunol Methods **267**(1): 13-26.

Glick, D., S. Barth and K. F. Macleod (2010). "Autophagy: cellular and molecular mechanisms." J Pathol **221**(1): 3-12.

- Goldfarb, M., K. Shimizu, M. Perucho and M. Wigler (1982). "Isolation and preliminary characterization of a human transforming gene from T24 bladder carcinoma cells." Nature **296**(5856): 404-409.
- Hanahan, D. and R. A. Weinberg (2011). "Hallmarks of cancer: the next generation." Cell **144**(5): 646-674.
- Harmon, J. T., T. B. Nielsen and E. S. Kempner (1985). "Molecular weight determinations from radiation inactivation." Methods Enzymol **117**: 65-94.
- He, C. and D. J. Klionsky (2010). "Analyzing autophagy in zebrafish." Autophagy **6**(5): 642-644.
- Hosokawa, N., T. Hara, T. Kaizuka, C. Kishi, A. Takamura, Y. Miura, S. Iemura, T. Natsume, K. Takehana, N. Yamada, J. L. Guan, N. Oshiro and N. Mizushima (2009). "Nutrient-dependent mTORC1 association with the ULK1-Atg13-FIP200 complex required for autophagy." Mol Biol Cell **20**(7): 1981-1991.
- Hoyer-Hansen, M. and M. Jaattela (2007). "Connecting endoplasmic reticulum stress to autophagy by unfolded protein response and calcium." Cell Death Differ **14**(9): 1576-1582.
- Huang, J., Y. Lin, L. Li, D. Qing, X. M. Teng, Y. L. Zhang, X. Hu, Y. Hu, P. Yang and Z. G. Han (2009). "ARHI, as a novel suppressor of cell growth and downregulated in human hepatocellular carcinoma, could contribute to hepatocarcinogenesis." Mol Carcinog **48**(2): 130-140.
- Itakura, E., C. Kishi, K. Inoue and N. Mizushima (2008). "Beclin 1 forms two distinct phosphatidylinositol 3-kinase complexes with mammalian Atg14 and UVRAG." Mol Biol Cell **19**(12): 5360-5372.
- Kabeya, Y., N. Mizushima, T. Ueno, A. Yamamoto, T. Kirisako, T. Noda, E. Kominami, Y. Ohsumi and T. Yoshimori (2000). "LC3, a mammalian homologue of yeast Apg8p, is localized in autophagosome membranes after processing." EMBO J **19**(21): 5720-5728.

Kalvari, I., S. Tsompanis, N. C. Mulakkal, R. Osgood, T. Johansen, I. P. Nezis and V. J. Promponas (2014). "iLIR: A web resource for prediction of Atg8-family interacting proteins." Autophagy **10**(5): 913-925.

Kang, S., J. P. Louboutin, P. Datta, C. P. Landel, D. Martinez, A. S. Zervos, D. S. Strayer, T. Fernandes-Alnemri and E. S. Alnemri (2013). "Loss of HtrA2/Omi activity in non-neuronal tissues of adult mice causes premature aging." Cell Death Differ **20**(2): 259-269.

Karnoub, A. E. and R. A. Weinberg (2008). "Ras oncogenes: split personalities." Nat Rev Mol Cell Biol **9**(7): 517-531.

Kastan, M. B. and J. Bartek (2004). "Cell-cycle checkpoints and cancer." Nature **432**(7015): 316-323.

Kaur, J. and J. Debnath (2015). "Autophagy at the crossroads of catabolism and anabolism." Nat Rev Mol Cell Biol **16**(8): 461-472.

Klionsky, D. J., K. Abdelmohsen, A. Abe, M. J. Abedin, H. Abeliovich, A. Acevedo Arozana, H. Adachi, C. M. Adams, P. D. Adams, K. Adeli, P. J. Adhihetty, S. G. Adler, G. Agam, R. Agarwal, M. K. Aghi, M. Agnello, P. Agostinis, P. V. Aguilar, J. Aguirre-Ghiso, E. M. Airoidi, S. Ait-Si-Ali, T. Akematsu, E. T. Akporiaye, M. Al-Rubeai, G. M. Albaiceta, C. Albanese, D. Albani, M. L. Albert, J. Aldudo, H. Algul, M. Alirezaei, I. Alloza, A. Almasan, M. Almonte-Beceril, E. S. Alnemri, C. Alonso, N. Altan-Bonnet, D. C. Altieri, S. Alvarez, L. Alvarez-Erviti, S. Alves, G. Amadoro, A. Amano, C. Amantini, S. Ambrosio, I. Amelio, A. O. Amer, M. Amessou, A. Amon, Z. An, F. A. Anania, S. U. Andersen, U. P. Andley, C. K. Andreadi, N. Andrieu-Abadie, A. Anel, D. K. Ann, S. Anoopkumar-Dukie, M. Antonioli, H. Aoki, N. Apostolova, S. Aquila, K. Aquilano, K. Araki, E. Arama, A. Aranda, J. Araya, A. Arcaro, E. Arias, H. Arimoto, A. R. Ariosia, J. L. Armstrong, T. Arnould, I. Arsov, K. Asanuma, V. Askanas, E. Asselin, R. Atarashi, S. S. Atherton, J. D. Atkin, L. D. Attardi, P. Auburger, G. Auburger, L. Aurelian, R. Autelli, L. Avagliano, M. L. Avantaggiati, L. Avrahami, S. Awale, N. Azad, T. Bachetti, J. M. Backer, D. H. Bae, J. S. Bae, O. N. Bae, S. H.

Bae, E. H. Baehrecke, S. H. Baek, S. Baghdiguian, A. Bagniewska-Zadworna, H. Bai, J. Bai, X. Y. Bai, Y. Bailly, K. N. Balaji, W. Balduini, A. Ballabio, R. Balzan, R. Banerjee, G. Banhegyi, H. Bao, B. Barbeau, M. D. Barrachina, E. Barreiro, B. Bartel, A. Bartolome, D. C. Bassham, M. T. Bassi, R. C. Bast, Jr., A. Basu, M. T. Batista, H. Batoko, M. Battino, K. Bauckman, B. L. Baumgarner, K. U. Bayer, R. Beale, J. F. Beaulieu, G. R. Beck, Jr., C. Becker, J. D. Beckham, P. A. Bedard, P. J. Bednarski, T. J. Begley, C. Behl, C. Behrends, G. M. Behrens, K. E. Behrns, E. Bejarano, A. Belaid, F. Belleudi, G. Benard, G. Berchem, D. Bergamaschi, M. Bergami, B. Berkhout, L. Berliocchi, A. Bernard, M. Bernard, F. Bernassola, A. Bertolotti, A. S. Bess, S. Besteiro, S. Bettuzzi, S. Bhalla, S. Bhattacharyya, S. K. Bhutia, C. Biagosch, M. W. Bianchi, M. Biard-Piechaczyk, V. Billes, C. Bincoletto, B. Bingol, S. W. Bird, M. Bitoun, I. Bjedov, C. Blackstone, L. Blanc, G. A. Blanco, H. K. Blomhoff, E. Boada-Romero, S. Bockler, M. Boes, K. Boesze-Battaglia, L. H. Boise, A. Bolino, A. Boman, P. Bonaldo, M. Bordi, J. Bosch, L. M. Botana, J. Botti, G. Bou, M. Bouche, M. Bouchecareilh, M. J. Boucher, M. E. Boulton, S. G. Bouret, P. Boya, M. Boyer-Guittaut, P. V. Bozhkov, N. Brady, V. M. Braga, C. Brancolini, G. H. Braus, J. M. Bravo-San Pedro, L. A. Brennan, E. H. Bresnick, P. Brest, D. Bridges, M. A. Bringer, M. Brini, G. C. Brito, B. Brodin, P. S. Brookes, E. J. Brown, K. Brown, H. E. Broxmeyer, A. Bruhat, P. C. Brum, J. H. Brumell, N. Brunetti-Pierri, R. J. Bryson-Richardson, S. Buch, A. M. Buchan, H. Budak, D. V. Bulavin, S. J. Bultman, G. Bultynck, V. Bumbasirevic, Y. Burelle, R. E. Burke, M. Burmeister, P. Butikofer, L. Caberlotto, K. Cadwell, M. Cahova, D. Cai, J. Cai, Q. Cai, S. Calatayud, N. Camougrand, M. Campanella, G. R. Campbell, M. Campbell, S. Campello, R. Candau, I. Caniggia, L. Cantoni, L. Cao, A. B. Caplan, M. Caraglia, C. Cardinali, S. M. Cardoso, J. S. Carew, L. A. Carleton, C. R. Carlin, S. Carloni, S. R. Carlsson, D. Carmona-Gutierrez, L. A. Carneiro, O. Carnevali, S. Carra, A. Carrier, B. Carroll, C. Casas, J. Casas, G. Cassinelli, P. Castets, S. Castro-Obregon, G. Cavallini, I. Ceccherini, F. Cecconi, A. I. Cederbaum, V. Cena, S. Cenci, C. Cerella, D. Cervia, S. Cetrullo, H. Chaachouay, H. J. Chae, A. S. Chagin, C. Y. Chai, G. Chakrabarti, G. Chamilos, E. Y. Chan, M. T. Chan, D. Chandra, P. Chandra, C. P. Chang, R.

C. Chang, T. Y. Chang, J. C. Chatham, S. Chatterjee, S. Chauhan, Y. Che, M. E. Cheetham, R. Cheluvappa, C. J. Chen, G. Chen, G. C. Chen, G. Chen, H. Chen, J. W. Chen, J. K. Chen, M. Chen, M. Chen, P. Chen, Q. Chen, Q. Chen, S. D. Chen, S. Chen, S. S. Chen, W. Chen, W. J. Chen, W. Q. Chen, W. Chen, X. Chen, Y. H. Chen, Y. G. Chen, Y. Chen, Y. Chen, Y. Chen, Y. J. Chen, Y. Q. Chen, Y. Chen, Z. Chen, Z. Chen, A. Cheng, C. H. Cheng, H. Cheng, H. Cheong, S. Cherry, J. Chesney, C. H. Cheung, E. Chevet, H. C. Chi, S. G. Chi, F. Chiacchiera, H. L. Chiang, R. Chiarelli, M. Chiariello, M. Chieppa, L. S. Chin, M. Chiong, G. N. Chiu, D. H. Cho, S. G. Cho, W. C. Cho, Y. Y. Cho, Y. S. Cho, A. M. Choi, E. J. Choi, E. K. Choi, J. Choi, M. E. Choi, S. I. Choi, T. F. Chou, S. Chouaib, D. Choubey, V. Choubey, K. C. Chow, K. Chowdhury, C. T. Chu, T. H. Chuang, T. Chun, H. Chung, T. Chung, Y. L. Chung, Y. J. Chwae, V. Cianfanelli, R. Ciarcia, I. A. Ciechomska, M. R. Ciriolo, M. Cirone, S. Claerhout, M. J. Clague, J. Claria, P. G. Clarke, R. Clarke, E. Clementi, C. Cleyrat, M. Cnop, E. M. Coccia, T. Cocco, P. Codogno, J. Coers, E. E. Cohen, D. Colecchia, L. Coletto, N. S. Coll, E. Colucci-Guyon, S. Comincini, M. Condello, K. L. Cook, G. H. Coombs, C. D. Cooper, J. M. Cooper, I. Coppens, M. T. Corasaniti, M. Corazzari, R. Corbalan, E. Corcelle-Termeau, M. D. Cordero, C. Corral-Ramos, O. Corti, A. Cossarizza, P. Costelli, S. Costes, S. L. Cotman, A. Coto-Montes, S. Cottet, E. Couve, L. R. Covey, L. A. Cowart, J. S. Cox, F. P. Coxon, C. B. Coyne, M. S. Cragg, R. J. Craven, T. Crepaldi, J. L. Crespo, A. Criollo, V. Crippa, M. T. Cruz, A. M. Cuervo, J. M. Cuezva, T. Cui, P. R. Cutillas, M. J. Czaja, M. F. Czyzyk-Krzeska, R. K. Dagda, U. Dahmen, C. Dai, W. Dai, Y. Dai, K. N. Dalby, L. Dalla Valle, G. Dalmasso, M. D'Amelio, M. Damme, A. Darfeuille-Michaud, C. Dargemont, V. M. Darley-Usmar, S. Dasarathy, B. Dasgupta, S. Dash, C. R. Dass, H. M. Davey, L. M. Davids, D. Davila, R. J. Davis, T. M. Dawson, V. L. Dawson, P. Daza, J. de Belleruche, P. de Figueiredo, R. C. de Figueiredo, J. de la Fuente, L. De Martino, A. De Matteis, G. R. De Meyer, A. De Milito, M. De Santi, W. de Souza, V. De Tata, D. De Zio, J. Debnath, R. Dechant, J. P. Decuypere, S. Deegan, B. Dehay, B. Del Bello, D. P. Del Re, R. Delage-Mourroux, L. M. Delbridge, L. Deldicque, E. Delorme-Axford, Y. Deng, J. Dengjel, M. Denizot, P. Dent, C. J. Der, V. Deretic, B.

Derrien, E. Deutsch, T. P. Devarenne, R. J. Devenish, S. Di Bartolomeo, N. Di Daniele, F. Di
 Domenico, A. Di Nardo, S. Di Paola, A. Di Pietro, L. Di Renzo, A. DiAntonio, G. Diaz-Araya, I.
 Diaz-Laviada, M. T. Diaz-Meco, J. Diaz-Nido, C. A. Dickey, R. C. Dickson, M. Diederich, P.
 Digard, I. Dikic, S. P. Dinesh-Kumar, C. Ding, W. X. Ding, Z. Ding, L. Dini, J. H. Distler, A. Diwan,
 M. Djavaheri-Mergny, K. Dmytruk, R. C. Dobson, V. Doetsch, K. Dokladny, S. Dokudovskaya,
 M. Donadelli, X. C. Dong, X. Dong, Z. Dong, T. M. Donohue, Jr., K. S. Doran, G. D'Orazi, G. W.
 Dorn, 2nd, V. Dosenko, S. Dridi, L. Drucker, J. Du, L. L. Du, L. Du, A. du Toit, P. Dua, L. Duan,
 P. Duann, V. K. Dubey, M. R. Duchen, M. A. Duchosal, H. Duez, I. Dugail, V. I. Dumit, M. C.
 Duncan, E. A. Dunlop, W. A. Dunn, Jr., N. Dupont, L. Dupuis, R. V. Duran, T. M. Durcan, S.
 Duvezin-Caubet, U. Duvvuri, V. Eapen, D. Ebrahimi-Fakhari, A. Echard, L. Eckhart, C. L.
 Edelstein, A. L. Edinger, L. Eichinger, T. Eisenberg, A. Eisenberg-Lerner, N. T. Eissa, W. S. El-
 Deiry, V. El-Khoury, Z. Elazar, H. Eldar-Finkelman, C. J. Elliott, E. Emanuele, U. Emmenegger,
 N. Engedal, A. M. Engelbrecht, S. Engelder, J. M. Enserink, R. Erdmann, J. Erenpreisa, R.
 Eri, J. L. Eriksen, A. Erman, R. Escalante, E. L. Eskelinen, L. Espert, L. Esteban-Martinez, T. J.
 Evans, M. Fabri, G. Fabrias, C. Fabrizi, A. Facchiano, N. J. Faergeman, A. Faggioni, W. D.
 Fairlie, C. Fan, D. Fan, J. Fan, S. Fang, M. Fanto, A. Fanzani, T. Farkas, M. Faure, F. B. Favier,
 H. Fearnhead, M. Federici, E. Fei, T. C. Felizardo, H. Feng, Y. Feng, Y. Feng, T. A. Ferguson,
 A. F. Fernandez, M. G. Fernandez-Barrena, J. C. Fernandez-Checa, A. Fernandez-Lopez, M. E.
 Fernandez-Zapico, O. Feron, E. Ferraro, C. V. Ferreira-Halder, L. Fesus, R. Feuer, F. C. Fiesel,
 E. C. Filippi-Chiela, G. Filomeni, G. M. Fimia, J. H. Fingert, S. Finkbeiner, T. Finkel, F. Fiorito, P.
 B. Fisher, M. Flajolet, F. Flamigni, O. Florey, S. Florio, R. A. Floto, M. Folini, C. Follo, E. A. Fon,
 F. Fornai, F. Fortunato, A. Fraldi, R. Franco, A. Francois, A. Francois, L. B. Frankel, I. D. Fraser,
 N. Frey, D. G. Freyssenet, C. Frezza, S. L. Friedman, D. E. Frigo, D. Fu, J. M. Fuentes, J. Fueyo,
 Y. Fujitani, Y. Fujiwara, M. Fujiya, M. Fukuda, S. Fulda, C. Fusco, B. Gabryel, M. Gaestel, P.
 Gailly, M. Gajewska, S. Galadari, G. Galili, I. Galindo, M. F. Galindo, G. Galliciotti, L. Galluzzi, L.
 Galluzzi, V. Galy, N. Gammoh, S. Gandy, A. K. Ganesan, S. Ganesan, I. G. Ganley, M. Gannage,

F. B. Gao, F. Gao, J. X. Gao, L. Garcia Nannig, E. Garcia Vescovi, M. Garcia-Macia, C. Garcia-Ruiz, A. D. Garg, P. K. Garg, R. Gargini, N. C. Gassen, D. Gatica, E. Gatti, J. Gavard, E. Gavathiotis, L. Ge, P. Ge, S. Ge, P. W. Gean, V. Gelmetti, A. A. Genazzani, J. Geng, P. Genschik, L. Gerner, J. E. Gestwicki, D. A. Gewirtz, S. Ghavami, E. Ghigo, D. Ghosh, A. M. Giammarioli, F. Giampieri, C. Giampietri, A. Giatromanolaki, D. J. Gibbings, L. Gibellini, S. B. Gibson, V. Ginet, A. Giordano, F. Giorgini, E. Giovannetti, S. E. Girardin, S. Gispert, S. Giuliano, C. L. Gladson, A. Glavic, M. Gleave, N. Godefroy, R. M. Gogal, Jr., K. Gokulan, G. H. Goldman, D. Goletti, M. S. Goligorsky, A. V. Gomes, L. C. Gomes, H. Gomez, C. Gomez-Manzano, R. Gomez-Sanchez, D. A. Goncalves, E. Goncu, Q. Gong, C. Gongora, C. B. Gonzalez, P. Gonzalez-Alegre, P. Gonzalez-Cabo, R. A. Gonzalez-Polo, I. S. Goping, C. Gorbea, N. V. Gorbunov, D. R. Goring, A. M. Gorman, S. M. Gorski, S. Goruppi, S. Goto-Yamada, C. Gotor, R. A. Gottlieb, I. Gozes, D. Gozuacik, Y. Graba, M. Graef, G. E. Granato, G. D. Grant, S. Grant, G. L. Gravina, D. R. Green, A. Greenhough, M. T. Greenwood, B. Grimaldi, F. Gros, C. Grose, J. F. Groulx, F. Gruber, P. Grumati, T. Grune, J. L. Guan, K. L. Guan, B. Guerra, C. Guillen, K. Gulshan, J. Gunst, C. Guo, L. Guo, M. Guo, W. Guo, X. G. Guo, A. A. Gust, A. B. Gustafsson, E. Gutierrez, M. G. Gutierrez, H. S. Gwak, A. Haas, J. E. Haber, S. Hadano, M. Hagedorn, D. R. Hahn, A. J. Halayko, A. Hamacher-Brady, K. Hamada, A. Hamai, A. Hamann, M. Hamasaki, I. Hamer, Q. Hamid, E. M. Hammond, F. Han, W. Han, J. T. Handa, J. A. Hanover, M. Hansen, M. Harada, L. Harhaji-Trajkovic, J. W. Harper, A. H. Harrath, A. L. Harris, J. Harris, U. Hasler, P. Hasselblatt, K. Hasui, R. G. Hawley, T. S. Hawley, C. He, C. Y. He, F. He, G. He, R. R. He, X. H. He, Y. W. He, Y. Y. He, J. K. Heath, M. J. Hebert, R. A. Heinzen, G. V. Helgason, M. Hensel, E. P. Henske, C. Her, P. K. Herman, A. Hernandez, C. Hernandez, S. Hernandez-Tiedra, C. Hetz, P. R. Hiesinger, K. Higaki, S. Hilfiker, B. G. Hill, J. A. Hill, W. D. Hill, K. Hino, D. Hofius, P. Hofman, G. U. Hoglinger, J. Hohfeld, M. K. Holz, Y. Hong, D. A. Hood, J. J. Hoozemans, T. Hoppe, C. Hsu, C. Y. Hsu, L. C. Hsu, D. Hu, G. Hu, H. M. Hu, H. Hu, M. C. Hu, Y. C. Hu, Z. W. Hu, F. Hua, Y. Hua, C. Huang, H. L. Huang, K. H. Huang, K. Y. Huang, S. Huang, S. Huang, W.

P. Huang, Y. R. Huang, Y. Huang, Y. Huang, T. B. Huber, P. Huebbe, W. K. Huh, J. J. Hulmi, G.
 M. Hur, J. H. Hurley, Z. Husak, S. N. Hussain, S. Hussain, J. J. Hwang, S. Hwang, T. I. Hwang,
 A. Ichihara, Y. Imai, C. Imbriano, M. Inomata, T. Into, V. Iovane, J. L. Iovanna, R. V. Iozzo, N. Y.
 Ip, J. E. Irazoqui, P. Iribarren, Y. Isaka, A. J. Isakovic, H. Ischiropoulos, J. S. Isenberg, M. Ishaq,
 H. Ishida, I. Ishii, J. E. Ishmael, C. Isidoro, K. Isobe, E. Isono, S. Issazadeh-Navikas, K. Itahana,
 E. Itakura, A. I. Ivanov, A. K. Iyer, J. M. Izquierdo, Y. Izumi, V. Izzo, M. Jaattela, N. Jaber, D. J.
 Jackson, W. T. Jackson, T. G. Jacob, T. S. Jacques, C. Jagannath, A. Jain, N. R. Jana, B. K.
 Jang, A. Jani, B. Janji, P. R. Jannig, P. J. Jansson, S. Jean, M. Jendrach, J. H. Jeon, N. Jessen,
 E. B. Jeung, K. Jia, L. Jia, H. Jiang, H. Jiang, L. Jiang, T. Jiang, X. Jiang, X. Jiang, X. Jiang, Y.
 Jiang, Y. Jiang, A. Jimenez, C. Jin, H. Jin, L. Jin, M. Jin, S. Jin, U. K. Jinwal, E. K. Jo, T. Johansen,
 D. E. Johnson, G. V. Johnson, J. D. Johnson, E. Jonasch, C. Jones, L. A. Joosten, J. Jordan, A.
 M. Joseph, B. Joseph, A. M. Joubert, D. Ju, J. Ju, H. F. Juan, K. Juenemann, G. Juhasz, H. S.
 Jung, J. U. Jung, Y. K. Jung, H. Jungbluth, M. J. Justice, B. Jutten, N. O. Kaakoush, K.
 Kaarniranta, A. Kaasik, T. Kabuta, B. Kaeffer, K. Kagedal, A. Kahana, S. Kajimura, O. Kakhlon,
 M. Kalia, D. V. Kalvakolanu, Y. Kamada, K. Kambas, V. O. Kaminsky, H. H. Kampinga, M.
 Kandouz, C. Kang, R. Kang, T. C. Kang, T. Kanki, T. D. Kanneganti, H. Kanno, A. G.
 Kanthasamy, M. Kantorow, M. Kaparakis-Liaskos, O. Kapuy, V. Karantza, M. R. Karim, P.
 Karmakar, A. Kaser, S. Kaushik, T. Kawula, A. M. Kaynar, P. Y. Ke, Z. J. Ke, J. H. Kehrl, K. E.
 Keller, J. K. Kemper, A. K. Kenworthy, O. Kepp, A. Kern, S. Kesari, D. Kessel, R. Ketteler, C.
 Kettelhut Ido, B. Khambu, M. M. Khan, V. K. Khandelwal, S. Khare, J. G. Kiang, A. A. Kiger, A.
 Kihara, A. L. Kim, C. H. Kim, D. R. Kim, D. H. Kim, E. K. Kim, H. Y. Kim, H. R. Kim, J. S. Kim, J.
 H. Kim, J. C. Kim, J. H. Kim, K. W. Kim, M. D. Kim, M. M. Kim, P. K. Kim, S. W. Kim, S. Y. Kim,
 Y. S. Kim, Y. Kim, A. Kimchi, A. C. Kimmelman, T. Kimura, J. S. King, K. Kirkegaard, V. Kirkin,
 L. A. Kirshenbaum, S. Kishi, Y. Kitajima, K. Kitamoto, Y. Kitaoka, K. Kitazato, R. A. Kley, W. T.
 Klimecki, M. Klinkenberg, J. Klucken, H. Knaevelsrud, E. Knecht, L. Knuppertz, J. L. Ko, S.
 Kobayashi, J. C. Koch, C. Koechlin-Ramonatxo, U. Koenig, Y. H. Koh, K. Kohler, S. D. Kohlwein,

M. Koike, M. Komatsu, E. Kominami, D. Kong, H. J. Kong, E. G. Konstantakou, B. T. Kopp, T. Korcsmaros, L. Korhonen, V. I. Korolchuk, N. V. Koshkina, Y. Kou, M. I. Koukourakis, C. Koumenis, A. L. Kovacs, T. Kovacs, W. J. Kovacs, D. Koya, C. Kraft, D. Krainc, H. Kramer, T. Kravic-Stevovic, W. Krek, C. Kretz-Remy, R. Krick, M. Krishnamurthy, J. Kriston-Vizi, G. Kroemer, M. C. Kruer, R. Kruger, N. T. Ktistakis, K. Kuchitsu, C. Kuhn, A. P. Kumar, A. Kumar, A. Kumar, D. Kumar, D. Kumar, R. Kumar, S. Kumar, M. Kundu, H. J. Kung, A. Kuno, S. H. Kuo, J. Kuret, T. Kurz, T. Kwok, T. K. Kwon, Y. T. Kwon, I. Kyrmizi, A. R. La Spada, F. Lafont, T. Lahm, A. Lakkaraju, T. Lam, T. Lamark, S. Lancel, T. H. Landowski, D. J. Lane, J. D. Lane, C. Lanzi, P. Lapaquette, L. R. Lapierre, J. Laporte, J. Laukkarinen, G. W. Laurie, S. Lavandero, L. Lavie, M. J. LaVoie, B. Y. Law, H. K. Law, K. B. Law, R. Layfield, P. A. Lazo, L. Le Cam, K. G. Le Roch, H. Le Stunff, V. Leardkamolkarn, M. Lecuit, B. H. Lee, C. H. Lee, E. F. Lee, G. M. Lee, H. J. Lee, H. Lee, J. K. Lee, J. Lee, J. H. Lee, J. H. Lee, M. Lee, M. S. Lee, P. J. Lee, S. W. Lee, S. J. Lee, S. J. Lee, S. Y. Lee, S. H. Lee, S. S. Lee, S. J. Lee, S. Lee, Y. R. Lee, Y. J. Lee, Y. H. Lee, C. Leeuwenburgh, S. Lefort, R. Legouis, J. Lei, Q. Y. Lei, D. A. Leib, G. Leibowitz, I. Lekli, S. D. Lemaire, J. J. Lemasters, M. K. Lemberg, A. Lemoine, S. Leng, G. Lenz, P. Lenzi, L. O. Lerman, D. Lettieri Barbato, J. I. Leu, H. Y. Leung, B. Levine, P. A. Lewis, F. Lezoualc'h, C. Li, F. Li, F. J. Li, J. Li, K. Li, L. Li, M. Li, M. Li, Q. Li, R. Li, S. Li, W. Li, W. Li, X. Li, Y. Li, J. Lian, C. Liang, Q. Liang, Y. Liao, J. Liberal, P. P. Liberski, P. Lie, A. P. Lieberman, H. J. Lim, K. L. Lim, K. Lim, R. T. Lima, C. S. Lin, C. F. Lin, F. Lin, F. Lin, F. C. Lin, K. Lin, K. H. Lin, P. H. Lin, T. Lin, W. W. Lin, Y. S. Lin, Y. Lin, R. Linden, D. Lindholm, L. M. Lindqvist, P. Lingor, A. Linkermann, L. A. Liotta, M. M. Lipinski, V. A. Lira, M. P. Lisanti, P. B. Liton, B. Liu, C. Liu, C. F. Liu, F. Liu, H. J. Liu, J. Liu, J. J. Liu, J. L. Liu, K. Liu, L. Liu, L. Liu, Q. Liu, R. Y. Liu, S. Liu, S. Liu, W. Liu, X. D. Liu, X. Liu, X. H. Liu, X. Liu, X. Liu, X. Liu, Y. Liu, Y. Liu, Z. Liu, Z. Liu, J. P. Liuzzi, G. Lizard, M. Ljubic, I. J. Lodhi, S. E. Logue, B. L. Lokeshwar, Y. C. Long, S. Lonial, B. Loos, C. Lopez-Otin, C. Lopez-Vicario, M. Lorente, P. L. Lorenzi, P. Lorincz, M. Los, M. T. Lotze, P. E. Lovat, B. Lu, B. Lu, J. Lu, Q. Lu, S. M. Lu, S. Lu, Y. Lu, F. Luciano, S. Luckhart, J. M. Lucocq, P. Ludovico, A.

Lugea, N. W. Lukacs, J. J. Lum, A. H. Lund, H. Luo, J. Luo, S. Luo, C. Luparello, T. Lyons, J. Ma, Y. Ma, Y. Ma, Z. Ma, J. Machado, G. M. Machado-Santelli, F. Macian, G. C. MacIntosh, J. P. MacKeigan, K. F. Macleod, J. D. MacMicking, L. A. MacMillan-Crow, F. Madeo, M. Madesh, J. Madrigal-Matute, A. Maeda, T. Maeda, G. Maegawa, E. Maellaro, H. Maes, M. Magarinos, K. Maiese, T. K. Maiti, L. Maiuri, M. C. Maiuri, C. G. Maki, R. Malli, W. Malorni, A. Maloyan, F. Mami-Chouaib, N. Man, J. D. Mancias, E. M. Mandelkow, M. A. Mandell, A. A. Manfredi, S. N. Manie, C. Manzoni, K. Mao, Z. Mao, Z. W. Mao, P. Marambaud, A. M. Marconi, Z. Marelja, G. Marfe, M. Margeta, E. Margittai, M. Mari, F. V. Mariani, C. Marin, S. Marinelli, G. Marino, I. Markovic, R. Marquez, A. M. Martelli, S. Martens, K. R. Martin, S. J. Martin, S. Martin, M. A. Martin-Acebes, P. Martin-Sanz, C. Martinand-Mari, W. Martinet, J. Martinez, N. Martinez-Lopez, U. Martinez-Outschoorn, M. Martinez-Velazquez, M. Martinez-Vicente, W. K. Martins, H. Mashima, J. A. Mastrianni, G. Matarese, P. Matarrese, R. Mateo, S. Matoba, N. Matsumoto, T. Matsushita, A. Matsuura, T. Matsuzawa, M. P. Mattson, S. Matus, N. Maugeri, C. Mauvezin, A. Mayer, D. Maysinger, G. D. Mazzolini, M. K. McBrayer, K. McCall, C. McCormick, G. M. McInerney, S. C. McIver, S. McKenna, J. J. McMahon, I. A. McNeish, F. Mechta-Grigoriou, J. P. Medema, D. L. Medina, K. Megyeri, M. Mehrpour, J. L. Mehta, Y. Mei, U. C. Meier, A. J. Meijer, A. Melendez, G. Melino, S. Melino, E. J. de Melo, M. A. Mena, M. D. Meneghini, J. A. Menendez, R. Menezes, L. Meng, L. H. Meng, S. Meng, R. Menghini, A. S. Menko, R. F. Menna-Barreto, M. B. Menon, M. A. Meraz-Rios, G. Merla, L. Merlini, A. M. Merlot, A. Meryk, S. Meschini, J. N. Meyer, M. T. Mi, C. Y. Miao, L. Micale, S. Michaeli, C. Michiels, A. R. Migliaccio, A. S. Mihailidou, D. Mijaljica, K. Mikoshiba, E. Milan, L. Miller-Fleming, G. B. Mills, I. G. Mills, G. Minakaki, B. A. Minassian, X. F. Ming, F. Minibayeva, E. A. Minina, J. D. Mintern, S. Minucci, A. Miranda-Vizueté, C. H. Mitchell, S. Miyamoto, K. Miyazawa, N. Mizushima, K. Mnich, B. Mograbi, S. Mohseni, L. F. Moita, M. Molinari, M. Molinari, A. B. Moller, B. Mollereau, F. Mollinedo, M. Mongillo, M. M. Monick, S. Montagnaro, C. Montell, D. J. Moore, M. N. Moore, R. Mora-Rodriguez, P. I. Moreira, E. Morel, M. B. Morelli, S. Moreno, M. J. Morgan, A. Moris, Y. Moriyasu, J. L. Morrison, L. A. Morrison, E.

Morselli, J. Moscat, P. L. Moseley, S. Mostowy, E. Motori, D. Mottet, J. C. Mottram, C. E. Moussa, V. E. Mpakou, H. Mukhtar, J. M. Mulcahy Levy, S. Muller, R. Munoz-Moreno, C. Munoz-Pinedo, C. Munz, M. E. Murphy, J. T. Murray, A. Murthy, I. U. Mysorekar, I. R. Nabi, M. Nabissi, G. A. Nader, Y. Nagahara, Y. Nagai, K. Nagata, A. Nagelkerke, P. Nagy, S. R. Naidu, S. Nair, H. Nakano, H. Nakatogawa, M. Nanjundan, G. Napolitano, N. I. Naqvi, R. Nardacci, D. P. Narendra, M. Narita, A. C. Nascimbeni, R. Natarajan, L. C. Navegantes, S. T. Nawrocki, T. Y. Nazarko, V. Y. Nazarko, T. Neill, L. M. Neri, M. G. Netea, R. T. Netea-Maier, B. M. Neves, P. A. Ney, I. P. Nezis, H. T. Nguyen, H. P. Nguyen, A. S. Nicot, H. Nilsen, P. Nilsson, M. Nishimura, I. Nishino, M. Niso-Santano, H. Niu, R. A. Nixon, V. C. Njar, T. Noda, A. A. Noegel, E. M. Nolte, E. Norberg, K. K. Norga, S. K. Noureini, S. Notomi, L. Notterpek, K. Nowikovsky, N. Nukina, T. Nurnberger, V. B. O'Donnell, T. O'Donovan, P. J. O'Dwyer, I. Oehme, C. L. Oeste, M. Ogawa, B. Ogretmen, Y. Ogura, Y. J. Oh, M. Ohmuraya, T. Ohshima, R. Ojha, K. Okamoto, T. Okazaki, F. J. Oliver, K. Ollinger, S. Olsson, D. P. Orban, P. Ordonez, I. Orhon, L. Orosz, E. J. O'Rourke, H. Orozco, A. L. Ortega, E. Ortona, L. D. Osellame, J. Oshima, S. Oshima, H. D. Osiewacz, T. Otomo, K. Otsu, J. H. Ou, T. F. Outeiro, D. Y. Ouyang, H. Ouyang, M. Overholtzer, M. A. Ozbun, P. H. Ozdinler, B. Ozpolat, C. Pacelli, P. Paganetti, G. Page, G. Pages, U. Pagnini, B. Pajak, S. C. Pak, K. Pakos-Zebrucka, N. Pakpour, Z. Palkova, F. Palladino, K. Pallauf, N. Pallet, M. Palmieri, S. R. Paludan, C. Palumbo, S. Palumbo, O. Pampliega, H. Pan, W. Pan, T. Panaretakis, A. Pandey, A. Pantazopoulou, Z. Papackova, D. L. Papademetrio, I. Papassideri, A. Papini, N. Parajuli, J. Pardo, V. V. Parekh, G. Parenti, J. I. Park, J. Park, O. K. Park, R. Parker, R. Parlato, J. B. Parys, K. R. Parzych, J. M. Pasquet, B. Pasquier, K. B. Pasumarthi, D. Patschan, C. Patterson, S. Pattingre, S. Pattison, A. Pause, H. Pavenstadt, F. Pavone, Z. Pedrozo, F. J. Pena, M. A. Penalva, M. Pende, J. Peng, F. Penna, J. M. Penninger, A. Pensalfini, S. Pepe, G. J. Pereira, P. C. Pereira, V. Perez-de la Cruz, M. E. Perez-Perez, D. Perez-Rodriguez, D. Perez-Sala, C. Perier, A. Perl, D. H. Perlmutter, I. Perrotta, S. Pervaiz, M. Pesonen, J. E. Pessin, G. J. Peters, M. Petersen, I. Petrache, B. J. Petrof, G. Petrovski, J. M. Phang, M. Piacentini, M. Pierdominici,

P. Pierre, V. Pierrefite-Carle, F. Pietrocola, F. X. Pimentel-Muinos, M. Pinar, B. Pineda, R. Pinkas-Kramarski, M. Pinti, P. Pinton, B. Piperdi, J. M. Piret, L. C. Platanias, H. W. Platta, E. D. Plowey, S. Poggeler, M. Poirot, P. Polcic, A. Poletti, A. H. Poon, H. Popelka, B. Popova, I. Poprawa, S. M. Poulouse, J. Poulton, S. K. Powers, T. Powers, M. Pozuelo-Rubio, K. Prak, R. Prange, M. Prescott, M. Priault, S. Prince, R. L. Proia, T. Proikas-Cezanne, H. Prokisch, V. J. Promponas, K. Przyklenk, R. Puertollano, S. Pugazhenth, L. Puglielli, A. Pujol, J. Puyal, D. Pyeon, X. Qi, W. B. Qian, Z. H. Qin, Y. Qiu, Z. Qu, J. Quadrilatero, F. Quinn, N. Raben, H. Rabinowich, F. Radogna, M. J. Ragusa, M. Rahmani, K. Raina, S. Ramanadham, R. Ramesh, A. Rami, S. Randall-Demllo, F. Randow, H. Rao, V. A. Rao, B. B. Rasmussen, T. M. Rasse, E. A. Ratovitski, P. E. Rautou, S. K. Ray, B. Razani, B. H. Reed, F. Reggiori, M. Rehm, A. S. Reichert, T. Rein, D. J. Reiner, E. Reits, J. Ren, X. Ren, M. Renna, J. E. Reusch, J. L. Revuelta, L. Reyes, A. R. Rezaie, R. I. Richards, D. R. Richardson, C. Richetta, M. A. Riehle, B. H. Rihn, Y. Rikihisa, B. E. Riley, G. Rimbach, M. R. Rippo, K. Ritis, F. Rizzi, E. Rizzo, P. J. Roach, J. Robbins, M. Roberge, G. Roca, M. C. Roccheri, S. Rocha, C. M. Rodrigues, C. I. Rodriguez, S. R. de Cordoba, N. Rodriguez-Muela, J. Roelofs, V. V. Rogov, T. T. Rohn, B. Rohrer, D. Romanelli, L. Romani, P. S. Romano, M. I. Roncero, J. L. Rosa, A. Rosello, K. V. Rosen, P. Rosenstiel, M. Rost-Roszkowska, K. A. Roth, G. Roue, M. Rouis, K. M. Rouschop, D. T. Ruan, D. Ruano, D. C. Rubinsztein, E. B. Rucker, 3rd, A. Rudich, E. Rudolf, R. Rudolf, M. A. Ruegg, C. Ruiz-Roldan, A. A. Ruparelia, P. Rusmini, D. W. Russ, G. L. Russo, G. Russo, R. Russo, T. E. Rusten, V. Ryabovol, K. M. Ryan, S. W. Ryter, D. M. Sabatini, M. Sacher, C. Sachse, M. N. Sack, J. Sadoshima, P. Saftig, R. Sagi-Eisenberg, S. Sahni, P. Saikumar, T. Saito, T. Saitoh, K. Sakakura, M. Sakoh-Nakatogawa, Y. Sakuraba, M. Salazar-Roa, P. Salomoni, A. K. Saluja, P. M. Salvaterra, R. Salvioli, A. Samali, A. M. Sanchez, J. A. Sanchez-Alcazar, R. Sanchez-Prieto, M. Sandri, M. A. Sanjuan, S. Santaguida, L. Santambrogio, G. Santoni, C. N. Dos Santos, S. Saran, M. Sardiello, G. Sargent, P. Sarkar, S. Sarkar, M. R. Sarrias, M. M. Sarwal, C. Sasakawa, M. Sasaki, M. Sass, K. Sato, M. Sato, J. Satriano, N. Savaraj, S. Saveljeva, L. Schaefer, U. E.

Schaible, M. Scharl, H. M. Schatzl, R. Schekman, W. Scheper, A. Schiavi, H. M. Schipper, H. Schmeisser, J. Schmidt, I. Schmitz, B. E. Schneider, E. M. Schneider, J. L. Schneider, E. A. Schon, M. J. Schonenberger, A. H. Schonthal, D. F. Schorderet, B. Schroder, S. Schuck, R. J. Schulze, M. Schwarten, T. L. Schwarz, S. Sciarretta, K. Scotto, A. I. Scovassi, R. A. Screaton, M. Screen, H. Seca, S. Sedej, L. Segatori, N. Segev, P. O. Seglen, J. M. Segui-Simarro, J. Segura-Aguilar, E. Seki, C. Sell, I. Seilliez, C. F. Semenkovich, G. L. Semenza, U. Sen, A. L. Serra, A. Serrano-Puebla, H. Sesaki, T. Setoguchi, C. Settembre, J. J. Shacka, A. N. Shajahan-Haq, I. M. Shapiro, S. Sharma, H. She, C. K. Shen, C. C. Shen, H. M. Shen, S. Shen, W. Shen, R. Sheng, X. Sheng, Z. H. Sheng, T. G. Shepherd, J. Shi, Q. Shi, Q. Shi, Y. Shi, S. Shibutani, K. Shibuya, Y. Shidoji, J. J. Shieh, C. M. Shih, Y. Shimada, S. Shimizu, D. W. Shin, M. L. Shinohara, M. Shintani, T. Shintani, T. Shioi, K. Shirabe, R. Shiri-Sverdlov, O. Shirihai, G. C. Shore, C. W. Shu, D. Shukla, A. A. Sibirny, V. Sica, C. J. Sigurdson, E. M. Sigurdsson, P. S. Sijwali, B. Sikorska, W. A. Silveira, S. Silvente-Poirot, G. A. Silverman, J. Simak, T. Simmet, A. K. Simon, H. U. Simon, C. Simone, M. Simons, A. Simonsen, R. Singh, S. V. Singh, S. K. Singh, D. Sinha, S. Sinha, F. A. Sinicrope, A. Sirko, K. Sirohi, B. J. Sishi, A. Sittler, P. M. Siu, E. Sivridis, A. Skwarska, R. Slack, I. Slaninova, N. Slavov, S. S. Smaili, K. S. Smalley, D. R. Smith, S. J. Soenen, S. A. Soleimanpour, A. Solhaug, K. Somasundaram, J. H. Son, A. Sonawane, C. Song, F. Song, H. K. Song, J. X. Song, W. Song, K. Y. Soo, A. K. Sood, T. W. Soong, V. Soontornniyomkij, M. Sorice, F. Sotgia, D. R. Soto-Pantoja, A. Sotthibundhu, M. J. Sousa, H. P. Spaink, P. N. Span, A. Spang, J. D. Sparks, P. G. Speck, S. A. Spector, C. D. Spies, W. Springer, D. S. Clair, A. Stacchiotti, B. Staels, M. T. Stang, D. T. Starczynowski, P. Starokadomskyy, C. Steegborn, J. W. Steele, L. Stefanis, J. Steffan, C. M. Stellrecht, H. Stenmark, T. M. Stepkowski, S. T. Stern, C. Stevens, B. R. Stockwell, V. Stoka, Z. Storchova, B. Stork, V. Stratoulis, D. J. Stravopodis, P. Strnad, A. M. Strohecker, A. L. Strom, P. Stromhaug, J. Stulik, Y. X. Su, Z. Su, C. S. Subauste, S. Subramaniam, C. M. Sue, S. W. Suh, X. Sui, S. Sukserree, D. Sulzer, F. L. Sun, J. Sun, J. Sun, S. Y. Sun, Y. Sun, Y. Sun, Y. Sun, V. Sundaramoorthy, J. Sung, H. Suzuki,

K. Suzuki, N. Suzuki, T. Suzuki, Y. J. Suzuki, M. S. Swanson, C. Swanton, K. Sward, G. Swarup, S. T. Sweeney, P. W. Sylvester, Z. Szatmari, E. Szegezdi, P. W. Szlosarek, H. Taegtmeyer, M. Tafani, E. Taillebourg, S. W. Tait, K. Takacs-Vellai, Y. Takahashi, S. Takats, G. Takemura, N. Takigawa, N. J. Talbot, E. Tamagno, J. Tamburini, C. P. Tan, L. Tan, M. L. Tan, M. Tan, Y. J. Tan, K. Tanaka, M. Tanaka, D. Tang, D. Tang, G. Tang, I. Tanida, K. Tanji, B. A. Tannous, J. A. Tapia, I. Tasset-Cuevas, M. Tatar, I. Tavassoly, N. Tavernarakis, A. Taylor, G. S. Taylor, G. A. Taylor, J. P. Taylor, M. J. Taylor, E. V. Tchetina, A. R. Tee, F. Teixeira-Clerc, S. Telang, T. Tencomnao, B. B. Teng, R. J. Teng, F. Terro, G. Tettamanti, A. L. Theiss, A. E. Theron, K. J. Thomas, M. P. Thome, P. G. Thomes, A. Thorburn, J. Thorner, T. Thum, M. Thumm, T. L. Thurston, L. Tian, A. Till, J. P. Ting, V. I. Titorenko, L. Toker, S. Toldo, S. A. Tooze, I. Topisirovic, M. L. Torgersen, L. Torosantucci, A. Torriglia, M. R. Torrisi, C. Tournier, R. Towns, V. Trajkovic, L. H. Travassos, G. Triola, D. N. Tripathi, D. Trisciuglio, R. Troncoso, I. P. Trougakos, A. C. Truttmann, K. J. Tsai, M. P. Tschan, Y. H. Tseng, T. Tsukuba, A. Tsung, A. S. Tsvetkov, S. Tu, H. Y. Tuan, M. Tucci, D. A. Tumbarello, B. Turk, V. Turk, R. F. Turner, A. A. Tveita, S. C. Tyagi, M. Ubukata, Y. Uchiyama, A. Udelnow, T. Ueno, M. Umekawa, R. Umemiya-Shirafuji, B. R. Underwood, C. Ungermann, R. P. Ureshino, R. Ushioda, V. N. Uversky, N. L. Uzcategui, T. Vaccari, M. I. Vaccaro, L. Vachova, H. Vakifahmetoglu-Norberg, R. Valdor, E. M. Valente, F. Vallette, A. M. Valverde, G. Van den Berghe, L. Van Den Bosch, G. R. van den Brink, F. G. van der Goot, I. J. van der Klei, L. J. van der Laan, W. G. van Doorn, M. van Egmond, K. L. van Golen, L. Van Kaer, M. van Lookeren Campagne, P. Vandenabeele, W. Vandenberghe, I. Vanhorebeek, I. Varela-Nieto, M. H. Vasconcelos, R. Vasko, D. G. Vavvas, I. Vega-Naredo, G. Velasco, A. D. Velentzas, P. D. Velentzas, T. Vellai, E. Vellenga, M. H. Vendelbo, K. Venkatachalam, N. Ventura, S. Ventura, P. S. Veras, M. Verdier, B. G. Vertessy, A. Viale, M. Vidal, H. L. Vieira, R. D. Vierstra, N. Vigneswaran, N. Vij, M. Vila, M. Villar, V. H. Villar, J. Villarroya, C. Vindis, G. Viola, M. T. Viscomi, G. Vitale, D. T. Vogl, O. V. Voitsekhovskaja, C. von Haefen, K. von Schwarzenberg, D. E. Voth, V. Vouret-Craviari, K. Vuori, J. M. Vyas, C. Waeber,

C. L. Walker, M. J. Walker, J. Walter, L. Wan, X. Wan, B. Wang, C. Wang, C. Y. Wang, C. Wang,
 C. Wang, C. Wang, D. Wang, F. Wang, F. Wang, G. Wang, H. J. Wang, H. Wang, H. G. Wang,
 H. Wang, H. D. Wang, J. Wang, J. Wang, M. Wang, M. Q. Wang, P. Y. Wang, P. Wang, R. C.
 Wang, S. Wang, T. F. Wang, X. Wang, X. J. Wang, X. W. Wang, X. Wang, X. Wang, Y. Wang,
 Y. Wang, Y. Wang, Y. J. Wang, Y. Wang, Y. Wang, Y. T. Wang, Y. Wang, Z. N. Wang, P.
 Wappner, C. Ward, D. M. Ward, G. Warnes, H. Watada, Y. Watanabe, K. Watase, T. E. Weaver,
 C. D. Weekes, J. Wei, T. Weide, C. C. Weihl, G. Weindl, S. N. Weis, L. Wen, X. Wen, Y. Wen,
 B. Westermann, C. M. Weyand, A. R. White, E. White, J. L. Whitton, A. J. Whitworth, J. Wiels, F.
 Wild, M. E. Wildenberg, T. Wileman, D. S. Wilkinson, S. Wilkinson, D. Willbold, C. Williams, K.
 Williams, P. R. Williamson, K. F. Winklhofer, S. S. Witkin, S. E. Wohlgemuth, T. Wollert, E. J.
 Wolvetang, E. Wong, G. W. Wong, R. W. Wong, V. K. Wong, E. A. Woodcock, K. L. Wright, C.
 Wu, D. Wu, G. S. Wu, J. Wu, J. Wu, M. Wu, M. Wu, S. Wu, W. K. Wu, Y. Wu, Z. Wu, C. P. Xavier,
 R. J. Xavier, G. X. Xia, T. Xia, W. Xia, Y. Xia, H. Xiao, J. Xiao, S. Xiao, W. Xiao, C. M. Xie, Z.
 Xie, Z. Xie, M. Xilouri, Y. Xiong, C. Xu, C. Xu, F. Xu, H. Xu, H. Xu, J. Xu, J. Xu, J. Xu, L. Xu, X.
 Xu, Y. Xu, Y. Xu, Z. X. Xu, Z. Xu, Y. Xue, T. Yamada, A. Yamamoto, K. Yamanaka, S.
 Yamashina, S. Yamashiro, B. Yan, B. Yan, X. Yan, Z. Yan, Y. Yanagi, D. S. Yang, J. M. Yang,
 L. Yang, M. Yang, P. M. Yang, P. Yang, Q. Yang, W. Yang, W. Y. Yang, X. Yang, Y. Yang, Y.
 Yang, Z. Yang, Z. Yang, M. C. Yao, P. J. Yao, X. Yao, Z. Yao, Z. Yao, L. S. Yasui, M. Ye, B.
 Yedvobnick, B. Yeganeh, E. S. Yeh, P. L. Yeyati, F. Yi, L. Yi, X. M. Yin, C. K. Yip, Y. M. Yoo, Y.
 H. Yoo, S. Y. Yoon, K. Yoshida, T. Yoshimori, K. H. Young, H. Yu, J. J. Yu, J. T. Yu, J. Yu, L.
 Yu, W. H. Yu, X. F. Yu, Z. Yu, J. Yuan, Z. M. Yuan, B. Y. Yue, J. Yue, Z. Yue, D. N. Zacks, E.
 Zacksenhaus, N. Zaffaroni, T. Zaglia, Z. Zakeri, V. Zecchini, J. Zeng, M. Zeng, Q. Zeng, A. S.
 Zervos, D. D. Zhang, F. Zhang, G. Zhang, G. C. Zhang, H. Zhang, H. Zhang, H. Zhang, H. Zhang,
 J. Zhang, J. Zhang, J. Zhang, J. Zhang, J. P. Zhang, L. Zhang, L. Zhang, L. Zhang, L. Zhang, M.
 Y. Zhang, X. Zhang, X. D. Zhang, Y. Zhang, Y. Zhang, Y. Zhang, Y. Zhang, Y. Zhang, M. Zhao,
 W. L. Zhao, X. Zhao, Y. G. Zhao, Y. Zhao, Y. Zhao, Y. X. Zhao, Z. Zhao, Z. J. Zhao, D. Zheng,

X. L. Zheng, X. Zheng, B. Zhivotovsky, Q. Zhong, G. Z. Zhou, G. Zhou, H. Zhou, S. F. Zhou, X. J. Zhou, H. Zhu, H. Zhu, W. G. Zhu, W. Zhu, X. F. Zhu, Y. Zhu, S. M. Zhuang, X. Zhuang, E. Ziparo, C. E. Zois, T. Zoladek, W. X. Zong, A. Zorzano and S. M. Zughaier (2016). "Guidelines for the use and interpretation of assays for monitoring autophagy (3rd edition)." Autophagy **12**(1): 1-222.

Knudson, A. G., Jr. (1971). "Mutation and cancer: statistical study of retinoblastoma." Proc Natl Acad Sci U S A **68**(4): 820-823.

Komatsu, M., S. Waguri, M. Koike, Y. S. Sou, T. Ueno, T. Hara, N. Mizushima, J. Iwata, J. Ezaki, S. Murata, J. Hamazaki, Y. Nishito, S. Iemura, T. Natsume, T. Yanagawa, J. Uwayama, E. Warabi, H. Yoshida, T. Ishii, A. Kobayashi, M. Yamamoto, Z. Yue, Y. Uchiyama, E. Kominami and K. Tanaka (2007). "Homeostatic levels of p62 control cytoplasmic inclusion body formation in autophagy-deficient mice." Cell **131**(6): 1149-1163.

Lamb, C. A., T. Yoshimori and S. A. Tooze (2013). "The autophagosome: origins unknown, biogenesis complex." Nat Rev Mol Cell Biol **14**(12): 759-774.

Levine, B. and G. Kroemer (2008). "Autophagy in the pathogenesis of disease." Cell **132**(1): 27-42.

Li, W. W., J. Li and J. K. Bao (2012). "Microautophagy: lesser-known self-eating." Cell Mol Life Sci **69**(7): 1125-1136.

Li, Y. C., L. W. Rodewald, C. Hoppmann, E. T. Wong, S. Lebreton, P. Safar, M. Patek, L. Wang, K. F. Wertman and G. M. Wahl (2014). "A versatile platform to analyze low-affinity and transient protein-protein interactions in living cells in real time." Cell Rep **9**(5): 1946-1958.

Liang, X. H., S. Jackson, M. Seaman, K. Brown, B. Kempkes, H. Hibshoosh and B. Levine (1999). "Induction of autophagy and inhibition of tumorigenesis by beclin 1." Nature **402**(6762): 672-676.

Lin, D., F. Cui, Q. Bu and C. Yan (2011). "The expression and clinical significance of GTP-binding RAS-like 3 (ARHI) and microRNA 221 and 222 in prostate cancer." J Int Med Res **39**(5): 1870-1875.

Lu, S., H. Jang, R. Nussinov and J. Zhang (2016). "The Structural Basis of Oncogenic Mutations G12, G13 and Q61 in Small GTPase K-Ras4B." Sci Rep **6**: 21949.

Lu, Z., M. T. Baquero, H. Yang, M. Yang, A. S. Reger, C. Kim, D. A. Levine, C. H. Clarke, W. S. Liao and R. C. Bast, Jr. (2014). "DIRAS3 regulates the autophagosome initiation complex in dormant ovarian cancer cells." Autophagy **10**(6): 1071-1092.

Lu, Z., R. Z. Luo, Y. Lu, X. Zhang, Q. Yu, S. Khare, S. Kondo, Y. Kondo, Y. Yu, G. B. Mills, W. S. Liao and R. C. Bast, Jr. (2008). "The tumor suppressor gene ARHI regulates autophagy and tumor dormancy in human ovarian cancer cells." J Clin Invest **118**(12): 3917-3929.

Lu, Z., R. Z. Luo, H. Peng, M. Huang, A. Nishimoto, K. K. Hunt, K. Helin, W. S. Liao and Y. Yu (2006). "E2F-HDAC complexes negatively regulate the tumor suppressor gene ARHI in breast cancer." Oncogene **25**(2): 230-239.

Lu, Z., R. Z. Luo, H. Peng, D. G. Rosen, E. N. Atkinson, C. Warneke, M. Huang, A. Nishimoto, J. Liu, W. S. Liao, Y. Yu and R. C. Bast, Jr. (2006). "Transcriptional and posttranscriptional down-regulation of the imprinted tumor suppressor gene ARHI (DRAS3) in ovarian cancer." Clin Cancer Res **12**(8): 2404-2413.

Lu, Z., H. Yang, M. N. Sutton, M. Yang, C. H. Clarke, W. S. Liao and R. C. Bast, Jr. (2014). "ARHI (DIRAS3) induces autophagy in ovarian cancer cells by downregulating the epidermal growth factor receptor, inhibiting PI3K and Ras/MAP signaling and activating the FOXo3a-mediated induction of Rab7." Cell Death Differ **21**(8): 1275-1289.

Luo, R. Z., X. Fang, R. Marquez, S. Y. Liu, G. B. Mills, W. S. Liao, Y. Yu and R. C. Bast (2003). "ARHI is a Ras-related small G-protein with a novel N-terminal extension that inhibits growth of ovarian and breast cancers." Oncogene **22**(19): 2897-2909.

Luo, R. Z., H. Peng, F. Xu, J. Bao, Y. Pang, R. Pershad, J. P. Issa, W. S. Liao, R. C. Bast, Jr. and Y. Yu (2001). "Genomic structure and promoter characterization of an imprinted tumor suppressor gene ARHI." Biochim Biophys Acta **1519**(3): 216-222.

Mahalingam, D., M. Mita, J. Sarantopoulos, L. Wood, R. K. Amaravadi, L. E. Davis, A. C. Mita, T. J. Curiel, C. M. Espitia, S. T. Nawrocki, F. J. Giles and J. S. Carew (2014). "Combined autophagy and HDAC inhibition: a phase I safety, tolerability, pharmacokinetic, and pharmacodynamic analysis of hydroxychloroquine in combination with the HDAC inhibitor vorinostat in patients with advanced solid tumors." Autophagy **10**(8): 1403-1414.

Matsunaga, K., T. Saitoh, K. Tabata, H. Omori, T. Satoh, N. Kurotori, I. Maejima, K. Shirahama-Noda, T. Ichimura, T. Isobe, S. Akira, T. Noda and T. Yoshimori (2009). "Two Beclin 1-binding proteins, Atg14L and Rubicon, reciprocally regulate autophagy at different stages." Nat Cell Biol **11**(4): 385-396.

Miranda, A., A. Mickle, B. Medda, Z. Zhang, R. J. Phillips, N. Tipnis, T. L. Powley, R. Shaker and J. N. Sengupta (2009). "Altered mechanosensitive properties of vagal afferent fibers innervating the stomach following gastric surgery in rats." Neuroscience **162**(4): 1299-1306.

Mizushima, N. and D. J. Klionsky (2007). "Protein turnover via autophagy: implications for metabolism." Annu Rev Nutr **27**: 19-40.

Mizushima, N. and M. Komatsu (2011). "Autophagy: renovation of cells and tissues." Cell **147**(4): 728-741.

Mukherjee, S., D. Ray, I. Lekli, I. Bak, A. Tosaki and D. K. Das (2010). "Effects of Longevinex (modified resveratrol) on cardioprotection and its mechanisms of action." Can J Physiol Pharmacol **88**(11): 1017-1025.

Muratcioglu, S., T. S. Chavan, B. C. Freed, H. Jang, L. Khavrutskii, R. N. Freed, M. A. Dyba, K. Stefanisko, S. G. Tarasov, A. Gursoy, O. Keskin, N. I. Tarasova, V. Gaponenko and R. Nussinov (2015). "GTP-Dependent K-Ras Dimerization." Structure **23**(7): 1325-1335.

Nan, X., T. M. Tamguney, E. A. Collisson, L. J. Lin, C. Pitt, J. Galeas, S. Lewis, J. W. Gray, F. McCormick and S. Chu (2015). "Ras-GTP dimers activate the Mitogen-Activated Protein Kinase (MAPK) pathway." Proc Natl Acad Sci U S A **112**(26): 7996-8001.

Nickerson, A., T. Huang, L. J. Lin and X. Nan (2014). "Photoactivated localization microscopy with bimolecular fluorescence complementation (BiFC-PALM) for nanoscale imaging of protein-protein interactions in cells." PLoS One **9**(6): e100589.

Parada, L. F., C. J. Tabin, C. Shih and R. A. Weinberg (1982). "Human EJ bladder carcinoma oncogene is homologue of Harvey sarcoma virus ras gene." Nature **297**(5866): 474-478.

Patel, S., V. Hurez, S. T. Nawrocki, M. Goros, J. Michalek, J. Sarantopoulos, T. Curiel and D. Mahalingam (2016). "Vorinostat and hydroxychloroquine improve immunity and inhibit autophagy in metastatic colorectal cancer." Oncotarget **7**(37): 59087-59097.

Plowman, S. J., C. Muncke, R. G. Parton and J. F. Hancock (2005). "H-ras, K-ras, and inner plasma membrane raft proteins operate in nanoclusters with differential dependence on the actin cytoskeleton." Proc Natl Acad Sci U S A **102**(43): 15500-15505.

Prior, I. A., P. D. Lewis and C. Mattos (2012). "A comprehensive survey of Ras mutations in cancer." Cancer Res **72**(10): 2457-2467.

Prior, I. A., C. Muncke, R. G. Parton and J. F. Hancock (2003). "Direct visualization of Ras proteins in spatially distinct cell surface microdomains." J Cell Biol **160**(2): 165-170.

Prior, I. A., R. G. Parton and J. F. Hancock (2003). "Observing cell surface signaling domains using electron microscopy." Sci STKE **2003**(177): PL9.

Pulciani, S., E. Santos, A. V. Lauver, L. K. Long, K. C. Robbins and M. Barbacid (1982). "Oncogenes in human tumor cell lines: molecular cloning of a transforming gene from human bladder carcinoma cells." Proc Natl Acad Sci U S A **79**(9): 2845-2849.

Qu, X., J. Yu, G. Bhagat, N. Furuya, H. Hibshoosh, A. Troxel, J. Rosen, E. L. Eskelinen, N. Mizushima, Y. Ohsumi, G. Cattoretti and B. Levine (2003). "Promotion of tumorigenesis by heterozygous disruption of the beclin 1 autophagy gene." J Clin Invest **112**(12): 1809-1820.

Rabinowitz, J. D. and E. White (2010). "Autophagy and metabolism." Science **330**(6009): 1344-1348.

Rangwala, R., Y. C. Chang, J. Hu, K. M. Algazy, T. L. Evans, L. A. Fecher, L. M. Schuchter, D. A. Torigian, J. T. Panosian, A. B. Troxel, K. S. Tan, D. F. Heitjan, A. M. DeMichele, D. J. Vaughn, M. Redlinger, A. Alavi, J. Kaiser, L. Pontiggia, L. E. Davis, P. J. O'Dwyer and R. K. Amaravadi (2014). "Combined MTOR and autophagy inhibition: phase I trial of hydroxychloroquine and temsirolimus in patients with advanced solid tumors and melanoma." Autophagy **10**(8): 1391-1402.

Rangwala, R., R. Leone, Y. C. Chang, L. A. Fecher, L. M. Schuchter, A. Kramer, K. S. Tan, D. F. Heitjan, G. Rodgers, M. Gallagher, S. Piao, A. B. Troxel, T. L. Evans, A. M. DeMichele, K. L. Nathanson, P. J. O'Dwyer, J. Kaiser, L. Pontiggia, L. E. Davis and R. K. Amaravadi (2014). "Phase I trial of hydroxychloroquine with dose-intense temozolomide in patients with advanced solid tumors and melanoma." Autophagy **10**(8): 1369-1379.

Reddy, E. P., R. K. Reynolds, E. Santos and M. Barbacid (1982). "A point mutation is responsible for the acquisition of transforming properties by the T24 human bladder carcinoma oncogene." Nature **300**(5888): 149-152.

Reggiori, F. and D. J. Klionsky (2013). "Autophagic processes in yeast: mechanism, machinery and regulation." Genetics **194**(2): 341-361.

Rosen, D. G., L. Wang, A. N. Jain, K. H. Lu, R. Z. Luo, Y. Yu, J. Liu and R. C. Bast, Jr. (2004). "Expression of the tumor suppressor gene ARHI in epithelial ovarian cancer is associated with increased expression of p21WAF1/CIP1 and prolonged progression-free survival." Clin Cancer Res **10**(19): 6559-6566.

Rosenfeld, M. R., X. Ye, J. G. Supko, S. Desideri, S. A. Grossman, S. Brem, T. Mikkelsen, D. Wang, Y. C. Chang, J. Hu, Q. McAfee, J. Fisher, A. B. Troxel, S. Piao, D. F. Heitjan, K. S. Tan, L. Pontiggia, P. J. O'Dwyer, L. E. Davis and R. K. Amaravadi (2014). "A phase I/II trial of hydroxychloroquine in conjunction with radiation therapy and concurrent and adjuvant temozolomide in patients with newly diagnosed glioblastoma multiforme." Autophagy **10**(8): 1359-1368.

Rous, P. (1910). "An Experimental Comparison of Transplanted Tumor and a Transplanted Normal Tissue Capable of Growth." J Exp Med **12**(3): 344-366.

Rous, P. (1911). "A Sarcoma of the Fowl Transmissible by an Agent Separable from the Tumor Cells." J Exp Med **13**(4): 397-411.

Santos, E., S. R. Tronick, S. A. Aaronson, S. Pulciani and M. Barbacid (1982). "T24 human bladder carcinoma oncogene is an activated form of the normal human homologue of BALB- and Harvey-MSV transforming genes." Nature **298**(5872): 343-347.

Scheffzek, K., M. R. Ahmadian, W. Kabsch, L. Wiesmuller, A. Lautwein, F. Schmitz and A. Wittinghofer (1997). "The Ras-RasGAP complex: structural basis for GTPase activation and its loss in oncogenic Ras mutants." Science **277**(5324): 333-338.

Scheidig, A. J., C. Burmester and R. S. Goody (1999). "The pre-hydrolysis state of p21(ras) in complex with GTP: new insights into the role of water molecules in the GTP hydrolysis reaction of ras-like proteins." Structure **7**(11): 1311-1324.

Schindelin, J., I. Arganda-Carreras, E. Frise, V. Kaynig, M. Longair, T. Pietzsch, S. Preibisch, C. Rueden, S. Saalfeld, B. Schmid, J. Y. Tinevez, D. J. White, V. Hartenstein, K. Eliceiri, P. Tomancak and A. Cardona (2012). "Fiji: an open-source platform for biological-image analysis." Nat Methods **9**(7): 676-682.

Settembre, C. and A. Ballabio (2011). "TFEB regulates autophagy: an integrated coordination of cellular degradation and recycling processes." Autophagy **7**(11): 1379-1381.

Shih, C., B. Z. Shilo, M. P. Goldfarb, A. Dannenberg and R. A. Weinberg (1979). "Passage of phenotypes of chemically transformed cells via transfection of DNA and chromatin." Proc Natl Acad Sci U S A **76**(11): 5714-5718.

Shih, C. and R. A. Weinberg (1982). "Isolation of a transforming sequence from a human bladder carcinoma cell line." Cell **29**(1): 161-169.

Shin, J. Y., H. T. Lim, A. Minai-Tehrani, M. S. Noh, J. E. Kim, J. H. Kim, H. L. Jiang, R. Arote, D. Y. Kim, C. Chae, K. H. Lee, M. S. Kim and M. H. Cho (2012). "Aerosol delivery of beclin1 enhanced the anti-tumor effect of radiation in the lungs of K-rasLA1 mice." J Radiat Res **53**(4): 506-515.

Singer, G., R. Oldt, 3rd, Y. Cohen, B. G. Wang, D. Sidransky, R. J. Kurman and M. Shih le (2003). "Mutations in BRAF and KRAS characterize the development of low-grade ovarian serous carcinoma." J Natl Cancer Inst **95**(6): 484-486.

Solman, M., A. Ligabue, O. Blazevis, A. Jaiswal, Y. Zhou, H. Liang, B. Lectez, K. Kopra, C. Guzman, H. Harma, J. F. Hancock, T. Aittokallio and D. Abankwa (2015). "Specific cancer-associated mutations in the switch III region of Ras increase tumorigenicity by nanocluster augmentation." Elife **4**: e08905.

Sparkes, R. S., A. L. Murphree, R. W. Lingua, M. C. Sparkes, L. L. Field, S. J. Funderburk and W. F. Benedict (1983). "Gene for hereditary retinoblastoma assigned to human chromosome 13 by linkage to esterase D." Science **219**(4587): 971-973.

Sridharan, S., K. Jain and A. Basu (2011). "Regulation of autophagy by kinases." Cancers (Basel) **3**(2): 2630-2654.

Stolz, A., A. Ernst and I. Dikic (2014). "Cargo recognition and trafficking in selective autophagy." Nat Cell Biol **16**(6): 495-501.

- Sun, Q., W. Fan, K. Chen, X. Ding, S. Chen and Q. Zhong (2008). "Identification of Barkor as a mammalian autophagy-specific factor for Beclin 1 and class III phosphatidylinositol 3-kinase." Proc Natl Acad Sci U S A **105**(49): 19211-19216.
- Sutton, M. N., Lu Z., Bast, R.C. Jr. (2014). The Role of Angiogenesis, Growth Arrest and Autophagy in Human Ovarian Cancer Xenograft Models for Tumor Dormancy. Tumor Dormancy, Quiescence, and Senescence, Vol. 3. M. A. Hayat, Springer. **3**: 99-109.
- Tabin, C. J., S. M. Bradley, C. I. Bargmann, R. A. Weinberg, A. G. Papageorge, E. M. Scolnick, R. Dhar, D. R. Lowy and E. H. Chang (1982). "Mechanism of activation of a human oncogene." Nature **300**(5888): 143-149.
- Takahashi, Y., D. Coppola, N. Matsushita, H. D. Cuaing, M. Sun, Y. Sato, C. Liang, J. U. Jung, J. Q. Cheng, J. J. Mule, W. J. Pledger and H. G. Wang (2007). "Bif-1 interacts with Beclin 1 through UVRAG and regulates autophagy and tumorigenesis." Nat Cell Biol **9**(10): 1142-1151.
- Taparowsky, E., Y. Suard, O. Fasano, K. Shimizu, M. Goldfarb and M. Wigler (1982). "Activation of the T24 bladder carcinoma transforming gene is linked to a single amino acid change." Nature **300**(5894): 762-765.
- Tsukamoto, S., A. Kuma, M. Murakami, C. Kishi, A. Yamamoto and N. Mizushima (2008). "Autophagy is essential for preimplantation development of mouse embryos." Science **321**(5885): 117-120.
- Vellai, T. (2009). "Autophagy genes and ageing." Cell Death Differ **16**(1): 94-102.
- Vogl, D. T., E. A. Stadtmauer, K. S. Tan, D. F. Heitjan, L. E. Davis, L. Pontiggia, R. Rangwala, S. Piao, Y. C. Chang, E. C. Scott, T. M. Paul, C. W. Nichols, D. L. Porter, J. Kaplan, G. Mallon, J. E. Bradner and R. K. Amaravadi (2014). "Combined autophagy and proteasome inhibition: a phase 1 trial of hydroxychloroquine and bortezomib in patients with relapsed/refractory myeloma." Autophagy **10**(8): 1380-1390.

Vucicevic, L., M. Misirkic, K. Janjetovic, U. Vilimanovich, E. Sudar, E. Isenovic, M. Prica, L. Harhaji-Trajkovic, T. Kravic-Stevovic, V. Bumbasirevic and V. Trajkovic (2011). "Compound C induces protective autophagy in cancer cells through AMPK inhibition-independent blockade of Akt/mTOR pathway." Autophagy **7**(1): 40-50.

Wang, L., A. Hoque, R. Z. Luo, J. Yuan, Z. Lu, A. Nishimoto, J. Liu, A. A. Sahin, S. M. Lippman, R. C. Bast, Jr. and Y. Yu (2003). "Loss of the expression of the tumor suppressor gene ARHI is associated with progression of breast cancer." Clin Cancer Res **9**(10 Pt 1): 3660-3666.

Weber, F., M. A. Aldred, C. D. Morrison, C. Plass, A. Frilling, C. E. Broelsch, K. A. Waite and C. Eng (2005). "Silencing of the maternally imprinted tumor suppressor ARHI contributes to follicular thyroid carcinogenesis." J Clin Endocrinol Metab **90**(2): 1149-1155.

Wennerberg, K., K. L. Rossman and C. J. Der (2005). "The Ras superfamily at a glance." J Cell Sci **118**(Pt 5): 843-846.

White, E. (2015). "The role for autophagy in cancer." J Clin Invest **125**(1): 42-46.

Wu, X., L. Liang, L. Dong, Z. Yu and X. Fu (2013). "Effect of ARHI on lung cancer cell proliferation, apoptosis and invasion in vitro." Mol Biol Rep **40**(3): 2671-2678.

Yu, Y., R. Luo, Z. Lu, W. Wei Feng, D. Badgwell, J. P. Issa, D. G. Rosen, J. Liu and R. C. Bast, Jr. (2006). "Biochemistry and biology of ARHI (DIRAS3), an imprinted tumor suppressor gene whose expression is lost in ovarian and breast cancers." Methods Enzymol **407**: 455-468.

Yu, Y., F. Xu, H. Peng, X. Fang, S. Zhao, Y. Li, B. Cuevas, W. L. Kuo, J. W. Gray, M. Siciliano, G. B. Mills and R. C. Bast, Jr. (1999). "NOEY2 (ARHI), an imprinted putative tumor suppressor gene in ovarian and breast carcinomas." Proc Natl Acad Sci U S A **96**(1): 214-219.

Yue, Z., S. Jin, C. Yang, A. J. Levine and N. Heintz (2003). "Beclin 1, an autophagy gene essential for early embryonic development, is a haploinsufficient tumor suppressor." Proc Natl Acad Sci U S A **100**(25): 15077-15082.

Zhou, W. J., R. Deng, G. K. Feng and X. F. Zhu (2009). "[A G-quadruplex ligand SYUIQ-5 induces autophagy by inhibiting the Akt-FOXO3a pathway in nasopharyngeal cancer cells]." Ai Zheng **28**(10): 1049-1053.

Zhou, Y., H. Liang, T. Rodkey, N. Ariotti, R. G. Parton and J. F. Hancock (2014). "Signal integration by lipid-mediated spatial cross talk between Ras nanoclusters." Mol Cell Biol **34**(5): 862-876.

Zhou, Y., P. Prakash, H. Liang, K. J. Cho, A. A. Gorfe and J. F. Hancock (2017). "Lipid-Sorting Specificity Encoded in K-Ras Membrane Anchor Regulates Signal Output." Cell **168**(1-2): 239-251 e216.

Zhou, Y., C. O. Wong, K. J. Cho, D. van der Hoeven, H. Liang, D. P. Thakur, J. Luo, M. Babic, K. E. Zinsmaier, M. X. Zhu, H. Hu, K. Venkatachalam and J. F. Hancock (2015). "SIGNAL TRANSDUCTION. Membrane potential modulates plasma membrane phospholipid dynamics and K-Ras signaling." Science **349**(6250): 873-876.

Zhu, Y. H., L. Fu, L. Chen, Y. R. Qin, H. Liu, F. Xie, T. Zeng, S. S. Dong, J. Li, Y. Li, Y. Dai, D. Xie and X. Y. Guan (2013). "Downregulation of the novel tumor suppressor DIRAS1 predicts poor prognosis in esophageal squamous cell carcinoma." Cancer Res **73**(7): 2298-2309.

VITA

Margie N. Sutton was born in San Antonio, Texas on November 12, 1987, the daughter of Cathy Schnitzer and Allen N. DeYoung. A San Antonio native, Margie attended Douglas MacArthur High School prior to completing a Bachelor of Science degree in Chemistry and Biology with highest honors from The University of Texas at San Antonio (UTSA) in December 2010. From January 2011 until August 2011, when she entered The University of Texas Graduate School of Biomedical Sciences she worked as a Research Scientist in the Department of Chemistry at UTSA, under the direction of her undergraduate thesis advisor Dr. Douglas E. Frantz. Upon joining The University of Texas Graduate School of Biomedical Sciences, Margie joined the laboratory of Dr. Robert C. Bast in May 2012 where she remained as a graduate research assistant throughout her doctoral research.

Address:

1115 W. 16th Street, Unit A

Houston, Texas 77008



Confirmation Number: 11630787
Order Date: 03/09/2017

Customer Information

Customer: Margie Sutton
Account Number: 3001123125
Organization: UT MD Anderson Cancer Center
Email: mnsutton@mdanderson.org
Phone: +1 (713) 792-3790
Payment Method: Invoice

This is not an invoice

Order Details

Scientific Reports

Billing Status:
N/A

Order detail ID: 70327122
ISSN: 2045-2322
Publication Type: e-Journal
Volume:
Issue:
Start page:
Publisher: Nature Publishing Group

Permission Status: **Granted**
Permission type: Republish or display content
Type of use: Republish in a thesis/dissertation
Order License Id: 4064880942249

Requestor type	Author of requested content
Format	Print
Portion	chart/graph/table/figure
Number of charts/graphs/tables/figures	1
Title or numeric reference of the portion(s)	Figure 8A
Title of the article or chapter the portion is from	The Structural Basis of Oncogenic Mutations G12, G13 and Q61 in Small GTPase K-Ras4B
Editor of portion(s)	Suzanne Farley, PhD
Author of portion(s)	Shaoyong Lu, Hyunbum Jang, Ruth Nussinov, Jian Zhang
Volume of serial or monograph	21949
Page range of portion	1
Publication date of portion	23 February 2016
Rights for	Main product
Duration of use	Life of current edition
Creation of copies for the disabled	no
With minor editing privileges	yes
For distribution to	Worldwide

In the following language(s)	Original language of publication
With incidental promotional use	no
Lifetime unit quantity of new product	Up to 499
Made available in the following markets	no
The requesting person/organization	Margie N. Sutton
Order reference number	
Author/Editor	Margie N. Sutton
The standard identifier of New Work	Dissertation
The proposed price	\$0
Title of New Work	The Role of the DIRAS family members in regulating Ras function, cancer growth and autophagy
Publisher of New Work	none
Expected publication date	May 2017
Estimated size (pages)	160

Note: This item was invoiced separately through our **RightsLink service**. [More info](#)

\$ 0.00

Total order items: 1

Order Total: \$0.00

[About Us](#) | [Privacy Policy](#) | [Terms & Conditions](#) | [Pay an Invoice](#)

Copyright 2017 Copyright Clearance Center